NTNU – Trondheim
Norwegian University of
Science and Technology

Experimental Investigations of Ice Rubble: Shear Box and Pile Testing

Oda Skog Astrup

Civil and Environmental Engineering
Submission date: June 2012
Supervisor: Knut Vilhelm Høyland, BAT

Norwegian University of Science and Technology
Department of Civil and Transport Engineering

NORWEGIAN UNIVERSITY OF SCIENCE AND TECHNOLOGY
DEPARTMENT OF CIVIL AND TRANSPORT ENGINEERING

Report Title:	Date: 09.06.2012			
Experimental Investigations and analytical Analysis of Ice Rubble: Shear Box and Pile Testing	Number of pages (incl. appendices): 145			
	Master Thesis	X	Project Work	
Name: Oda Skog Astrup				
Professor in charge/supervisor: Knut Høyland				
Other external professional contacts/supervisors:				

Abstract:

The largest part of an ice ridge consists of unconsolidated ice rubble, whose material properties decide the load from ridges on ships and structures. Material resistance is attributed to the initial freeze-bonds and the friction and interlocking between blocks. The objective of the thesis was to investigate rubble behaviour by two tests: shear box test at NTNU and pile test at HSVA. The shear box test was aimed at investigating freeze-bond mechanisms in rubble. The pile test was aimed at suggesting values for rubble properties for a model scale experiment.

The shear box had dimensions 600 mm x 400 mm x 40 mm, and was filled with ice blocks of 60 mm x 22 mm x 40 mm simulating rubble. Confinement was added, the box was submerged for 10 minutes, and tested in a rig by forcing the rubble to fail in shear. Force vs. displacement was measured. Different types of saline ice and submerging water temperatures were used. Pile testing consisted of making an elongated pyramid-shaped pile, baseline 600 mm, of rubble collected from the ice tank at HSVA. The pile was tilted and geometry was measured before and after failure happened in the pile.

Main results from the shear box tests were the observation of a first phase deformation of rubble, that displayed a near linear force-displacement relation and a first peak shear stress. Magnitude of first peaks was measured in the range 8.9 kPa to 59.7 kPa, and depended on submersion water temperature, salinity of ice, how blocks were cut in respect to crystal structure in the ice sheet and confining pressure. Pile tests had repose angles ranging from 36.0° to 47.3°, and cohesion for an assumed angle of friction of 30° was in the range of 172 Pa to 342 Pa.

First phase shear stress was compared to shear strength of single freeze-bond tests of the same ice, and direct relations were found. The magnitude of first peak shear stress in tests varied most with ice salinity and crystal structure. The measured repose angles for pile tests give an upper limit for internal angles of friction, and values seemed reasonable. The ice was warm, and this may the reason for the low cohesions.

Keywords:

1. Ice rubble
2. Shear box
3. Pile test
4. Freeze-bonds

Preface

This thesis is the documentation of the work done in the course TBA4920 at NTNU Department of Civil and Transport Engineering in the spring semester of 2012. The main topic of the thesis is experimental and analytical investigation of ice rubble, shear box and pile testing. My supervisor was Knut Høyland.

Laboratory work was executed in two different test facilities, and would not have been possible without the help, assistance and support of several individuals and organizations.

The shear box testing was executed at the cold lab at NTNU Department of Civil and Transport Engineering together with fellow master student Henning Helgøy. He lead testing of single freeze-bond strength, that was conducted simultaneously with the shear box tests. The testing was conducted with support from the SAMCoT CRI through the Research Council of Norway and all the SAMCoT partners.

The pile tests were conducted at HSVA (Hamburg Ship Model Basin) as a part of the test matrix for the RITAS-project. RITAS is short for Rubble Ice Transportation on Arctic Offshore Structures. This project is a cooperation between Multiconsult, Statoil, HYDRALAB-IV, HSVA, NTNU and SAMCoT. My participation was made possible by the economic support from HYDRALAB-IV, the European Community's Seventh Framework Programme through the grant to the budget of the Integrating Activity HYDRALAB IV, Contract no. 261520.[1]

Trondheim, June 9th, 2012

Oda Skog Astrup

[1]This document reflects only the authors' views and not those of the European Community. This work may rely on data from sources external to the HYDRALAB IV project Consortium. Members of the Consortium do not accept liability for loss or damage suffered by any third party as a result of errors or inaccuracies in such data. The information in this document is provided "as is" and no guarantee or warranty is given that the information is fit for any particular purpose. The user thereof uses the information at its sole risk and neither the European Community nor any member of the HYDRALAB IV Consortium is liable for any use that may be made of the information.

Acknowledgments

Several people and organizations have contributed to this thesis.

I'd like to thank my supervisor Knut Høyland for his guidance. I'd also like to thank Professor Lars Grande for his guidance on geotechnical topics and pile-testing.

This thesis is based on a great deal of lab work, almost all of it conducted together with Henning Helgøy. I would like to thank him for his never failing good mood, for all help, for all the good laughs inside and outside the lab, and of course for all the work he put down in forming, executing and discussing the experiments.

The laboratory work conducted at NTNU was conducted together with Henning. We received a lot of help, and I would like to thank Johan Wåhlin, Per Asbjørn Østesen and the guys at the geotechnical lab for all help with set-up and equipment. Also I would like to acknowledge the support from the NTNU centre for research-based innovation SAMCot.

The laboratory work executed at the ice basin of HSVA (Hamburgerische Schiffbau Versuchs Anstanlt) in Hamburg, Germany, was a part of the RITAS-project. I would like to thank all of Multiconsult Tromsø and Nicolas Serré who lead the project, and he whole RITAS-team for all help and guidance, and for making my stay in Hamburg unforgettable. I would also like to thank HYDRALAB-IV for the economic support that made it possible for me to participate in the project.

Parts of the work described in this publication were supported by the European Community's 7th Framework Program through the grant to the budget of the Integrated Infrastructure Initiative HYDRALAB-IV, Contract no. 261520. I would like to thank the Hamburg Ship Model Basin (HSVA), especially the ice tank crew, for the hospitality, technical and scientific support and the professional execution of the test program in the Research Infrastructure ARCTECLAB.

Abstract

The largest part of an ice ridge consists of unconsolidated ice rubble, whose material properties decide the load from ridges on ships and structures. Material resistance is attributed to the initial freeze-bonds and the friction and interlocking between blocks. The objective of the thesis was to investigate rubble behaviour by two tests: shear box test at NTNU and pile test at HSVA. The shear box test was aimed at investigating freeze-bond mechanisms in rubble. The pile test was aimed at suggesting values for rubble properties for a model scale experiment.

The shear box had dimensions 600 mm x 400 mm x 40 mm, and was filled with ice blocks of 60 mm x 22 mm x 40 mm simulating rubble. Confinement was added, the box was submerged for 10 minutes, and tested in a rig by forcing the rubble to fail in shear. Force vs. displacement was measured. Different types of saline ice and submerging water temperatures were used. Pile testing consisted of making an elongated pyramid-shaped pile, baseline 600 mm, of rubble collected from the ice tank at HSVA. The pile was tilted and geometry was measured before and after failure happened in the pile.

Main results from the shear box tests were the observation of a first phase deformation of rubble, that displayed a near linear force-displacement relation and a first peak shear stress. Magnitude of first peaks was measured in the range 8.9 kPa to 59.7 kPa, and depended on submersion water temperature, salinity of ice, how blocks were cut in respect to crystal structure in the ice sheet and confining pressure. Pile tests had repose angles ranging from 36.0° to 47.3°, and cohesion for an assumed angle of friction of 30° was in the range of 172 Pa to 342 Pa.

First phase shear stress was compared to shear strength of single freeze-bond tests of the same ice, and direct relations were found. The magnitude of first peak shear stress in tests varied most with ice salinity and crystal structure. The measured repose angles for pile tests give an upper limit for internal angles of friction, and values seemed reasonable. The ice was warm, and this may the reason for the low cohesions.

Sammendrag (Abstract in Norwegian)

Skrugarder består hovedsakelig av ukonsolidert skruis, og dette materialet bestemmer belastningen fra en skrugard på skip og konstruksjoner. Materialstyrken av-henger av frysebåndene mellom blokker, friksjon og sperremekanismer mellom blokker. Hovedmålet med oppgaven var å undersøke ukonsolidert skruis materiale ved hjelp av to tester: skjærboksforsøk ved NTNU og forsøk med skråningsstabilitet ved HSVA. Skjærboksforsøkene hadde som mål å undersøke frysebåndsmekanismer i skruis. Skråningsstabilitetsforsøkene hadde som mål å foreslå skruis parametere for et modellskala forsøk.

Skjærboksen hadde dimensjoner 600 mm x 400 mm x 40 mm, og var fylt med isblokker på 60 mm x 22 mm x 40 mm som simulerte skruis. Overlagringstrykk ble satt på, boksen ble senket ned i vann i 10 minutter og testet ved å tvinge skruisen til å gå til skjærbrudd. Kraft og forskyvning ble målt. Skråningsstabilitetsforsøket besto i å lage en avlang triangulær haug, grunnlinje 600 mm, av skruisen fra isbasenget på HSVA. Så vippe haugen til sida, måle opprinnelig geometri og rasvinkler.

Hovedresultater fra skjærboksforsøkene var at en første fase i deformasjonsforløpet til skruis ble observert. Kraft-forsyningsrelasjonen var nærmest lineær fram til en toppverdi. Toppspenningen varierte fra 8.9 kPa til 59.7 kPa avhengig av nedsenkningstemperaturen til vannet, saltinnhold i isen, med hvilken orientering blokkene var kuttet fra isen og overlagringstrykket. Den naturlige skråningsvinkelen i skruis haugene ved HSVA ble målt mellom 36.0° og 47.3°, kohesjonen for en antatt friksjonsvinkel på 30° var mellom 172 Pa og 342 Pa.

Topp spenningen målt i første fase i skjærboksførsøkene ble sammenlignet med styrken av enkle frysebåndstester, og det ble konstatert målbare sammenhenger. Toppspenningen i første fase varierte mest med saltinnholdet og krystallstrukturen i isen. De målte skråningsvinklene i skråningsstabilitetsforsøkene gir en øvre grense for indre friksjonsvinkel, og verdiene var ikke urimelige. Isen var varm, og det kan være forklaringen på lav kohesjon.

Contents

List of Figures

List of Tables

List of Abbreviations and Symbols

Abbreviations

HSVA	Hamburgerische Schiffbau und Versuchsanstalt (Hamburg Ship Model Basin), test facilities in Hamburg Germany
NTNU	Norwegian University of Science and Technology
RITAS	Rubble Transport on Arctic Offshore Structures, a research program
RVE	Representative Volume Element
SAMCoT	Sustainable Arctic Marine and Coastal Technology, a centre for research-based innovation at NTNU
SB	Shear Box
ppt	parts per thousand, measure for salinity
2D	Two dimensional
3D	Three dimensional

Symbols

A	[m^2]	Areal
c	[Pa]	Cohesion
d_{SB}	[m]	Depth of shear box
E	[Pa]	Young's modulus
F	[N]	Force
$\overline{F}$	[N]	Average force
G	[Pa]	Shear modulus
g	[m/s^2]	Gravity
H_c	[m]	Thickness of consolidated layer
H_i	[m]	Level ice thickness
H_k	[m]	Keel depth
H_s	[m]	Sail height
h_b	[m]	Thickness of block
h_r	[m]	Height of rubble
L	[m]	Length
L_b	[m]	Length of block
L_{SB}	[m]	Length of shear box
N_b		Number of blocks
s	[m]	Length of a line segment

s_0	[m]	Original length of a line segment
t	[s]	Time
$\overline{t}$	[s]	Average time
V	[m^3]	Volume
v	[m/s]	Velocity
w	[m]	Width

α	[deg]	Angle
β	[deg]	Angle
γ		Shear strain
γ_{xy}		Engineering shear strain
γ_{max}		Maximum shear strain
ϵ		Longitudinal strain
ϵ_E		Engineering longitudinal strain
ϵ_L		Logarithmic longitudinal strain
ϵ_v		Volumetric strain
ϵ_1		Principal stain (the algebraic largest)
ϵ_2		Principal stain (the algebraic intermediate)
ϵ_3		Principal stain (the algebraic smallest)
η		Porosity
θ_k	[deg]	Keel angle
λ		Length scaling factor
λ_T		Time scaling factor
ν		Poisson ratio
ρ	[kg/m^3]	Density
σ_n	[Pa]	Normal stress
σ_{fl}	[Pa]	Flexural strength
σ_1	[Pa]	Principal stress (the algebraic largest)
σ_2	[Pa]	Principal stress (the algebraic intermediate)
σ_3	[Pa]	Principal stress (the algebraic smallest)
τ	[Pa]	Shear stress
τ_0	[Pa]	Nominal shear stress
τ_t	[Pa]	Time-adjusted shear stress
τ_{ave}	[Pa]	Average shear stress
ϕ	[deg]	Internal angle of friction
ϕ_c	[deg]	Internal angle of friction for continuous shear
ϕ_{cv}	[deg]	Internal angle of friction for a material with constant volume
ϕ_p	[deg]	Internal angle of friction for the first peak strength
ψ	[deg]	Angle of dilation

1 Introduction

1.1 Background

For structures and ships located in waters with seasonal ice, encounters with first-year ice ridges may give significant loading. The ridges are created by shear and pressure processes in open ocean or in front of structures, and can reach a great volume. The largest part of an ice ridge consists of unconsolidated ice rubble. The knowledge about the material properties and the mechanical behaviour of unconsolidated ice rubble is still limited. To be able to decide the loading from ice ridges, this must be investigated.

For ice rubble, this is difficult for several reasons. Firstly, in-situ investigation is expensive and comprehensive. Secondly, it is challenging to make good laboratory tests due to the peculiar nature of sea ice, and ice rubble.

Common for most studies is that the ice rubble have been idealized as a elastic-plastic material, where the yield limit is described by the Mohr-Coulomb criterion (Liferov and Bonnemaire, 2005). The initial failure springs from the breaking of the rubble skeleton, which is attributed to the freeze-bonds that initially exist between individual blocks. After the initial freeze-bonds are broken, the ice rubble display mainly frictional resistance (Ettema and Urroz-Aguirre, 1987). Knowledge about this processes are still limited, and further study is necessary.

To better understand the behaviour of ice rubble, two types of tests have been common: punch tests and shear box tests. Punch tests out in the field, like pushing down a plug of rubble, are convenient since you test full scale real rubble and have natural condition. The boundary conditions of such testing are on the contrary hard to decide. Shear box testing can be conducted in the lab. The concept is to fill a box with ice blocks simulating the rubble, apply a shear force and measure the failure load and behaviour of the rubble. Such tests do not test rubble in its natural state, but have well defined boundary conditions.

The freeze-bonding mechanism in ice ruble have been investigated by doing small-scale freeze-bond tests. Repetto-Llamazares et al. (2011) and Serré et al. (2011) studied how freeze-bonding effected rubble behaviour, by combining tests of freeze-bond strength between two ice blocks and shear box testing of rubble made with the same ice. They found that stronger freeze-bonds gave higher first peak strength in rubble, and gave an increased dilation due to blocks sticking together in block assemblies.

The starting point of this thesis, was the laboratory study of single freeze-bonds be-

tween ice blocks in the project work of TBA4550 autumn of 2011 (Astrup, 2011). Based on the laboratory set-up of Repetto-Llamazares et al. (2011), the shear strength of freeze-bonds related to surface structure, and strain rate, were tested. We (Helgøy, 2011; Astrup, 2011) defined several parameters that could have considerable effects on freeze-bond strength: Submersion water temperature, surface roughness of blocks, surface crystal structure and ice storage time. In his thesis, fellow master student Helgøy (2012) aimed to investigate further the effects of these parameters on freeze-bond strength.

Since freeze-bonding is merely one of the mechanisms when rubble deform, it was interesting to investigate further the relation between freeze-bond strength and rubble behaviour. That is, to find out if the same parameters as suggested to effect freeze-bonds, also effect rubble strength, and how strong the relation between freeze-bond tests and rubble strength is.

Rubble interactions with structures are often studied with model scale experiments. To validate observations in small scale, the model scale rubble parameters for the experiment should also be investigated. Pile testing is one way to access rubble parameters such as the angle of internal friction and cohesion. The concept of the test is to pour or stack rubble in a random way, allowing it to form a pyramid-shaped pile. By measuring the initial repose angle one gets an indication of the internal angle of friction in the pile, and by tilting the pile afterwards one may quantify how much cohesion have developed in the rubble. Pile testing have been conducted earlier by Serré et al. (2009).

Little work has been done on evaluating the set-up and the results of such tests for ice rubble. It may be possible to develop the method further, and use principles of soil mechanics and slope stability to extract give more information from the testing.

1.2 Scope and Objectives

The main goal of the thesis is to investigate rubble behaviour by experimental and analytical methods, using two tests: the shear box test and the pile test. This includes a literature study on the mechanical properties of ice rubble, earlier shear box studies, scaling and other aspects of forming experiments. Two laboratory set-ups are formed; one for the shear box experiment at NTNU, and one for the pile testing at HSVA. The following research goals were set for each experiment:

The main goal for the laboratory work at NTNU was to investigate the freeze-bond mechanisms in rubble. To investigate this, three major objectives or research goals were formed.

(a) Earlier studies on freeze-bonds often report submersion water temperatures "at the freezing point". Such a description can be used both for water in the process of freezing (super cooled water), or for water at a stable temperature in

a cold room. The first objective was to investigate how sensitive the ice rubble strength was to the temperature of the surrounding water. The hypothesis was that water temperatures kept exactly at the freezing point (super cooled) will give significantly higher strength of the rubble than water kept above but near the freezing point.

(b) During testing of single freeze-bonds it became evident that the orientation of crystals in the individual ice blocks gave a considerable effect on the freeze-bond strength (Helgøy, 2012). The hypothesis was that also shear boxes with this variation of blocks would display different behaviour. To verify this was the second main objective.

(c) The last main objective was to do a throughout investigation of rubble behaviour in the shear box, analyse typical behaviour and evaluate the limitations of the test method.

The pile testing at HSVA had four main objectives.

(a) The initial purpose of the test is to access rubble properties, and the first objective was to report the model scale rubble properties for the RITAS-project.

(b) As the testing implies creating slides in a pile, concepts of slope stability may be used to extract more information from the testing. To use slope stability to analyse tests was another objective.

(c) The third objective was to investigate the time-dependence of cohesion in a pile.

(d) Since pile testing is not a very common test for ice rubble, the last objective was to do an evaluation of the method and the credibility of results.

1.3 Limitations

The author assumes that the reader has a basic knowledge of sea ice properties and behaviour, and of material mechanics.

Laboratory work at NTNU was conducted together with fellow master student Henning Helgøy. He had the main responsibility for forming a set-up and reporting results for single freeze-bond tests, see Helgøy (2012). I had the main responsibility for forming a set-up and reporting results from the shear box testing.

In the set-up values for initial ice temperature, submersion time and deformation velocity was not varied, the study does not aim on investigating how rubble behaviour depends on this parameters.

Laboratory work at HSVA was a part of the RITAS-project, where all worked together to execute all the planned tests. I had the main responsibility for executing and reporting results from the pile tests. As the pile test where only one item on

the test matrix, it was some restrictions on what type of rubble that was available and to the time available for testing.

1.4 Structure of Study

The study is structured with a theory part (chap. 2), a description of the experiments executed at NTNU (chap. 3.1 and 4.1), a description of the experiments executed at HVSA (chap. 3.2 and 4.2), and a common discussion and conclusion (chap. 5 and 6). Section 2.1 is a modified version of the section with the same name from Astrup (2011).

2 Theory

2.1 Formation and Composition of Ice Ridges

An ice ridge is a volume of broken sea ice pushed together. The ridges can reach a great volume, and can be created in front of structures or by shear and pressure processes in the ocean.

In nature you may find single ridges or ridge fields of varying shape, but the simple, symmetrical geometry in figure 1 is normally used for calculations. We separate the ridge into two parts, the sail and the keel. The sail consists of the blocks above water, and the keel of the submerged blocks. Further we separate the keel into a consolidated layer where the ice blocks are fully frozen together, and the unconsolidated rubble where the ice blocks may, or may not be frozen together (Løset et al., 2006, Chap. 4.6.3.).

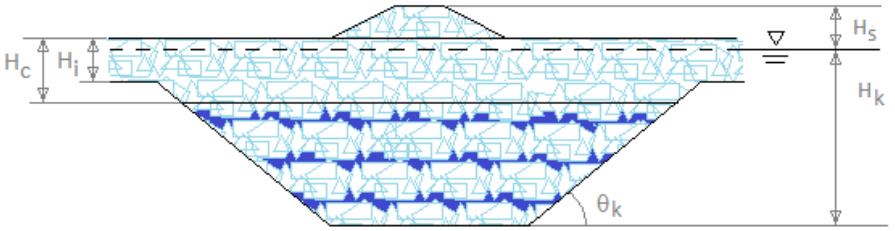

Figure 1: Generalized geometry of an ice ridge

In the literature you may find statistical values for the geometry of first-year ridges. Some suggested values are (ISO/FDIS/19906, 2010, A.8.2.4.5.1):

- Keel to sail ratio: $H_k/H_s = 4.5$
- Consolidated layer to level ice thickness: $H_c/H_i = 1.6$
- Keel angle $\theta_k = 26°$

The rubble, that is the unconsolidated part of the keel, takes up most of the volume in a ridge. When a ridge is created, the blocks are pushed down under water and pressed together by the overlaying weight and the buoyancy. The gaps between the blocks are filled with water and slush. The submerged blocks initially keep a

lower temperature than the surrounding water, and may freeze together. We call this the formation of ad freeze-bonds.

Values for the porosity of the rubble have been reported in a range of 0.25-0.45 (Liferov, 2005, Chap. 2.2). The porosity also increase with depth, and seem to have an almost linear variance from top to bottom (Mellor, 1983). The block size depends on the initial thickness of the ice cover, and can be predicted by looking at the block size in the sail.

Ice ridges have a limited lifetime, and develop and change continuously with time. In general we separate ridges into first-year and old ridges, were old means that they were preserved over one or several summers. First-year ridges are the most relevant features for waters with only seasonal ice cover, and are the type that is addressed in this paper.

2.2 Deformation and Failure Criteria

To describe deformation in a material one uses the strain measures. To predict failure or fracture in a material one typically uses failure criteria, based on stress states and strain energy in the material.

2.2.1 Strain

The local deformation of a material is measured in strain. It is given as a dimensionless number, and expresses relative deformation of a material segment. One may use the measures longitudinal strain ε (eq:1)

$$\varepsilon = \lim_{s_0 \to 0} \frac{s - s_0}{s_0} \tag{1}$$

where s is the length of a strait line segment.

Strain may also be expressed as shear strain $\gamma = \alpha + \beta$ (figure 2), and volumetric strain ε_v (eq:2).

Shear strain is defined as the change of the right angle between two lines in the material, that originally were orthogonal to each other, see figure 2. The shear strains are given in radians, and are defined as positive when the angle is reduced.

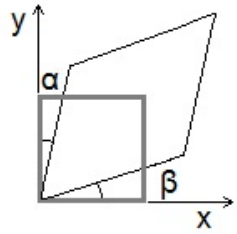

Figure 2: Definition of shear strain as sum of the two angles α and β

The volumetric strain ε_v is defined as the change in volume per unit undeformed volume:

$$\varepsilon_v = \lim_{\Delta V_0 \to 0} \frac{\Delta V - \Delta V_0}{\Delta V_0} \tag{2}$$

where ΔV is the volume of a segment.

Several different strain measures exist, and two of the most common are given in (eq: 3).

$$\varepsilon_E = \frac{s - s_0}{s_0} \quad \varepsilon_L = ln\left(\frac{s}{s_0}\right) \tag{3}$$

For small strains the engineering strain ε_E is a good approximation, for larger strains this measure is unfit, and the logarithmic strain ε_L is often used.

Analyses with small strains are easier than working with large strains, due to the simplifications of the expressions. If the displacements are small, the angles of figure 2 can be simplified and the engineering shear strain can be written as:

$$\gamma_{xy} = \frac{\partial u_x}{\partial y} + \frac{\partial u_y}{\partial x} \tag{4}$$

The whole three dimensional strain matrix in the xyz-coordinate system will then be:

$$\begin{bmatrix} \varepsilon_{xx} & \frac{1}{2}\gamma_{xy} & \frac{1}{2}\gamma_{xz} \\ \frac{1}{2}\gamma_{yx} & \varepsilon_{yy} & \frac{1}{2}\gamma_{yz} \\ \frac{1}{2}\gamma_{zx} & \frac{1}{2}\gamma_{zy} & \varepsilon_{zz} \end{bmatrix} \tag{5}$$

Note that the strain shear tensors are taken as an average angle reduction, and is therefore expressed as $\frac{1}{2}\gamma_{xy}$. For a complete proof of (eq:4) and further explanation of the strain measure, see Irgens (2008, Chap. 5).

2.2.2 Linear Stress-Strain Relation and Strain Energy Density

In elastic material behaviour it is a linear relation between stress and strain. If you consider an element exposed to uniaxial stress, this can be stated by Hooke's law:

$$\sigma_x = E\varepsilon_x \tag{6}$$

where E is the elasticity or Young's modulus. Similarly this linear relation can be stated for a segment exposed to pure shear, as:

$$\tau_{xy} = G\gamma_{xy} \tag{7}$$

where G is the shear modulus, which stand in relation to Young's modulus as

$$E = 2G(1 - \nu) \tag{8}$$

Where ν is the Poisson ratio.

The strain energy U is defined as the work absorbed in a material volume due to forces acting on it. The general formulation is:

$$U = \int_{V_0}^{V_1} \int_{\varepsilon_0}^{\varepsilon_1} \sigma \, d\varepsilon \, dV \tag{9}$$

2.2.3 The Mohr-Coulomb Failure Criterion

The Mohr-Coulomb failure criterion is often used for materials that have strength depending on the level of hydrostatic pressure, like soils, ice, and other materials that are stronger in compression than in tension. The Mohr-Coulomb criterion has the physical explanation that shear-resistance at a plane, is proportional to the friction created by the normal force at that plane. Mathematically this is stated:

$$\tau = \sigma_n \, tan(\phi) + c \tag{10}$$

Where τ is the shear strength, σ_n is the normal compression stress, ϕ is the angle of internal friction and c is the cohesion.

This relation can also be represented in a diagram, see figure 3.

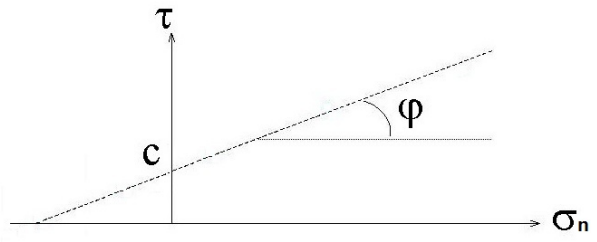

Figure 3: The Mohr-Coulomb failure criterion, $\sigma_n > 0$ in compression

The use of Mohr-coulomb failure criterion is well developed for geotechnics, the study of soils as a granular material. Houlsby (1991) discusses the behaviour of sand, and explains how the phenomena of dilation complicate the material model. Dilation is the expansion of materials during shearing, starting just after a short initial compression of the material. In soil mechanics this applies especially to dense sands, the denser the sand the more rapid expansion (Houlsby, 1991).

In the Mohr-Coulomb criteria the dilation is taken into account as an angle of dilation ψ, that together with the angle of friction at no volume expansion ϕ_{cv}, constitute the observed angle of friction ϕ (Houlsby, 1991). This can be expressed:

$$\tau = \sigma_n \, tan(\phi) + c = \sigma_n \, tan(\phi_{cv} + \psi) + c \tag{11}$$

The angle of friction is defined as a ratio of shear stress to normal stress, and can be expressed in terms of principal stresses (Houlsby, 1991):

$$\sin\phi = \frac{\sigma_1 - \sigma_3}{\sigma_1 + \sigma_3} \tag{12}$$

Where σ_1 and σ_3 are the algebraic largest and smallest principal stress, see (Irgens, 2008, chap. 3.3.1).

In a similar way the angle of dilation is expressed as the ratio between a volumetric strain rate and a shear strain rate (Houlsby, 1991). This can also be written as a ratio between a volumetric strain increment and a shear strain increment as in equation (13).

$$\sin\psi = -\frac{\delta\varepsilon_v}{\delta\gamma_{max}} = \frac{-(\delta\varepsilon_1 + \delta\varepsilon_2 + \delta\varepsilon_3)}{\delta\varepsilon_1 - \delta\varepsilon_3} \tag{13}$$

Where ε_1, ε_2 and ε_3 are principal strains, see (Irgens, 2008, chap. 5.3.4). The negative sign is due to that compressive deformation is considered positive in soil mechanics.

A physical illustration of the dilation angle is given in the sawtooth model shown in figure 4.

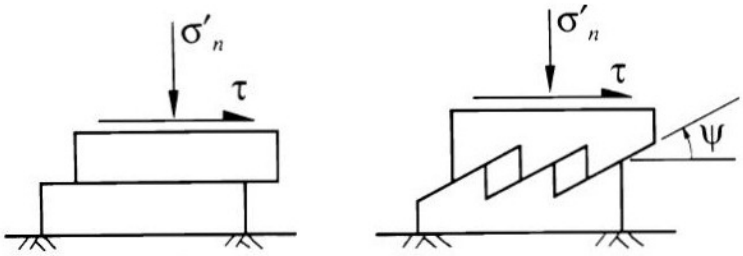

(a) Volume without dilation (b) Volume with dilation

Figure 4: A physical model for dilation, described by Houlsby (1991)

In figure 4 (a) a smooth block slides on top of another without any volume expansion. Then ϕ=ϕ_{cv}. While in figure 4 (b) two rough blocks slide on top of each other and you get a volume expansion. Then ϕ=ϕ_{cv}+ψ applies. So the angle of internal friction is dependent on the angle of dilation, which again depends on the density of the material and the confinement pressure.

2.3 Scaling of Experiments

Scaling of experiments is a large topic. The approach is to identify variables, use dimensional analysis and scale by dimensionless numbers. One uses symbols like F, M, L, T and θ for force, mass, length, time and temperature. Using these symbols, one can express the dimension of many physical parameters.

For example the dimensions of stress will be:

$$stress = \frac{Force}{Area} = \frac{MLT^{-2}}{L^2} = ML^{-1}T^{-2} \tag{14}$$

One defines the length scaling factor λ as the ratio of full scale (f) to model scale (m):

$$\lambda = \frac{L_f}{L_m} \tag{15}$$

In model studies when making a model of some prototype construction, one needs to scale the model with consideration to what physical phenomena one would like

to investigate. It is usually not possible to scale for all physical phenomena at the same time, and one must choose the most important ones.

For mechanical testing of ice there are four phenomena, or force contributions, that are believed to be important: kinematic or inertia force ($F_{kinetic}$), gravity force ($F_{gravity}$), elastic strength ($F_{elastic}$) and flexural strength ($F_{flexural}$). Using these forces, one can define the three most relevant dimensionless numbers to scale by: Froude number, the Cauchy Number and the flexural strength ratio.

2.3.1 Froude Scaling

When kinematic and gravity forces are important, the Froude number (eq: 16) is the appropriate dimensionless number to scale by.

$$Fr = \frac{F_{kinetic}}{F_{gravity}} = \frac{v}{\sqrt{gL}} \tag{16}$$

Where v is velocity, g is gravity and L is a characteristic length.

The Froude number must stay the same for the model and the full scale problem. Using this, and assuming g is constant, one can derive the other scaling factors as a function of λ. Velocity will scale as:

$$Fr_m = Fr_f \;\Rightarrow\; \frac{v_m}{\sqrt{gL_m}} = \frac{v_f}{\sqrt{gL_f}} \;\Rightarrow\; \frac{v_f}{v_m} = \frac{\sqrt{L_f}}{\sqrt{L_m}} \;\Rightarrow\; \boxed{\frac{v_f}{v_m} = \sqrt{\lambda}} \tag{17}$$

Similarly time t will scale as

$$\boxed{\lambda_T = \frac{T_f}{T_m} = \sqrt{\lambda}} \tag{18}$$

2.3.2 Cauchy Scaling

When kinematic and elastic forces are important, the Cauchy number (eq: 19) is the appropriate dimensionless number to scale by.

$$Ca = \frac{F_{kinetic}}{F_{elastic}} = \frac{\rho v^2}{E} \tag{19}$$

Where ρ is the density and E is the elastic modulus.

The Cauchy number must stay the same for the model and the full scale problem. Using this, and assuming that ρ is constant and the time scaling factor λ_T is given, one can derive the elastic modulus scaling as a function of λ and λ_T:

$$Ca_m = Ca_f \quad \Rightarrow \quad \frac{\rho v_m^2}{E_m} = \frac{\rho v_f^2}{E_f} \quad \Rightarrow \quad \frac{E_f}{E_m} = \sqrt{\frac{L_f^2 T_f^{-2}}{L_m^2 T_m^{-2}}} \quad \Rightarrow \quad \boxed{\frac{E_f}{E_m} = \lambda^2 \lambda_T^{-2}} \tag{20}$$

If the time scaling is already given by the Froude scaling (eq: 18), this can be inserted in (eq: 20) and the expression will be simplified:

$$\boxed{\frac{E_f}{E_m} = \lambda} \tag{21}$$

2.3.3 Scaling with Flexural Strength Ratio

When kinematic forces and flexural strength are important, the flexural strength ratio (eq: 22) is the appropriate dimensionless number to scale by.

$$Fl = \frac{F_{kinetic}}{F_{gravity}} = \frac{\rho v^2}{\sigma_{fl}} \tag{22}$$

Where σ_{fl} is the flexural strength of the material. When ρ is a constant, the flexural strength will scale as:

$$Fl_m = Fl_f \quad \Rightarrow \quad \frac{\rho V_m^2}{\sigma_{flm}} = \frac{\rho V_f}{\sigma_{flf}} \quad \Rightarrow \quad \frac{\sigma_{flf}}{\sigma_{flm}} = \frac{v_f^2}{v_m^2} \quad \Rightarrow \quad \boxed{\frac{\sigma_{flf}}{\sigma_{flm}} = \lambda^2 \lambda_T^2} \tag{23}$$

If the time scaling is given already by the Froude scaling (eq: 18), this can be inserted in (eq: 20) and the expression will be simplified:

$$\boxed{\frac{\sigma_{fl_f}}{\sigma_{fl_m}} = \lambda} \tag{24}$$

Assuming the force acting on a structure is governed by the flexural stress of ice, the force will scale as:

$$\frac{F_{fl_f}}{F_{fl_m}} = \frac{\sigma_{fl_f} L_f^2}{\sigma_{fl_m} L_m^2} \Rightarrow \boxed{\frac{F_{fl_f}}{F_{fl_m}} = \lambda^3} \tag{25}$$

2.3.4 Scaling Methods for Ice

For ice experiments one often wish to scale by all the dimentionless numbers presented in this section. To satisfy the previous calculations in ice experiments, one needs to scale down the strength and the elasticity of the ice. This is mostly archived by heating the ice. It is also common to "seed" the ice, which means spaying the water surface with cold water when the ice is forming. In this way you can scale down the crystals diameter of the ice, and may adjust the ice strength and composition.

In the previous calculations the density is considered a constant, but using a sophisticated method to release small air bubbles during the ice formation, the density can be changed. This is for example done at the test facilities of HSVA in Hamburg.

2.4 Deformation of Ice Rubble

As mentioned, rubble is the unconsolidated part of the ice ridge keel, whose mechanical behaviour most commonly is described by the Mohr-Coulomb failure criteria. Its strength depends on the material properties, which is listed by Prodanovic (1979) below:

- Mechanical properties of parental ice sheet
- Degree of consolidation (refreezing)
- Confining pressure
- Size of ice pieces
- Void ratio (packing)
- Temperature
- Load or strain rate

2.4.1 Failure Mechanisms

When considering a volume of rubble subjected to shear, the resistance in the material spring from two processes (Ettema and Urroz-Aguirre, 1987). The mechanical friction and interlocking between blocks and from the freeze-bond formed between blocks. It is argued in several studies that failure of rubble happens in two modes (Liferov and Bonnemaire, 2005), each attributed to one of these resistance processes.

It is suggested that the primary mode is related to the initial failure of the rubble skeleton, governed by the strength of the ad freeze-bond between blocks, often

considered as a form of cohesion. The second mode is dominated by friction resistance and the dilatancy effects that is activated after substantial deformation of the rubble (Liferov and Bonnemaire, 2005). In the second mode rubble is undergoing continuous shear, and can be considered as a near cohesionless material (Ettema and Urroz-Aguirre, 1987).

Several authors have addressed the phenomenon of ad freeze-bonds in rubble ice, and earlier work is referred to by Repetto-Llamazares et al. (2011). The main findings in these studies were that key parameters for the freeze-bond strength were the confinement pressure, the contact (submersion) time and the initial temperature of the ice. They found the freeze bonds to act either ductile or brittle, with a mean strength of 2 kPa and 9 kPa respectively. This was for small-scale tests, with short submersion times (1 to 20 min). No authors have yet related the freeze-bond properties to the cohesive properties of rubble.

Helgøy (2011) and Astrup (2011) did the same types of test following the same set-up as Repetto-Llamazares et al. (2011), getting much higher values for the freeze-bond strength (46.6kPa $\pm$ 19.9). The most plausible explanation seemed to be differences in the ice properties, or surface structure, compared to the first study. It seemed that more saline, more porous or more small-grained ice blocks gave stronger ad freeze-bonds.

2.4.2 Ice Rubble as a Mohr-Coulomb Material

A Mohr-Coulomb material give a linear relationship between the shear strength and the normal confinement, uniquely described by the two parameters ϕ and c. For ice rubble the picture is not so simple.

Ettema and Urroz-Aguirre (1989) explain the meaning of the angle of internal friction, and the various ways it has been reported in previous studies. The angle of internal friction springs from the processes of contact friction and interlocking of adjacent particles. The processes are influenced by confinement, constrains, strength of the particles, porosity, size distribution and shape of the particles and presents of contaminants.

Ettema and Urroz-Aguirre (1989) introduce the notation of ϕ_p and ϕ_c corresponding to the angle of friction for the initial peak of the stress-strain curve (ϕ_p), and for the peak stress during continuous shear or constant volume of the rubble (ϕ_c). Which measure that should be applied, depend on the nature of the ice rubble process. If the rubble is densely packed and deformation is small, ϕ_p may be a good measure, whereas ϕ_c may be used in large strain deformation processes.

Different measures and definitions for the internal angle of friction has been developed and reported, but in their review of earlier studies Liferov and Bonnemaire (2005) suggest that the internal angle of friction is in the range of 30-45°. In earlier studies the angle of internal friction have been reported as high as 70°. Ettema and Urroz-Aguirre (1989) suggest that the unrealistic values for ice rubble (over

50°) spring from that many studies have neglected the presents of cohesion in the rubble.

The cohesion can be understood as the shear resistance when the normal stress is zero (Ettema and Urroz-Aguirre, 1989). The cohesion between ice blocks have been studied by several authors and it has been suggested that cohesion is proportional to the thickness of the blocks. Liferov and Bonnemaire (2005) report the cohesion to thickness ratio, c/t, from several laboratory studies within a large range (2-30 kPa/m). The studies of Weiss et al. (1981) suggest a relationship of $c/t = 16 \pm 8kPa/m$, and corrected for hydrostatic pressure (as suggested by Ettema and Urroz-Aguirre (1989)) a ratio of $c/t = 12 \pm 6kPa/m$ (Liferov and Bonnemaire, 2005).

2.5 The Shear Box Test

The most common way to investigate ice rubble behaviour in the laboratory has been to use shear boxes. Using shear boxes to investigate rubble, give information on rubble parameters and behaviour. It is important to point out that the rubble response in such studies is a result of both the material properties of the tested ice rubble, and the influence of the test set-up and imposed constrains. Therefore different set-ups have been developed, and several authors have investigated rubble using shear boxes of various kinds.

The earliest studies, Prodanovic (1979), Weiss et al. (1981), Hellmann (1984) and Fransson and Sandkvist (1985) tested rubble behaviour with a direct shear box. Later Ettema and Urroz-Aguirre (1987) used a simple shear test, Sayed (1987) developed a biaxial plain-strain apparatus and Wong et al. (1990), Sayed et al. (1992) and Timco and Cornet (1999) used triaxial cells. Many of these studies were aimed at finding values for cohesion and internal angle of friction, and values were reported within a large range. Earlier work on behaviour of rubble have been systematically reviewed by Liferov and Bonnemaire (2005) and Timco and Cornet (1999). In addition the articles by Ettema and Urroz-Aguirre (1989) and Ettema and Urroz-Aguirre (1991) offers a review of the reported parameters of the earliest studies.

2.5.1 Direct Shear Box

The first laboratory studies of rubble properties used a direct shear box. The studies were done with different apparatus of the same principle. The main idea was to create a shear deformation in a volume of rubble by allowing the rubble to fail along a specific shear plane. Two examples of direct shear boxes are shown in figure 5.

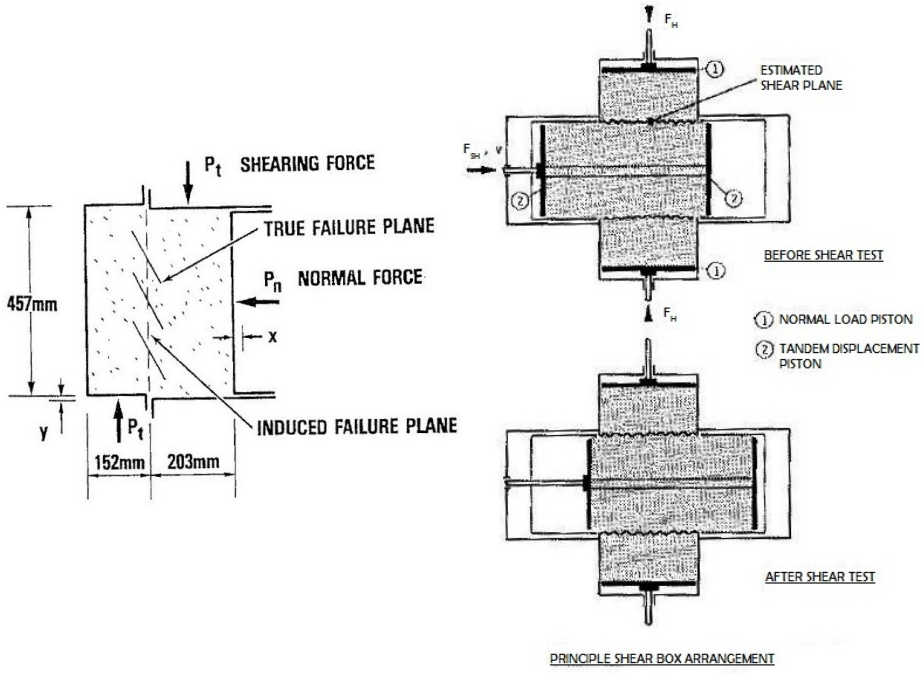

(a) (b)

Figure 5: The principle of the direct shear box used by (a) Prodanovic (1979) and (b) Hellmann (1984)

For such apparatus it is possible to vary and measure the applied shear force, the confining pressure and the strain rate. The advantages are that the set-up is simple and relatively cheap. The drawbacks are that the testing introduce a failure plane which is not the same as the true failure plane of rubble, as indicated in figure 5 (a). This means that the rubble sample is exposed to a non-uniform stress and strain distribution, and material is not in a pure shear state. Instead the stress and strain distributions heavily depend on the boundary conditions. Since the results depend on the test set-up, several authors have questioned results from these tests. Timco and Cornet (1999) conclude that only index values and not the quantitative results from such tests can be trusted.

Hellmann (1984) observed that the deformation of rubble seemed to go through three phases associated to different types of friction resistance. In the first phase the shear force increased due to the denser packing of blocks before shearing started. In the second face the normal force and the shear force increased until it peaked as a result of dilation of the ice blocks. In the third phase the shear force stabilized and the rubble deform continuously. Hellmann (1984) related cohesion to the two first phases only.

Hellmann (1984) reported the transition between phases in displacement. His study was executed with a direct shear box with two side chambers as shown in figure 5 (b). The first phase lasted for the first 2 mm of displacement, the second phase until a maximum was reached after 50-150 mm displacement, and the third and final phase lasted the rest of the test, 480 mm. To be able to compare this numbers with studies with different shear boxes, the relative displacement is a better measure. The relative displacement can be calculated as:

$$relative\ displacement = \frac{displacement\ [m]}{length\ of\ side\ chamber\ [m]} \cdot 100\ \% \tag{26}$$

The cross section of the square side chambers in Hellmann's study was 0.5 m^2. Using this in (eq:26) relative displacement of the first phase is 0.4 %, the second phase last until a maximum stress occurs after a relative displacement between 10 % and 30 %. The third phase last until the end of the test, that has a total relative displacement of 96 %.

More recently Serré et al. (2011) used a direct shear box to investigate the relation between freeze-bonds and rubble strength. The apparatus they used is described in section 3.1.1. The authors were able to identify the same three phase behaviour of rubble as Hellmann (1984), but linked the initial rubble failure to freeze-bond failure. They defined the faces a little different, with a 6 second first phase, a second phase described so that the peak load was included from 6 to 120 seconds and a third phase from 120 to 230 seconds. The deformation velocity was 2 mm/s and the length of the shear plane was 0.6 m. Using this and (eq:26), relative displacement of the first phase was 2 %, relative displacement in the end of the second phase was 40 %. The relative displacement of the whole test was 77 %. The reported first phase strength of tests with short sumbergion times (10 minutes), and 3 kPa confinement was ca. 10 kPa.

The limitations of the set-up is discussed by the authors, and later also by Ji (2011) who did a finite element modelling of the same shear box experiments. The main weakness of the set-up was that the RVE (Representative Volume Element) was to small to ensure continuum material behaviour. That means that the material behaviour may be strongly influenced by the behaviour of one block.

Some investigations have been made on the significance of the number of blocks filling a shear box volume. Shafrova (2007) did simulation of a shear box with a pseudo-discrete continuum model with a constant volume, but varying the size of blocks, and thereby the number of blocks. In short, she found a relation between maximum shear stress and the ratio of the shear box length to block thickness. The relation is plotted in figure 6.

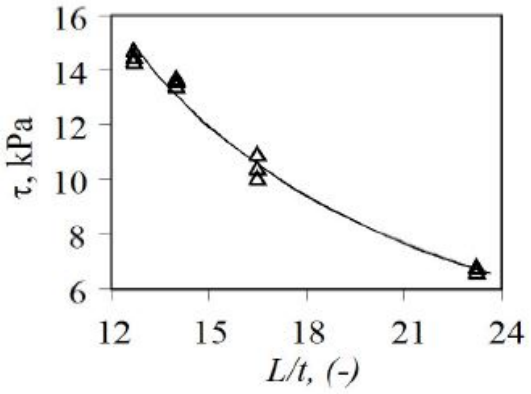

Figure 6: The measured shear stress versus the ratio between the shear box length to block thickness, in a rubble volume (Shafrova, 2007)

The relation implies that stress is over estimated when the number of blocks in a shear box is small.

2.5.2 Simple Shear Box

Ettema and Urroz-Aguirre (1987) executed simple shear tests on a horizontally floating layer of ice. The set-up can be seen in figure 7.

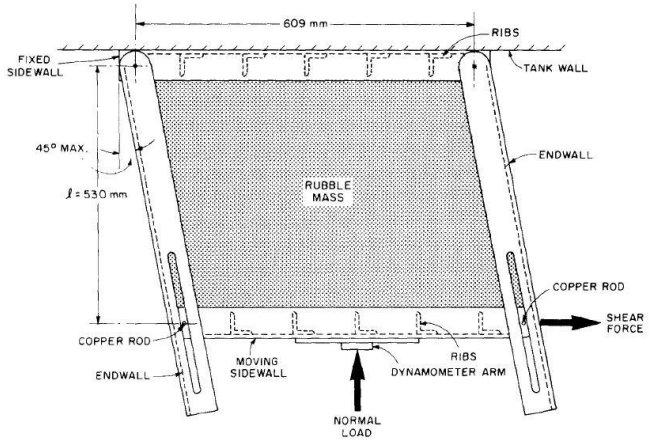

Figure 7: View from above of the the shear box used by Ettema and Urroz-Aguirre (1987)

The advantage of such a set-up was that the state of stress and strain was the same in the whole sample, and close to a state of pure shear. The drawbacks were that the set-up had no way of increasing the normal pressure (Timco and Cornet, 1999), and that the set-up was restricted to only floating rubble and low confinements.

2.5.3 Biaxial Plain Strain Apparatus

Timco et al. (1992) developed a more sophisticated shear box, that could be used in either plane-stress or plane-strain configuration. This set-up solved several of the flaws of the simpler shear boxes, such as well controlled boundary conditions and the possibility of testing rubble under a large range of deformation and stress states.

With this shear box Sayed et al. (1992) found that all deformation was irrecoverable (plastic), that it was a logarithmic dependence between shear stress and strain. They also suggested that the initial porosity of the rubble had no influence on the stress-strain relationship. They tried to describe the material behaviour of ice rubble as they would describe clay, but concluded that the material behaviour of rubble was complex and could not be simplified by a single parameter like the angle of friction.

2.5.4 Triaxial Cell

Several authors use results from a tri-axial cell filled with ice rubble, which is described by for example Gale et al. (1987) and is sketched in figure 8.

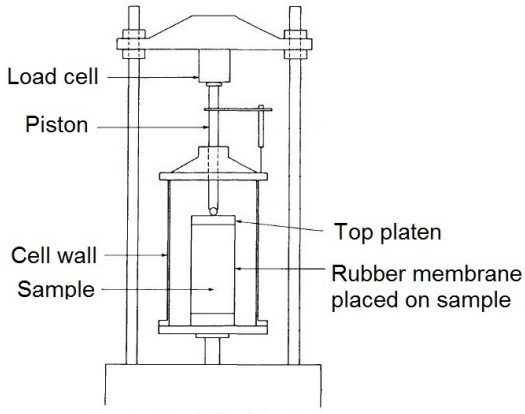

Figure 8: A sketch of the triaxial cell used by Wong et al. (1990) and Gale et al. (1987). The sample had a diameter of 65 mm, a height of 130-150 mm

The triaxial cell is not exactly a shear box, but tests rubble in the same way as the more box-shaped apparatus, and has the advantage of controlling the 3D state of stress.

Some of the results from this studies was that rubble in a loose state seemed to be dominated by a frictional behaviour, whereas for dense rubble the cohesion seamed to play a more important role (Wong et al., 1990).

2.6 Pile Testing

2.6.1 The Method

The purpose of investigating ice rubble properties is to obtain input values for load models and simulation tools. The load models can be validated by model scale testing. To get true validation of the models, the model ice rubble properties should also be tested. It is common to use punch tests, but the results from punch tests are hard to interpret due to the unknown boundary conditions. One could also use a shear box test, but it demands quite comprehensive equipment. Another alternative is the pile test.

The principle of the test is to collect rubble, and in some way let it pile up in a shape only governed by the material. To have a 2D simplification of the pile, it should be shaped as a elongated crest, see figure 9.

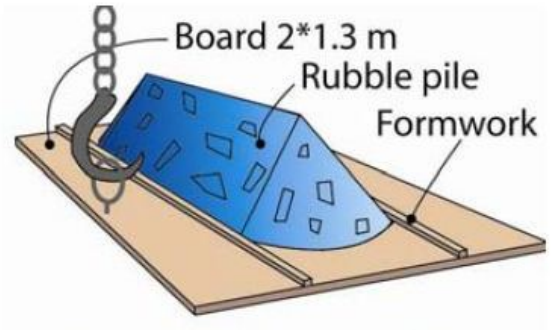

Figure 9: Sketch of a elongated pile (Serré et al., 2009)

Primarily one can measure the repose angle of the pile, that is the angle between the horizontal and the side of the pile, see figure 10. In a completely cohesionless material the repose angle would be equal to the internal angle of friction. For a material with cohesion the repose angle would be steeper than the angle of internal friction.

In ice rubble cohesion develops and strengthens over time. This means that even if it initially was not possible to stack the rubble with a steeper angle than the repose angle, it may be possible to tilt the pile afterwards without blocks falling off. Eventually if one continues to tilt the pile, a failure will occur. If this failure takes shape as a slide in the pile, one can also measure the critical angle and the failure angle, see figure 10. Such tests have been executed by for example Serré et al. (2009), and the purpose was to make visible how much cohesion had developed in a pile.

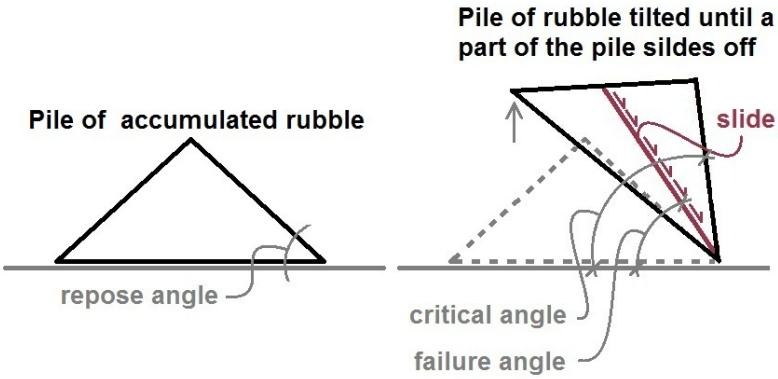

Figure 10: 2D sketch of the pile test with definitions of angles: repose angle, critical angle and failure angle

There are some important considerations that must be taken into account when interpreting results from the pile test. As mentioned the cohesion in ice rubble change with time, so how long time one use to test will affect the results. Also the pile test is dry, and will not behave as a rubble accumulation under water.

Another issue is the scaling of the experiment. The shear stress should scale with the Froude number, as $\frac{\sigma_f}{\sigma_m} = \lambda$. There are two different contributions to the shear stress, friction and cohesion. The problem is that we have no way of controlling the scaling the cohesion, whereas the friction will scale proportional to the size of the sample.

The problem can be illustrated by dimensional analysis:

$$\tau \;=\; \sigma_n tan(\phi) + c \;=\; \frac{\rho g V}{A} tan(\phi) + c \;=\; \rho g L tan(\phi) + c$$

Where ρ g and c are constants. This means that the contribution from friction will increase as the size of the sample (L) grow. In other words the cohesion will be more important in a small pile than in a big one, and values for ϕ and c obtained for a pile test are not material constants, but depend on the set-up.

2.6.2 Derivation of the c-ϕ-relation

Since failure happens as a slide, it is possible to analyse the rubble failure with principles of slope stability in soil mechanics. In geothecnics this is called $a\phi$-analysis, and is described by Emdal et al. (2006). Attraction a is another measure of cohesion. In figure 3 attraction is the normal stress where the yield function intercepts with the x-axis.

Here the principle of slope analyses is applied to a slide in a pyramid-shaped pile. For simplicity cohesion is kept as the measure, and this section show the derivation of a c-ϕ-relation for the pile test.

Assuming that the pile fail mainly in one slide, one can estimate the volume V_{slide} that slides off. This is possible since the initial geometry, the measured failure angle and the angle of the pile board at failure is known. By using trigonometry, the slide area A_{slide} can be found, and by multiplying it by a unit width (in the longitudinal direction of a pile) w the volume is obtained. See figure 11.

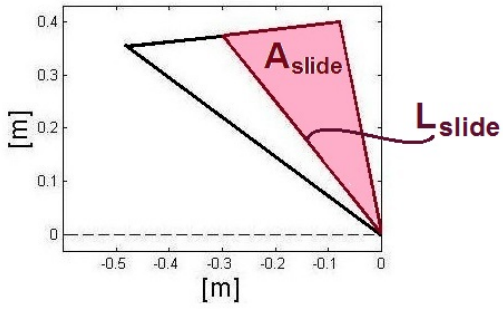

Figure 11: Area and length (baseline) of a slide used to derive the c-ϕ-relation

Assuming values for rubble density ρ_{rubble} and the gravity g, the gravity force $F_{gravity}$ of the slide can be found as:

$$F_{gravity} = A_{slide}\, w\, \rho_{rubble}\, g = V_{slide}\, \rho_{rubble}\, g \tag{27}$$

As seen in figure 12, gravity force can be decomposed to a normal and a shear force component, by using failure angle $\alpha_{failure}$.

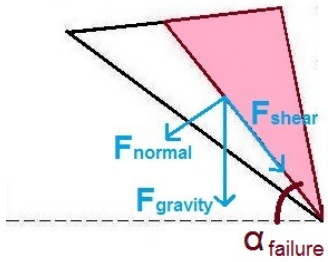

Figure 12: Derivation of force components for the c-ϕ-relation

$$F_{Normal} = F_{gravity} \cos \alpha_{failure} \tag{28}$$

$$F_{shear} = F_{gravity} \sin \alpha_{failure} \tag{29}$$

Stress is found by dividing the forces on the area of the slide, given by the length of the slide L_{slide} and the unith width w.

$$\sigma_n = \frac{F_{Normal}}{L_{slide}\, w} \tag{30}$$

$$\tau = \frac{F_{shear}}{L_{slide}\, w} \tag{31}$$

These results can be entered in the Mohr-Coulomb failure criteria (eq: 10) so that the equation only has two unknowns, c and ϕ. This is the c-ϕ-relation.

$$\tau = c + \sigma_n \tan \phi \Rightarrow c = \tau - \sigma_n \tan \phi \tag{32}$$

This relation may be plotted as shown in figure 13.

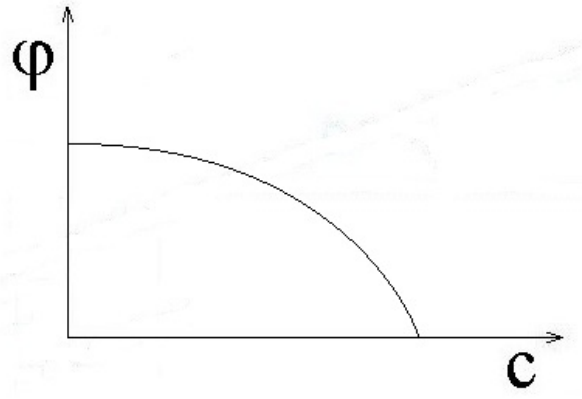

Figure 13: A plot of cohesion c versus internal angle of friction ϕ

Inserting (eq: 27-32) in (eq: 32) the full expression related to all pile parameters will be:

$$c = \frac{A_{slide}\ \rho_{rubble}\ g}{L_{slide}}(\sin\alpha_{failure} - \cos\alpha_{failure}\ \tan\phi) \tag{33}$$

3 Experiments

Two experiments are described: shear box testing at NTNI and pile testing at HSVA.

Shear box testing was conducted together with Henning Helgøy in the cold lab at the Department of Civil and Transport engineering at NTNU. Single freeze-bond tests were conducted simultaneously with the shear box testing, under the lead of Henning.

The pile testing were conducted at HSVA as a part of the RITAS-project, which was led by Nicolas Serré from Multiconsult Tromsø. For in-depth description of the project, I refer to his documentation and the daily reports, that can be made available if relevant.

3.1 Experiment NTNU: Shear Box

The set-up is based on earlier experiments with a shear box described by Serré et al. (2011). The shear box experiment was conducted in combination with strength testing of individual freeze-bonds, see Helgøy (2012).

Based on results from single freeze-bond testing, we had three main objectives with the shear box testing:

(a) Investigate water temperature sensitivity

(b) Investigate the significance of block orientation

(c) Investigate rubble behaviour in shear box in general

These objectives where studied by:

- Varying water conditions ("cold" and "warm")
- Varying block orientation (horizontal and vertical)
- Varying confining pressure (3.1 kPa, 18.4 kPa and 26.6 kPa)
- Running dry (unsubmerged) tests

Necessary for the testing were: a shear box apparatus, artificial created ice rubble, a submersion basin, a cold room for testing and a rig to apply and measure force and displacement.

3.1.1 The Apparatus

The apparatus is a direct shear box, built to simulate 2D conditions. It is built in plexiglass, and consists of a square box of 600 mm x 600 mm, with a depth of 40 mm. The square box is cut in two in the middle, and the parts are connected with a lubricated rail and wheels. The bottom of the box has holes which allows water to drain, and on top there is a detachable lid that enable you to apply confining pressure by adding weights. Figure 14 and 15 show the principle of the shear box, and figure 16 show a photo.

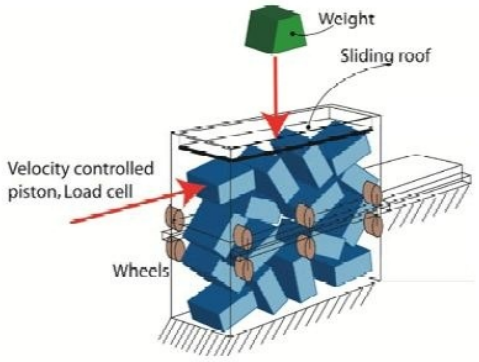

Figure 14: A 3D sketch of the shear box used by Serré et al. (2011)

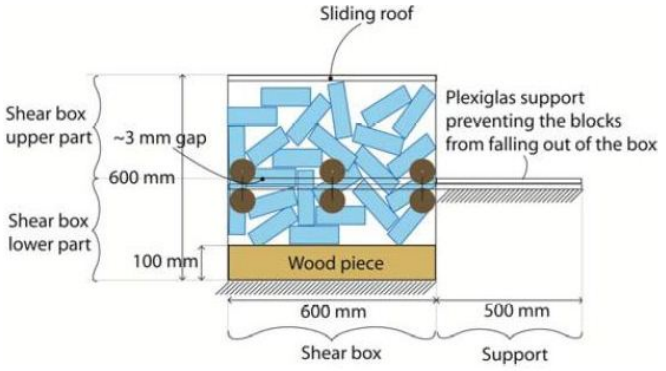

Figure 15: A 2D sketch of the shear box used by Serré et al. (2011)

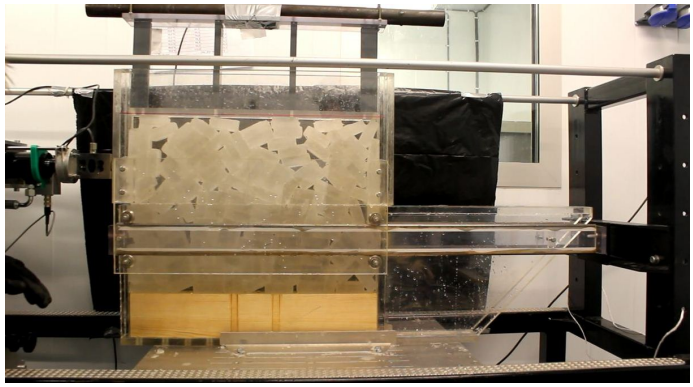

Figure 16: A photo of the shear box

The box was designed to contain one RVE of blocks. RVE is short for Representative Volume Element, and is the smallest volume that should ensure continuum behaviour of the material. It has been common to set the RVE to 10 times the size of the heterogeneities, as referred to by Serré et al. (2011).

The RVE was calculated based on a block size of 60 mm x 40 mm x 22 mm. The single block size was chosen to scale with a ratio of 1:20 from full scale observations in the Barents Sea (1.2 m x 0.8 m x 0.44 m). This meant that the RVE was set to 600 mm x 400 mm. Since the box originally was squared, the volume of the box was reduced by putting a 100 mm piece of wood in the bottom. The test volume was set to 600 mm x 400 mm. This assumption were adopted from Serré et al. (2011), even though it was proven that the RVE was too small to ensure continuous behaviour of the ice rubble. If the RVE were to be increased, a new apparatus would have to be built.

3.1.2 The Ice Rubble

Saline ice was created in the tank FRYSIS II (0.8 m x 1.2 m x 1.3 m) in the cold lab of the Department of Civil and Transport Engineering at NTNU . Room temperature was -7°C when the room was in use (for sawing), and when ice was removed from the tank. The rest of the time room temperature was -20°C. The water had a salinity of 8 ppt. From experience we know that water with a salinity of 8 ppt form ice with a salinity of 3 ppt when exposed to temperatures of -20°C. In three turns, each of around 7 days, a 11-17 cm thick layer of ice was formed. The three batches of ice were named ice type 1, 2 and 3.

The ice was removed from the tank, and stored in boxes or plastic bags in a room of -7°C for at least 24 hours. Then the ice was cut to pieces of 60 x 40 x 22 mm with a band saw. The ice blocks where cut out from the ice sheet oriented horizontally or vertically, see figure 17.

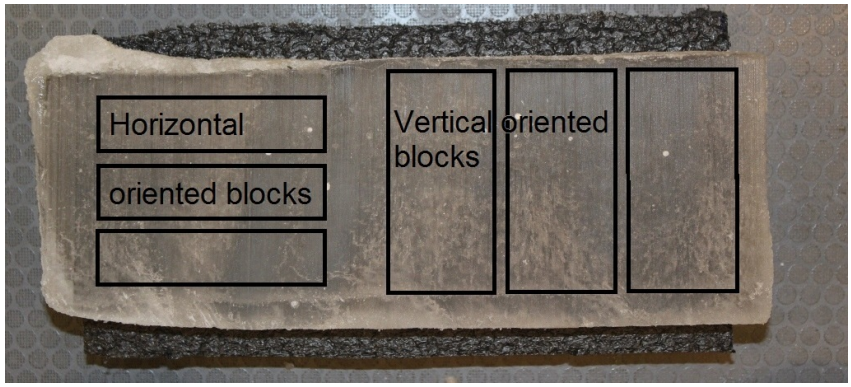

Figure 17: The two possible orientations of blocks in the cross section of an ice sheet

3.1.3 Testing Procedure

The shear box was filled manually with ice blocks to a height of ca. 400 mm. A lid with weights was added, and the whole box was submerged in saline water of 8 ppt. The water temperature in the submersion basin was monitored by two temperature sensors, and was close to the freezing point. Air temperature of the room was -1°C, for "warm" tests (all tests but three). For the three "cold" tests air temperature was -7°C.

After 10 minutes, the box was taken out of the water and given a couple of minutes to drain. Then it was placed in a rig where the bottom was restrained from moving. The room temperature while testing was -7°C for all tests. The rig had a velocity controlled hydraulic piston that pushed the upper part of the shear box, forcing the rubble to fail. The piston was attached to a load cell that recorded force and displacement. See illustration of the procedure in figure 18.

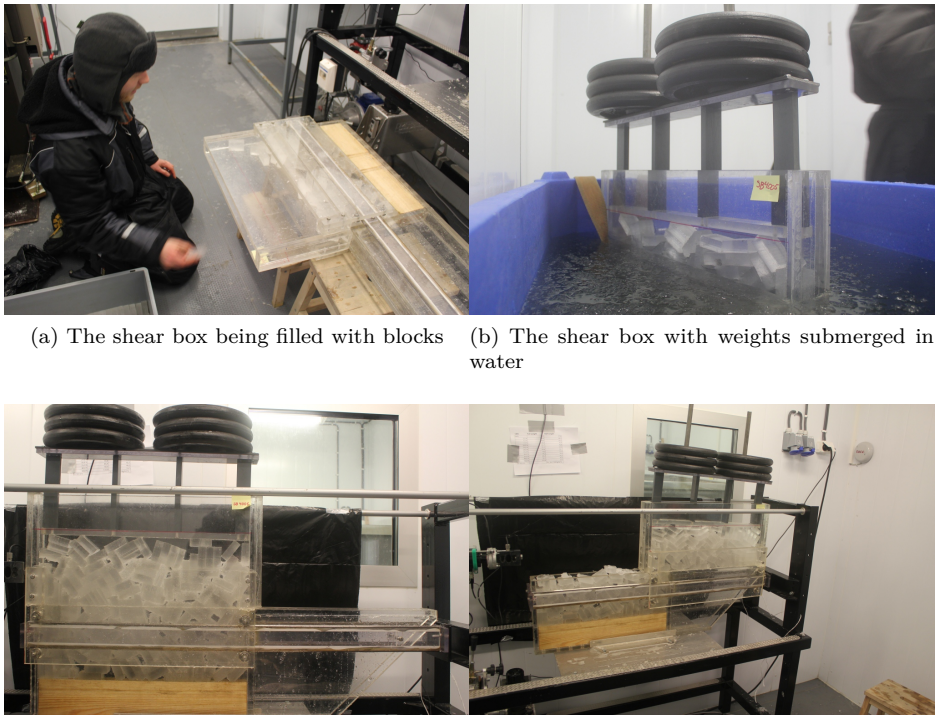

(a) The shear box being filled with blocks (b) The shear box with weights submerged in water

(c) Box placed in the rig before testing (d) After testing

Figure 18: The procedure of testing rubble with the shear box

The instantaneous velocity was displayed on the computer screen at all times, and the velocity could be regulated manually by a screw mechanism. The velocity during all tests was kept at 2 mm/s.

A confinement of 3.1 kPa (7.5 kg) was chosen for most tests, also higher confinements of 18.4 kPa (45 kg) and 26.6 kPa (65 kg) were tested. The lover confinement is within the range of pressures that may develop in a 10 m thick layer of rubble (Ettema and Schaefer, 1986). Higher confinements may be relevant in cases where ice ridges are scouring the seabed or interacting with structures. The confinement was the same during submersion and testing.

3.1.4 Single Freeze-bond Testing

The shear box testing was carried out together with testing of the shear strengths of freeze-bond between two ice blocks. The procedure is based on earlier work by Repetto-Llamazares et al. (2011). The main idea is to put together two ice blocks, add confinement and submerge them in saline water, so that a freeze-bond forms between the blocks. All tests were

Shear strength of the freeze-bond is tested by applying a force on the upper block, while retaining the lower block, recording force and displacement. Freeze-bond tests in this study is submerged in 10 minutes, have a confinement pressure of ca. 2 kPa and deformation velocity of 2 mm/s. In-depth description of the set-up and the result from this testing is given in the master thesis of Helgøy (2012). A simple 2D sketch of the testing procedure is given in figure 19.

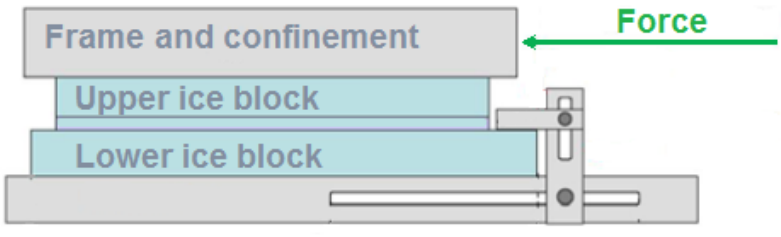

Figure 19: A sketch of how the freeze-bond shear strength was tested

3.1.5 Definitions

The rubble porosity η is calculated by the following formula:

$$\eta = 1 - \frac{N_b h_b L_b}{h_r L_{SB}} \tag{34}$$

where N_b is the number of blocks, h_b and L_b are the block thickness and length respectively, h_r is the rubble height and L_{SB} is the shear box length.

The nominal shear stress τ_0 is computed by the formula:

$$\tau_0 = \frac{F(t)}{A_0} = \frac{F(t)}{d_{SB} L_{SB}} \tag{35}$$

where $F(t)$ is the piston force at any time t, and d_{SB} is the depth of the shear box.

The time-adjusted shear stress τ_t takes into account that the shear area is reduced as the test proceeds. It can be computed by the formula:

$$\tau_t = \frac{F(t)}{A(t)} = \frac{F(t)}{d_{SB}(L_{SB} - vt)} \tag{36}$$

where v is the piston velocity.

Average shear stress τ_{ave}, use the average force over an average area.

$$\tau_{ave} = \frac{\overline{F}}{A(\bar{t})} = \frac{\overline{F}}{d_{SB}(L_{SB} - v\bar{t})} \tag{37}$$

Where $\overline{F}$ is the average force and $\bar{t}$ is the middle time in the considered time interval.

Displacement in the tests may be reported in second from interaction starts, millimeter of displacement or relative displacement by (eq:26).

Notation for the internal angle of friction ϕ, depend on in what deformation state the rubble is. It can be reported as ϕ_p, related to the first peak strength or as ϕ_c related to stress during continuous deformation. See section 2.4.2.

3.2 Experiment HSVA: Pile Test

Pile tests has earlier been conducted at HSVA earlier by Serré et al. (2009), and the set-up is based on this study.

The pile testing was conducted as a part of the RITAS-project. There were four objectives with the pile tests:

(a) To report model scale ice rubble properties for the RITAS-project

(b) To analyse results by principles of slope stability (c-ϕ-relation)

(c) To study the time-dependence of cohesion

(d) To evaluate the testing method

Two control parameters were varied in the testing:

- The type of rubble
- Consolidation time

3.2.1 The RITAS-Project

During the weeks 15-18 in spring 2012, the RITAS project was carried out at HSVA, Hamburg. The RITAS-project is short for Rubble Ice Transport on Arctic structures. The objectives of the project were to study ice transport around a model scale structure, ice accumulation with a buoyancy box and the model scale ice conditions in general. The facilities that were at disposal were the 78 m long, 10 m wide and 2.5 m deep ice basin, and the nearby workshop.

Five times an ice cover was created, and the model structure, the buoyancy box and the ice properties were tested. One or two pile tests were conducted each test day. Froude, Cauchy and flexural strength ratio scaling was applied with a length scaling factor λ of 1:20. The general test matrix is given in table 1.

Table 1: Test matrix for the RITAS project

date	*test number*	*ice condition*
23.04.12	1000	Base case (thickness 40 mm, density 870 kg/m^3)
25.04.12	2000	Base case
27.04.12	3000	Low density ice (800 kg/m^3)
30.04.12	4000	Thick ice sheet (60 mm)
03.05.12	5000	Base case

For a closer description of the RITAS-project and the test matrix, see the documentation of the RITAS-project.

3.2.2 Set-up for Pile Testing

Necessary for testing were: the pile board, a crane with constant velocity, a box to collect rubble from the tank, and a place by the tank to conduct tests.

The pile tests were executed in the far end of the tank at the time when the ice cover was broken into rubble for structure interaction tests. Ice rubble was collected from the ice tank using a crane and a flat rectangular box that was perforated, and could be submerged and lifted as soon as rubble had floated into it. See figure 20.

(a) (b) (c)

Figure 20: How the rubble was gathered from the tank at HSVA

The rubble drained for about one minute, and was poured out on the testing board. The pile board was a 2.0 x 1.3 meter plate with two pieces of wood (framework) whose position could be regulated. See figure 21. Distance of frame pieces was set to 0.6 m for all tests but one.

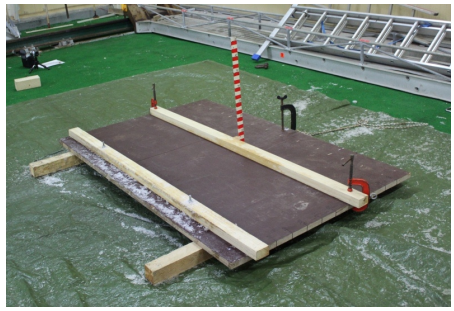

Figure 21: Picture of the pile board geometry

Rubble was collected two or three times until an elongated pile was created between the two frame pieces. Figure 22 shows an example of a pile created in this way.

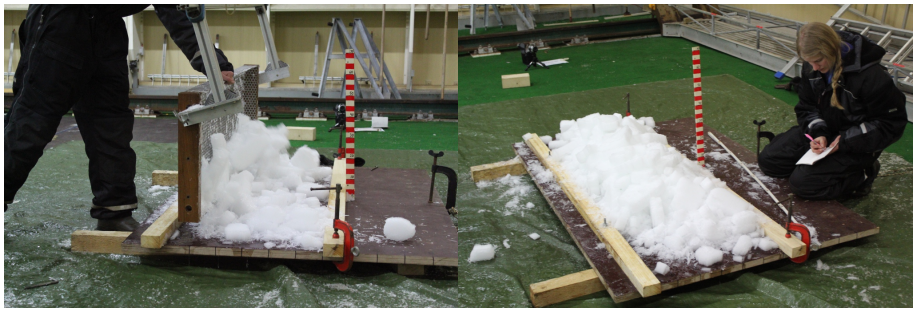

(a) Making the pile (b) Finished pile

Figure 22: How pile test 3060 was made

The initial geometry (length and heights) of the pile was then measured. From this the repose angle (see figure 10) could be estimated. Then the crane was attached to one side of the plate in order to tilt the board to one side. The crane moved upwards with a constant velocity of 7 mm/s.

Some tests were tested immideately after they were made, while some were left to consolidate for 30 minutes.

The board was tilted until some blocks fell off, or a slide happened in the pile. When this happened, the test was stopped and two angles were measured: The angle of the plate and the angle of the slope where the slide had happened. This was necessary in order to decide the critical angle and the failure angle (see figure 10). How the board was tilted can be seen in figure 23.

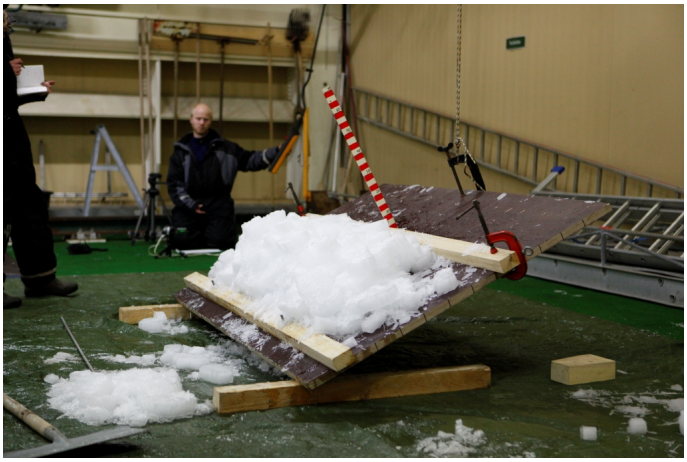

Figure 23: Tilting of pile test 2060

All experiments were filmed, photographed, and described during the testing. The rubble density was estimated two times using a bucket with a known volume and a scale.

4 Results

Results from the testing are reported separately for the shear box and the pile testing. The shear box testing also includes results from single freeze-bond testing. Fellow master student Henning Helgøy had the main responsibility of reporting results from these tests, and for further description then given here, I refer to Helgøy (2012).

4.1 Results NTNU: Shear Box

All together 22 shear box tests were conducted. Tests carried out at the same day where given the same series number, except for tests in series SB1000 which was carried out over two days. Table 2 shows the variation of control parameters for each test.

Table 2: Overview of tests and control parameters. *Ice type* is the ice batch number, *Block orientation* describe how ice was cut from an ice sheet (see figure 17), *Water temp.* is the temperature in the submersion basin, *Porosity* is rubble porosity calculated by (eq:34), *Confinement* is the normal stress of the weights put on top of the box and *Average velocity* is the average applied speed of the piston during testing.

Test name	*Ice type*	*Block orientation*	*Water (and air*) temp. [°C]*	*Porosity*	*Confinement [kPa]*	*Average velocity [mm/s²]*
SB1000	1	vertical	-0.43	0.24	3.1	2.06
SB1001	1	vertical	-0.43	0.20	3.1	1.81
SB1002	1	vertical	-0.53 (-7.0)	0.23	3.1	1.95
SB1003	1	vertical	-0.53 (-7.0)	0.21	3.1	1.84
SB1004	1	vertical	-0.53 (-7.0)	0.24	3.1	1.96
SB2000	2	horizontal	-0.50	0.19	3.1	1.90
SB2001	2	vertical	-0.50	0.20	3.1	2.02
SB2002	2	horizontal	-0.50	0.19	3.1	1.83
SB2003	2	vertical	-0.50	0.23	3.1	2.08
SB3000	2	vertical	-0.44	0.23	3.1	1.97
SB3001	2	horizontal	-0.44	0.23	3.1	2.02
SB3002	2	vertical	-0.44	0.25	3.1	1.93
SB3003	2	horizontal	-0.44	0.26	3.1	1.90
SB4000	3	horizontal	-0.51	0.22	3.1	2.01
SB4001	3	horizontal	-0.51	0.24	3.1	1.99
SB4002	3	horizontal	-0.51	0.21	26.6	1.80
SB4003	3	horizontal	(dry)	0.22	3.1	2.04
SB4004	3	horizontal	(dry)	0.20	26.6	1.98
SB4005	3	horizontal	-0.51	0.25	26.6	1.89
SB4006	3	horizontal	-0.51	0.25	26.6	1.98
SB4007	3	horizontal	-0.51	0.23	18.4	1.99
SB4008	3	horizontal	-0.51	0.27	18.4	2.01

* The submerging basin was placed in a room with air temperature -1°C in all tests but three tests of the series SB1000

4.1.1 Ice Properties

Ice for the experiments was grown in FRYSISII three times. Ice of type 1 was classified as S2 ice, ice of type 2 and 3 had a columnar structure, but since the crystal size was large it was difficult to confirm that also this were S2 ice. From a plain visual inspection it was obvious that ice of type 1 had more evenly distributed brine and gas inclusions then ice of type 2 and 3. As can be seen in figure 24 the brine channels where not evenly distributed in ice of type 2, and some parts of the ice sheet was completely transparent. This was also the case for ice of type 3, but

not for ice of type 1 where the ice looked more uniform and opaque.

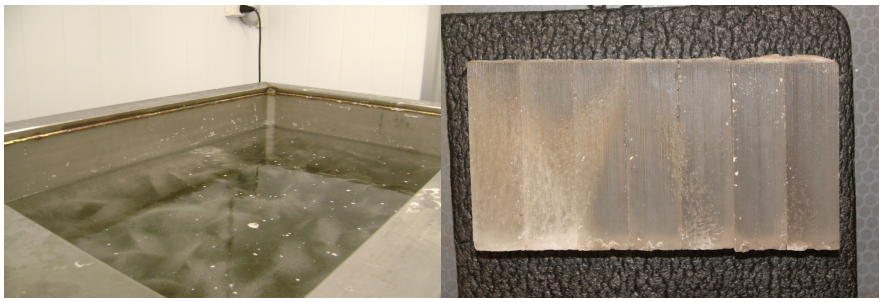

(a) Ice of type 2 in FRYSISII (b) A piece of ice of type 2 cut in blocks

Figure 24: Uneven distributed brine channels in ice of type 2

Ice properties varied notably between the three types. Table 3 show the key parameters for each type.

Table 3: The characteristics of the ice that was used at NTNU

Ice type	*Days of growth*	*Thickness [mm]*	*Salinity [ppt]*	*Crystal diameter [mm]*	*Density g/cm^3*
1	12	160	2.27	5	0.853
2	7	140	1.52	20	0.889
3	8	110	1.37	35	0.889

The intended salinity of the ice was 3 ppt, but the produced ice was less saline. The measure of the crystal diameter is a generalization based on the thin sections that we made of each type of ice, presented in figure 25. More thin sections are given in appendix C.

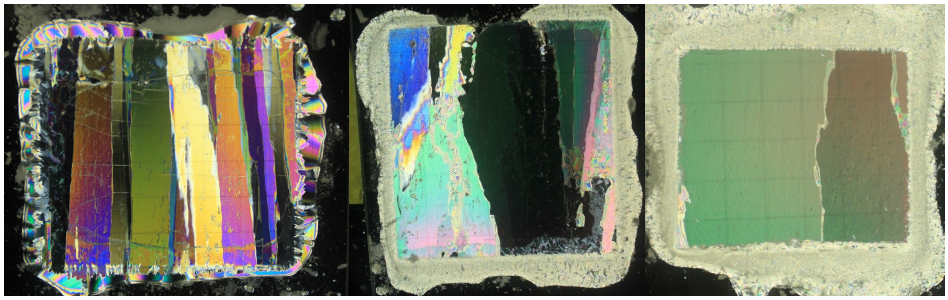

(a) Ice type 1 (3x3.5 cm) (b) Ice type 2 (3.5x3.5 cm) (c) Ice type 3 (2.5x3 cm)

Figure 25: Photos of thin sections of the three ice types, height x width given in brackets

4.1.2 Control Parameters

In the set-up specific values were chosen for the control parameters. When testing, it became evident that the measured values deviated from the intended values. This concerns the ice block temperature and salinity, the submersion basin temperature and salinity and the piston velocity. In addition the mechanical system itself displayed some friction that added to the measured friction in tests.

The room temperature was set to -7°C, which was also the intended temperature of the ice blocks. When measured the temperature of the ice blocks were in average -6.1 ± 0.4 °C.

Salinity of the blocks in the shear box was measured two times after each shear box test. The intended value was close to 3 ppt, but as shown in table 3 the produced ice was less saline. The salinity of blocks after testing is given for each series in table 4.

Table 4: Salinity of blocks after testing at NTNU

Test series	*Type of ice*	*salinity*
SB1000	1 (vertical)	2.4 ± 0.3 ppt
SB2000/SB3000	2 (vertical)	1.9 ± 0.5 ppt
SB2000/SB3000	2 (horizontal)	1.9 ± 0.5 ppt
SB4000	3 (horizontal)	1.0 ± 0.3 ppt

The temperature of the submersion basin was monitored by two temperature sensors. The recorded temperature from series SB2000 and SB3000 can be seen in the figure 26.

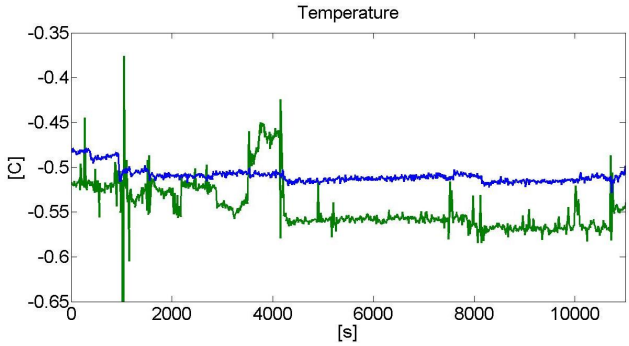

(a) series SB2000

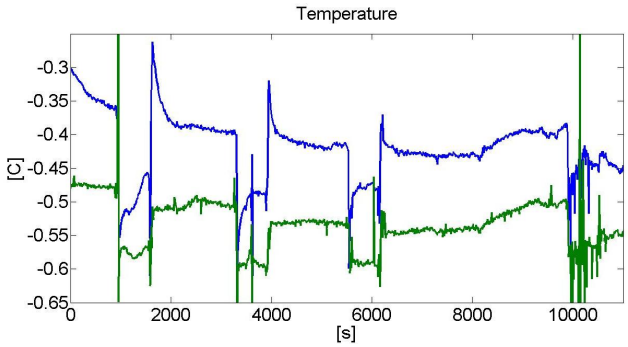

(b) series SB3000

Figure 26: Two plots of the temperature measured by the two sensors in the basin

As can be seen in the figure the thermometers deviated in their measurements, and for test series SB4000 one sensor failed. We chose to use only the measurement from the sensor that functioned trough all tests. In figure 26 this sensor represent the blue, upper line. In figure 26 (b) one can see that the temperature in the basin dropped every time a shear box was submerged. This was only observed for this test series.

The reported water temperature may not describe the true situation in the basin. When the submersion basin was placed in a cold room (-7°C) there was quite some slush present in the water, but the difference in temperature to a basin placed in a warm (-1°C) room was small. Therefore air temperature in the room is also reported in table 2.

The salinity of the submersion basin, was initially 8.1 ppt, but gradually increased to a value of 8.5 ppt on the last testing day.

The load vs. displacement relation was recorded for each test. However, the displacement signal was exposed to significant amounts of noise. To avoid unphysical fluctuations in the force vs. displacement relation, it was more convenient to plot

the force versus time. The time measure was an independent measure, directly related to the displacement when the velocity was constant. To validate this way of presenting results, the true velocity in each test was checked. The average recorded velocity for all 22 tests were 1.95 ± 0.08 mm/s, with an average variation of ± 0.31 mm/s within each test.

Also, using the force-time relation is only a good approximation if the piston velocity was truly constant at the time of interaction with the box. For all tests the velocity vs. time and the force vs. time were plotted, to see if a constant velocity was reached at the time of interaction. Such a plot can be seen in figure 27

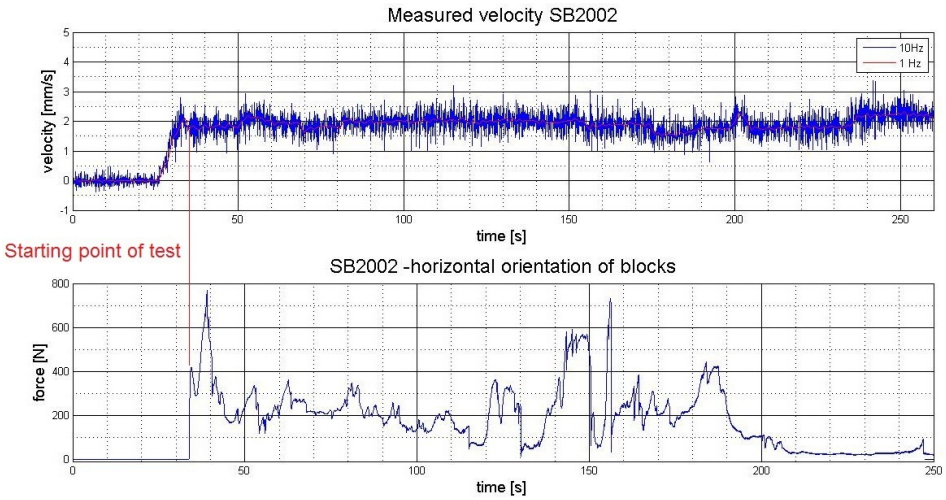

Figure 27: Plot made to check if the velocity was constant at the time of interaction, both a 10 Hz average and a 1 Hz average of the displacement signal was plotted

Out of 22 tests only test SB2001 did not have an average velocity close to 2 mm/s as the displacement of the box started. For this test the velocity was closer to 1.25 mm/s, slowly increasing to 2mm/s over the first 15 seconds.

The friction of the system (an empty box) was measured for all confinements (3.1 kPa, 18.4 kPa and 26.6 kPa), and an average value (9.7 N, 14.8 N and 17.8 N) was subtracted from all results.

4.1.3 General Behaviour

All tests started with a sudden increase in the force that dropped or flattened out after only a few millimetres of displacement. This is identified and referred to as the first phase. It was not possible to detect visually that this was happening, but after

an additional small displacement cracks between the ice blocks were appearing. See figure 28.

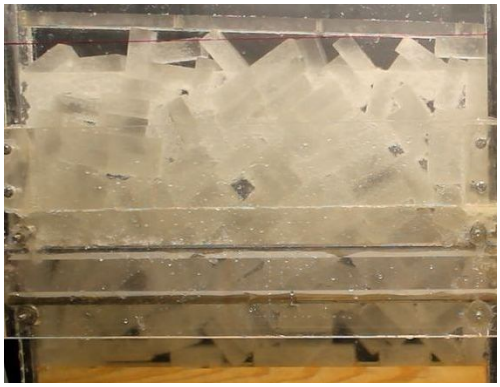

(a) Picture taken before testing

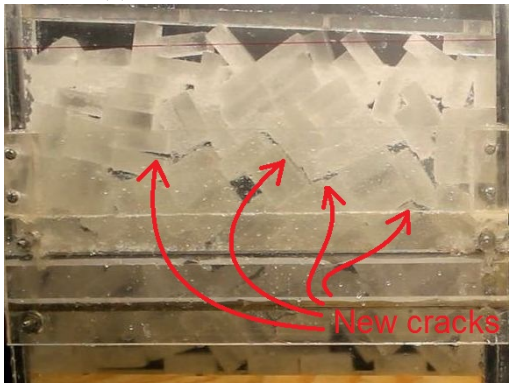

(b) Picture taken 7 seconds out in the test

Figure 28: Pictures of a crack appearing in test SB2003

The first phase only lasted for the first second, or occasionally little longer (up to 5 seconds), and was followed by a second phase where rearrangement of the rubble could be observed.

If one study picture 28 carefully, one can see that the rubble volume has expanded upwards. This dilation of the rubble blocks started immediately as the deformation of the box started. It was hard to determinate visually if the volume expansion where only attributed to the second phase, or if it started as early as in the first phase.

Volume expansion was greater for low confinement tests than for high confinement tests. After extensive displacement the rubble often rearranged itself as shown in figure 29.

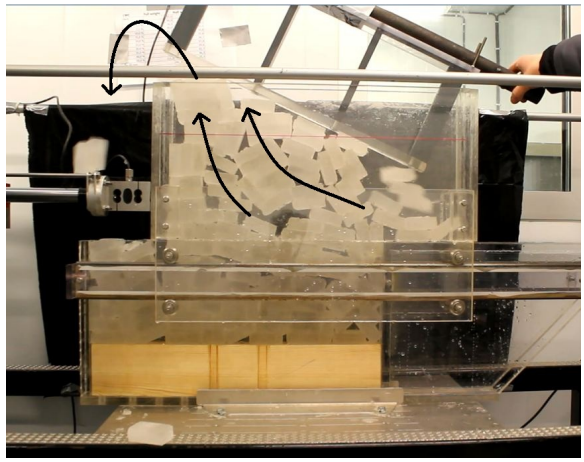

Figure 29: Dilation and expulsion of blocks in test SB1001 (84 seconds out in the test). Arrows indicate the movement of rubble

It was typical that the rubble gathered at the left side of the box, and that the lid tilted, as seen in figure 29. For the high confinement tests the rubble did not move as much, and often the volume was cut in two exactly at the shear plane. Occasionally the rubble moved downwards, and one could see the whole of the rubble volume involved in the deformation. This was not the case in the low confinement tests, where rubble motion happened mostly in the upper part of the box.

In at least 50% of the tests (11 tests), the blocks formed an arch lifting the rubble upwards during the second phase. See figure 30.

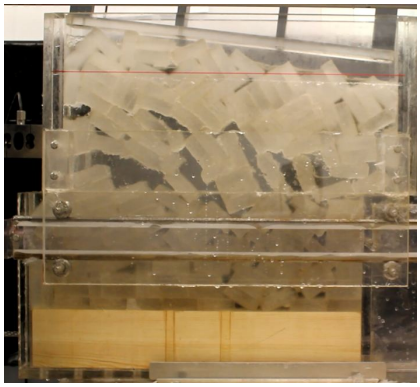

(a) Low confinement test (3.1 kPa) after 36 seconds

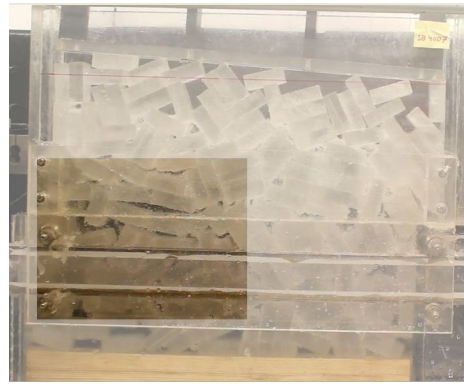

(b) High confinement test (18.4 kPa) after 17 seconds

Figure 30: Arching of blocks in test SB1000 and SB4007

This especially concerned the tests of series SB1000, the vertical oriented tests of SB2000/3000 and the dry test with low confinement. For the higher confinements this tendency could also be observed, but less obvious as the arch collapsed much sooner.

Common for all tests was that the rubble blocks moved together in lumps, or block assemblies, that stayed together for the whole test. An example can be seen in figure 31, and some thin sections are given in appendix C.4.

Figure 31: Block assembly from test SB1004

The size and number of block assemblies are evaluated for each test after 70 seconds of displacement. The block assemblies seemed to be few but large in the SB1000 series, and smaller and more numerous for test series SB2000, SB3000 and SB4000. Commonly the block assemblies consisted of 3-4 blocks. The largest block assemblies consisted of up to 20 blocks, but mostly of no more than 7 blocks. Figure 32 show a typical distribution of blocks with some block assemblies in test after 70 seconds.

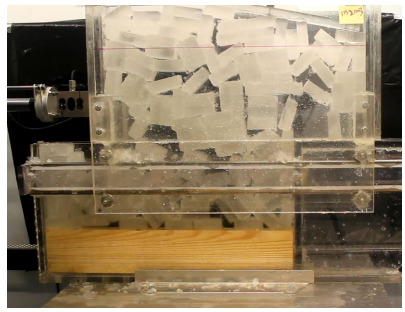

Figure 32: Test SB2003 after 70 seconds of displacement

Some force-time diagrams are represented in figure 33, and all plots are given in appendix B.

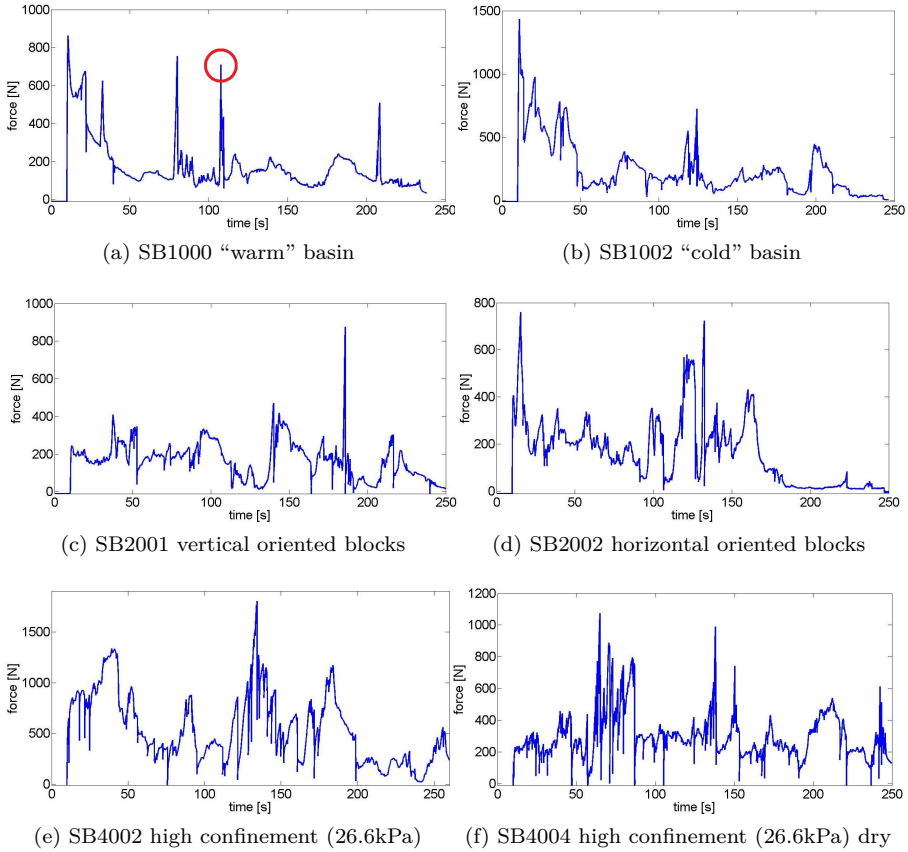

(a) SB1000 “warm” basin

(b) SB1002 “cold” basin

(c) SB2001 vertical oriented blocks

(d) SB2002 horizontal oriented blocks

(e) SB4002 high confinement (26.6kPa)

(f) SB4004 high confinement (26.6kPa) dry

Figure 33: Some force-time diagrams

The marked peak in figure 33 a) arise from a block being locked and broken at the shear plane. Figure 34 show the block seconds before, and after it breaks.

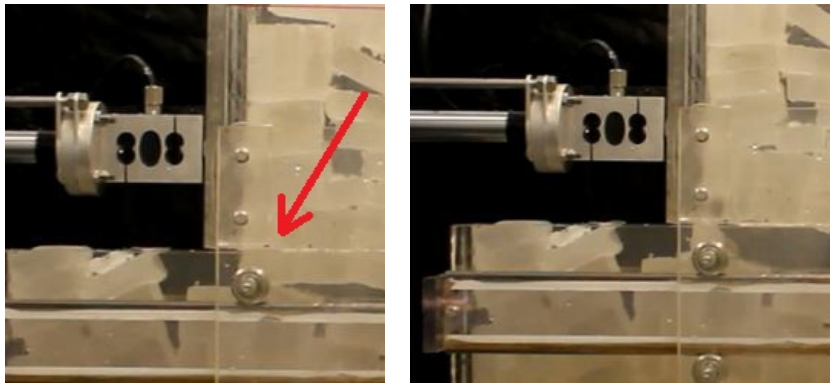

(a) before (b) after

Figure 34: Block breaking at the shear plane in test SB1000

In all tests some blocks broke or were crushed, except for the dry test with low (3.1 kPa) confinement. For the submerged tests with a low confinement we observed that in average 3.3 blocks broke, and in all tests but two, it was obseved broken pieces at the shear box interphase after testing. In the higher confinement tests (18.4 kPa and 26.6 kPa) the number of broken blocks exceeded 10, and the exact number was hard to count. The dry test with high confinement (26.6 kPa) showed no less breaking of blocks than the submerged tests.

In the plots the breaking of a single block result in a sharp single peak, while the crushing of one or several blocks, due to jamming of blocks at the shear interphase, mostly resulted in a more rounded peak.

In an attempt to measure ice strength, two blocks of ice type 1 were crushed in compression. The ice block was placed in the freeze-bond frame, which constrains it on the sides. The principle is shown in figure 35

Figure 35: How a block was crushed in the freeze-bond frame

The two blocks showed a compression strength of 1.0 and 1.2 MPa, but is was questionable whether this testing method generated a pure crushing failure mode, and no further testing with this method was conducted.

Further the shear box deformation is simply described by two phases, where the second phase includes all deformation from the first phase has ended, to the end of the test.

4.1.4 The First Phase

For almost all tests an almost linear phase and a first peak, were distinguishable. This peak (or end of linear behaviour) occurred within the first second for most test, as reported in figure 36.

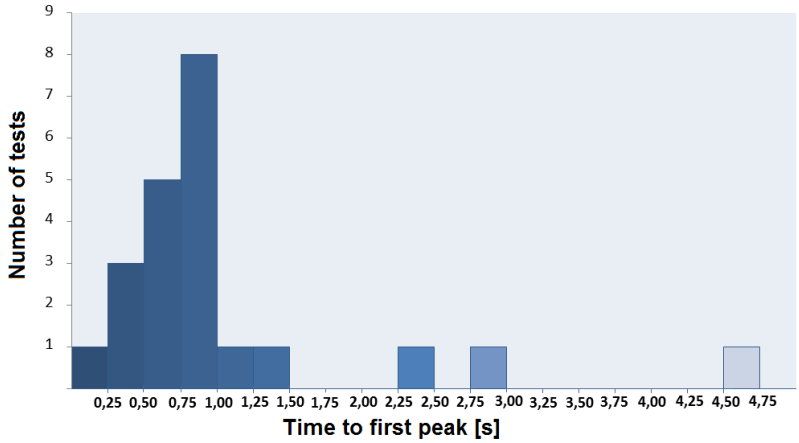

Figure 36: Occurrence of first peak

Series SB1000 had in general the strongest and most distinguished peaks and series SB4000 the weakest and less obvious. For one high confinement test (SB4002) the first peak seamed to be related to a block that broke. The first 6 seconds in each test series is plotted in figure 37, 38, 39 and 40.

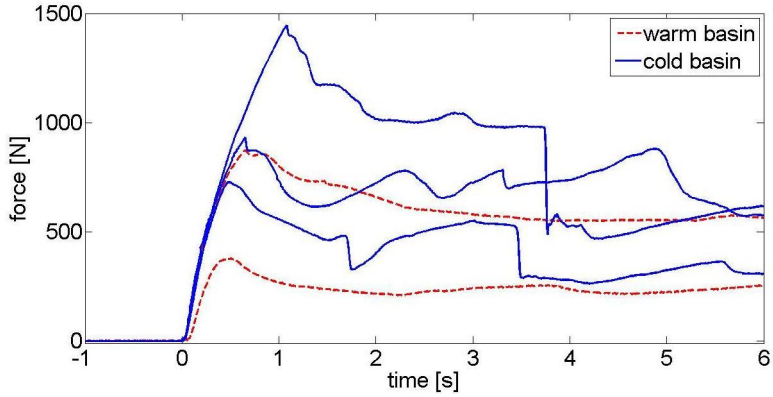

Figure 37: The first 6 seconds of tests in series SB1000

It was noted that shear boxes in cold tests seemed to contain more slush than in

the warm tests.

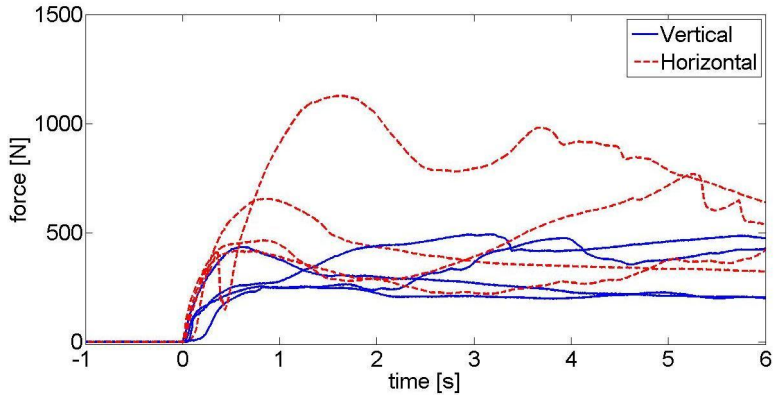

Figure 38: The first 6 seconds of tests in series SB2000 and SB3000

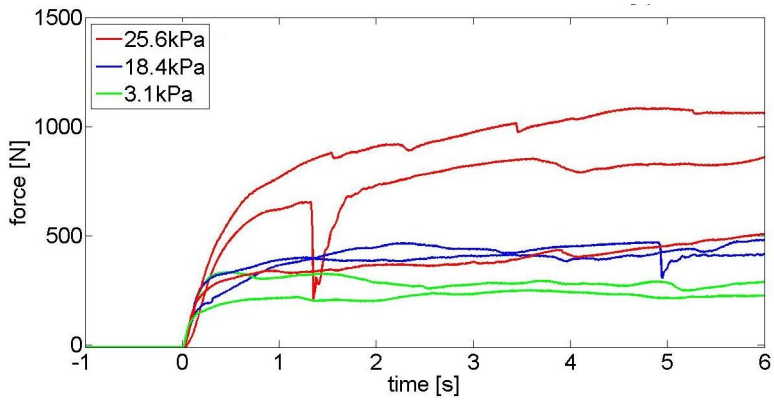

Figure 39: The first 6 seconds of tests in series SB4000

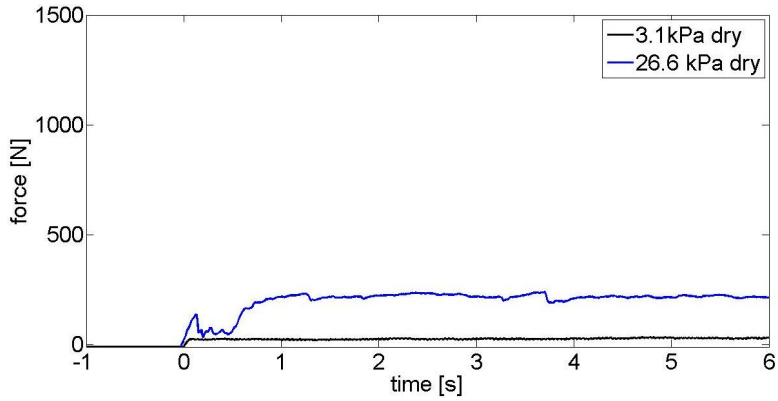

Figure 40: The first 6 seconds of the unsubmerged (dry) tests in series SB4000

The shear modulus G was calculated for each test as $G = \Delta\tau/\Delta\gamma$. For the calculation the first linear part of the force-time-relation was chosen (for a shear strains up to $\gamma = 0.0012 - 0.0024$). For the initial deformation of the box, the force-displacement relation was near linear, and the displacements were small, so the engineering strain was used. Figure 41 (a) illustrate the linear part chosen for calculations, and 41 (b) illustrate how shear strain was calculated. $\Delta\tau$ was calculated as the difference in nominal shear stress (by (eq:35)).

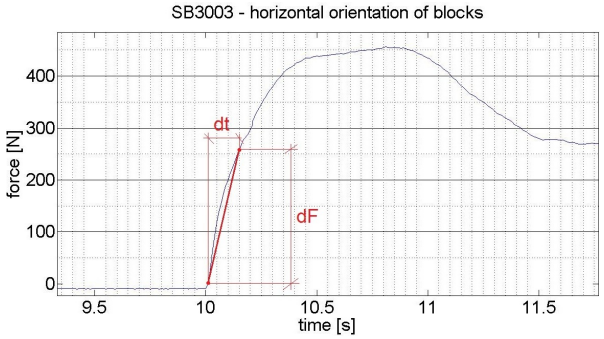

(a) Force-time plot where values was chosen

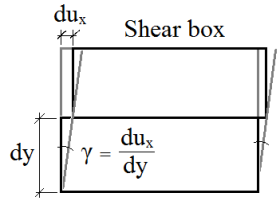

(b) How the shear strain was calculated

Figure 41: How values for calculating the G-modulus were chosen

The average values for first peak shear strength and the shear modulus distributed on test series are given in table 5.

Table 5: Key values for the first phase in shear box tests

Test series	*Test configuration*	*Number of tests*	*Peak shear stress [kPa]*	*Shear modulus [MPa]*
SB1000	"warm basin"	2	25.6	8.4
(ice type 1)	"cold basin"	3	42.7	9.2
SB2000/3000	vertical oriented ice	4	12.3	4.5
(ice type 2)	horizontal oriented ice	4	25.1	7.8
SB4000	3.1 kPa	2	11.4	5.4
(ice type 3)	3.1 kPa (dry)	1	1.0	2.3 *
	18.4 kPa	2	15.9	5.9
	26.6 kPa	3	24.1	5.5
	26.6 kPa (dry)	1	9.1	3.9 *

* Not very distinguished first phase

The values for the first peak shear stress can also be sorted by type in a diagram, as in figure 42. Here, results from all low confinement (3.1 Pa) tests are plotted sorted on test configuration and test series.

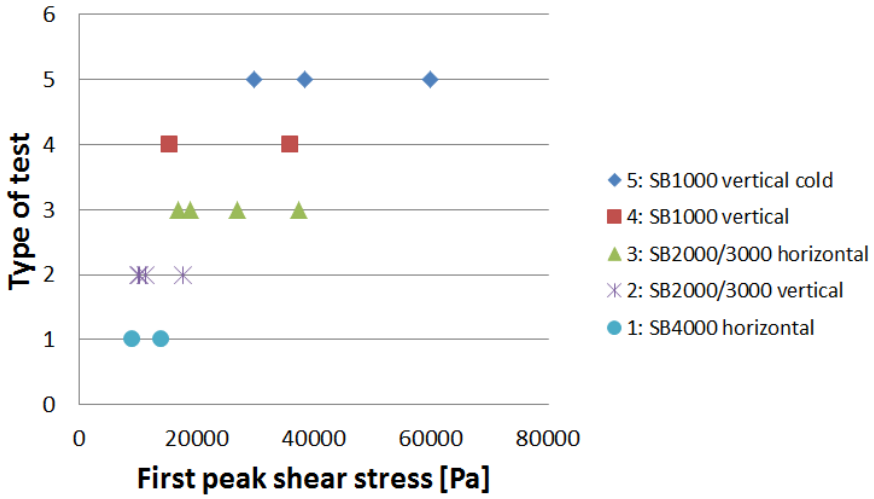

Figure 42: The distribution of first peak shear stress on test type

Figure 43 show the first peak shear stress by (eq:35) plotted versus normal confining pressure, for series SB4000.

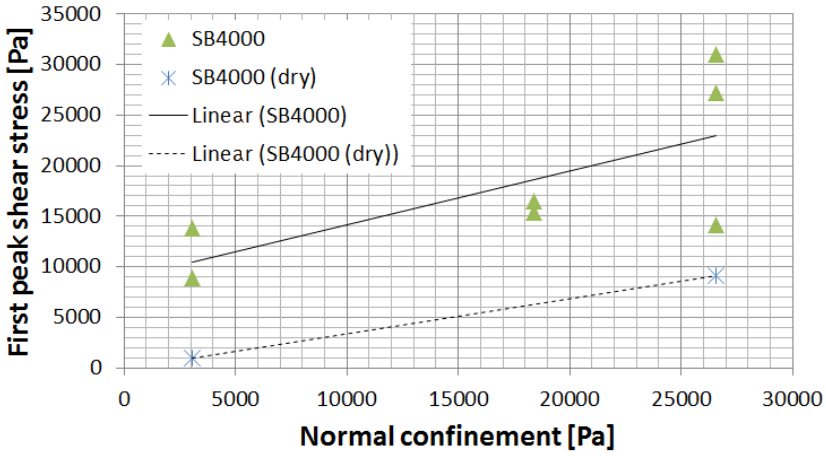

Figure 43: The first peak shear stress plotted versus normal confinement for SB4000

Using linear regression, the constants for the Mohr-Coulomb failure criteria for the first peak can be decided. For the submerged tests cohesion c=8830.6 Pa, and internal angle of friction ϕ_p=28.0°. For the unsubmerged tests cohesion c=41.3 Pa, and internal angle of friction ϕ_p=19.0°.

4.1.5 The Second Phase

The second phase is simply a name for all deformation after the first phase. There are some trends that can be detected in the force-time plots. All low confinement tests are plotted together in figure 44.

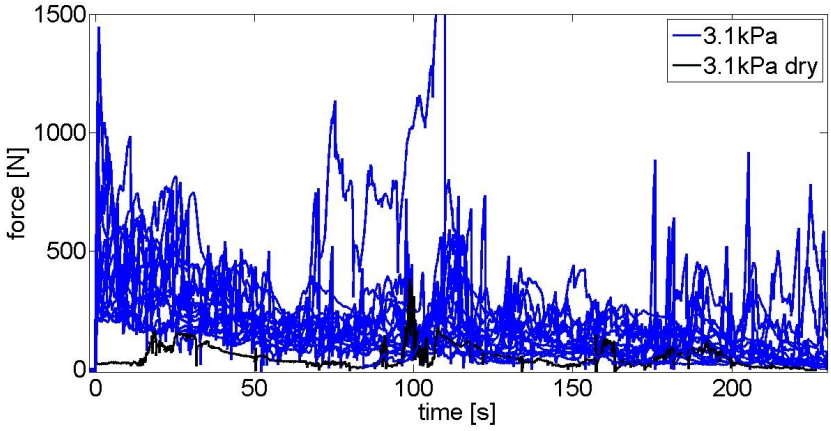

Figure 44: Force-time plot with all 3.1 kPa tests

From the force-time plots, a typical development of resistance in a shear box test were described. From an initial peak, the force level was typically slowly reduced and stabilised within the first 50 seconds (100 mm or 16.7 % deformation). Then a period with an average force level interrupted by random peaks followed. Towards the end of the test, after 175 seconds (350 mm or 58.3 % deformation), there was an increase in the density of random peaks (more blocks breaking). Often the peak force in a test was one of the late random peaks. Test SB2001 which is plotted in figure 33 (c) is an example of this.

Average Shear Stress

The middle value of shear force vas found between 50 and 175 seconds of displacement for test series SB4000. The shear stress was calculated as the average shear stress by (eq:37) for a middle time of 112.5 seconds. How the average value was found for a test is indicated in figure 45, and the plot of averaged shear stress versus normal confinement for series SB4000 is shown in figure 46.

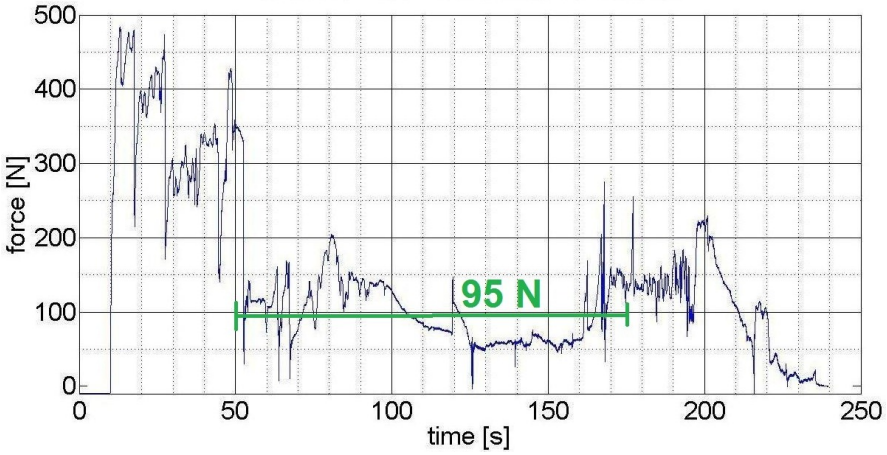

Figure 45: How an average force in a test was found for an interval from 50-175 seconds

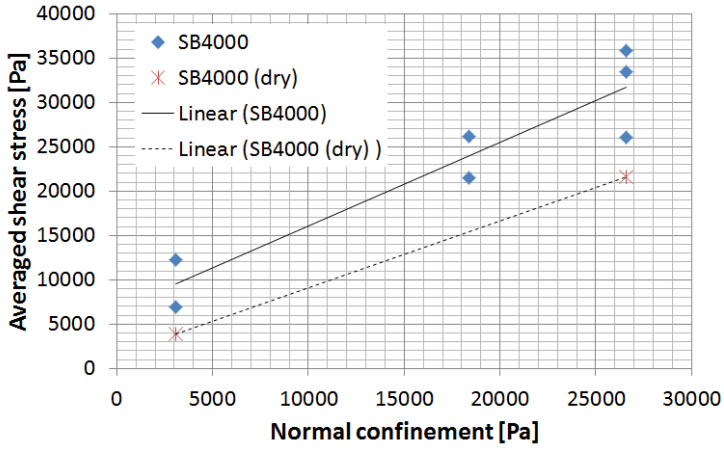

Figure 46: Normal confinement versus average shear stress for series SB4000

Using linear regression, the constants for the Mohr-Coulomb failure criteria can be decided for the average shear stress plotted versus normal confinement. For the submerged tests cohesion was c=6647 Pa and internal angle of friction ϕ_c=43.3°. For the unsubmerged tests cohesion was c=1510 Pa and internal angle of friction ϕ_c=37.2°.

Maximum Shear Stress

The overall greatest shear force and the time it occurred were identified for all tests. The maximum load occurred early (within the first 7 seconds) in the testing for series SB1000, and in the testing with horizontal oriented blocks for series SB2000 and SB3000. The maximum occurred later (7-125 seconds) for the tests with vertically oriented block of series SB2000 and SB3000, and series SB4000. For some tests the peak occurred very late (175-230 seconds).

Based on the maximum shear force, the maximum shear stress was calculated nominally by (eq:35), and time adjusted (corrected for the real area) by (eq:36). Figure 47 show the nominal maximum shear stress plotted versus normal confinement, and figure 48 show the maximum time-adjusted shear stress plotted versus the normal confinement in series SB4000.

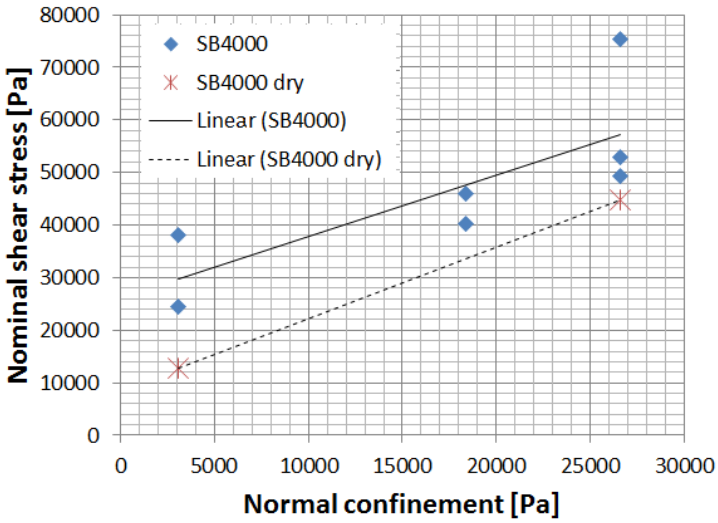

Figure 47: The nominal maximum shear stress plotted versus normal stress in series SB4000

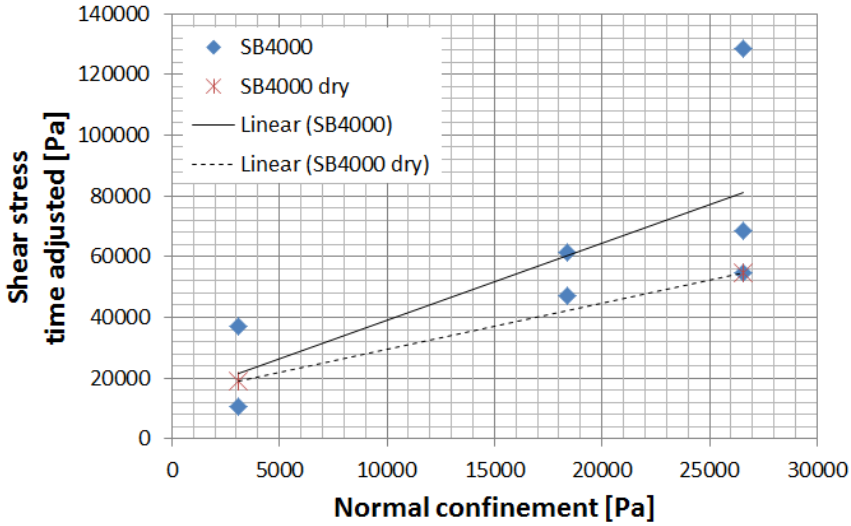

Figure 48: The time-adjusted maximum shear stress plotted versus normal stress in series SB4000

Using linear regression, the constants for the Mohr-Coulomb failure criteria can be decided for the time-adjusted maximum shear stress diagram (figure 48). For the submerged tests cohesion was c=13809 Pa and internal angle of friction was

ϕ_{max}=68.5°. For the unsubmerged tests cohesion was c=14555 Pa and internal angle of friction was ϕ_{max}=56.6°.

Effect of Confining Pressure

The effects of confining pressure was investigated in series SB4000. Figure 49 shows the first 30 seconds in tests with three different confinements.

The sudden drops in the force for the high confinement tests (red lines), were the result of the abrupt compression of the volume due to the high confinement placed on the lid of the shear box.

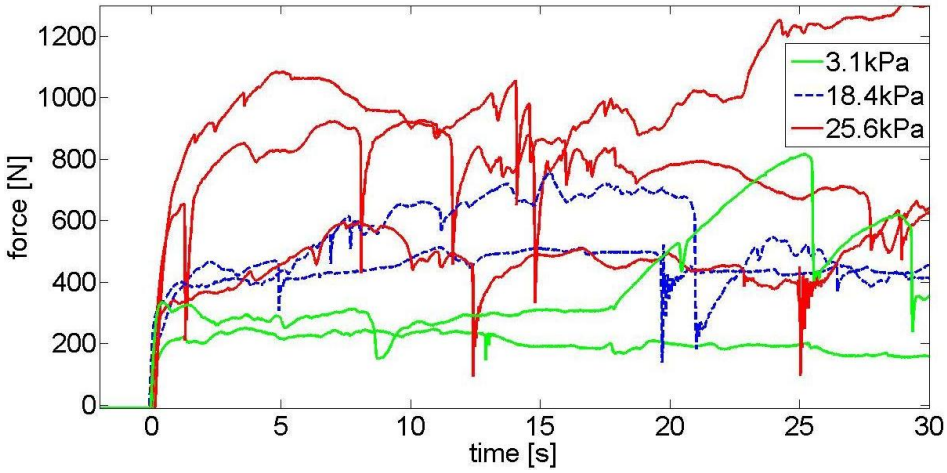

Figure 49: The first 30 seconds for submerged tests in series SB4000

4.1.6 Single Freeze-bond Strength

The strength of single freeze-bonds were tested for the same type of ice blocks as used in the shear box experiments. The results for nominal shear strength are reported in detail by Helgøy (2012), but relevant results are summarized in table 6.

Table 6: Results from single freeze-bond testing at NTNU

Ice type	*Orientation of blocks*	*Air temp. [°C]*	*Number of samples*	*Mean shear strength [kPa]*	*Std shear strength [kPa]*	*Relevant for shear box series*
1	vertical	-1	21	15.6	± 7.0	SB1000,SB1001
1	vertical	-7	19	17.0	± 9.2	SB1002-SB1004
2	vertical	-1	6	11.7	± 7.0	SB2000/SB3000
2	horizontal	-1	5	18.5	± 11.3	SB2000/SB3000
3	horizontal	-1	5	20.2	± 11.9	SB4000

4.2 Results HSVA: Pile Test

4.2.1 Ice Properties

Ice properties were measured throughout the whole testing day, each 10 meters of the ice tank. Temperature was measured at 1 cm depth, in the morning and just before the pile test was performed. An average of the ice temperature just before the pile test is reported (if available). The mean values for level ice thickness, salinity and density are reported. All values are from RITAS-participants et al. (2012) and are represented in table 7.

Table 7: The measured ice properties of the different ice sheets at HSVA

Test series	*Thickness [mm]*	*Temperature [°C]*	*Salinity [ppt]*	*Density kg/m^3*
1000	43	-0.73 (morning)	NA	905.6
2000	43	-0.70 (morning)	3.4	901.7
3000	47	-0.71	3.4	805.8
4000	61	-0.78	3.4	925.3
5000	41	-0.59	NA	887.8

The water had a salinity of 6.9 ppt, and the room temperature during testing was kept at + 1 °C.

The dry density of rubble was estimated two times for the pile tests, for series 3000 and series 5000. The density was estimated to 560 kg/m^3 (3000-series, low density) and 558 kg/m^3 (5000-series, base case). The scale that was used had an accuracy of 0.5 kg, and the volume measure had an accuracy of ca. ± 5000 cm^3, this gave the density an accuracy of roughly around ± 100 kg/m^3.

Combined with the level ice properties from table 7, the porosity of the rubble can be estimated as 30.5% for the 3000-series and 37.1% for the 5000-series.

4.2.2 Pile and Slide Geometry

In total 8 pile tests were conducted. They are numbered according to the RITAS test matrix, and an overview of the initial geometry is given in table 8. The meaning of the different geometry-measures are indicated in figure 50, and the pile heights were calculated as an average over three measuring points.

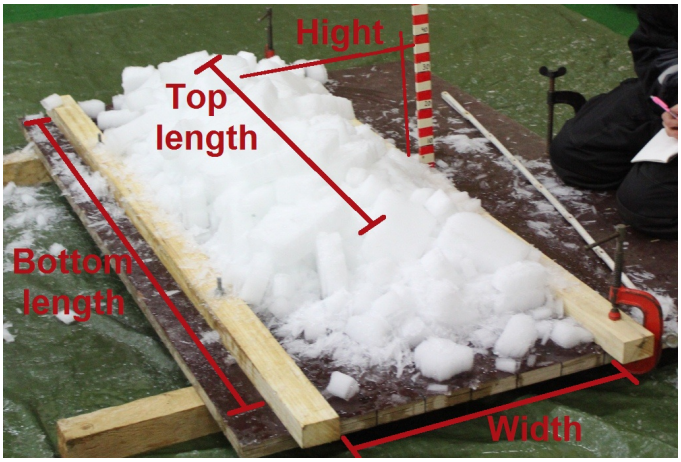

Figure 50: Geometry of a pile

Since the piles did not deform uniformly over the length and did not all behave in the same way, the results were somewhat difficult to report in a general way. Therefore we introduce a distinction between *the first slide*, *the main slide* and *the final slide*.

When the piles were tilted, several small local slides were registered and the local failure angles were measured in-situ. The first of these local slides is referred to as *the first slide*. It also occurred that all, or most of the pile deformed at the same time. This is referred to as *the main slide*. In some of the tests the pile simply failed in friction with the pile board, and rubble slid off the board. After such a failure the test was stopped and this is referred to as *the final slide*. Figure 51, 52 and 53 show examples of how the different types of slides could look like.

Table 8: Overview of the initial geometry of the conducted pile tests at HSVA

Test name	*Bottom width [mm]*	*Bottom length [mm]*	*Top length [mm]*	*Average height [mm]*	*Repose angle [deg]*	*Block thickness (other comment)*	*Consolidation time [min]*
1060	600	1800	-	308	45.7	43 mm (very mushy pile, rubble went over framework)	0 (20 *)
2060	600	1400	-	272	42.2	43 mm (quite distinguished pieces)	0 (20 *)
2061	600	1500	-	325	47.3	43 mm (used some of the rubble from 2060	33 (5 *)
3060	600	1600	800	308	45.8	47 mm (quite distinguished pieces)	0 (18 *)
3061	600	1470	690	267	41.7	47 mm (used some of the rubble from 3060)	32 (5 *)
4060	600	1800	1000	260	40.9	61 mm	0 (15 *)
5060	400	1300	1200	180	42.0	41 mm	0 (6 *)
5061	600	1800	800	218	36.0	41 mm (used some of the rubble from 5060)	0 (6 *)

* Time to make the pile

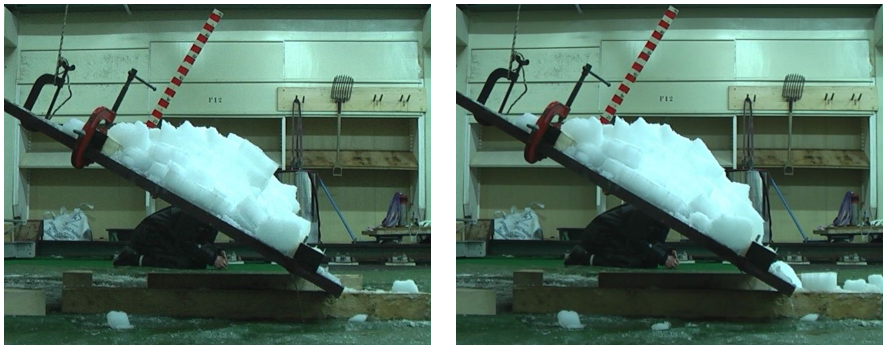

(a) Before first slide (b) After first slide

Figure 51: Snapshot from video of *the first slide* in test 3060, some blocks slid off in two locations

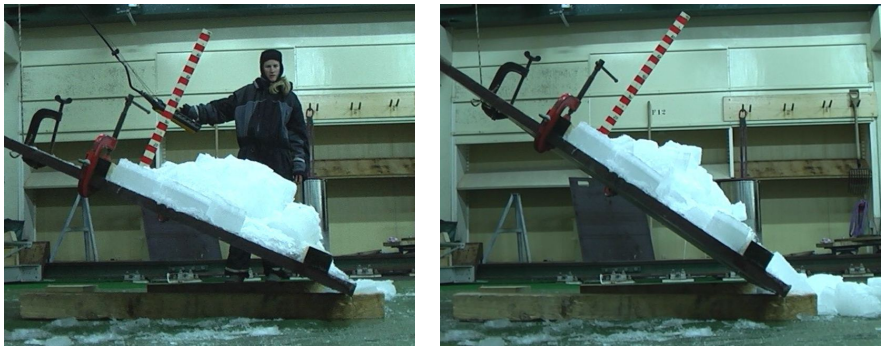

(a) Before main slide (b) After main slide

Figure 52: Snapshot from video of *the main slide* in test 4060, a failure happened inside the pile, and the top slided off

(a) Before final slide (b) After final slide

Figure 53: Snapshot from video of *the final slide* in test 2061, failure along the board, all blocks slide off

During the testing it was some problems with the attachment of the crane to the plate, so that the crane would tug the plate and make it shake. Sometimes this seemed like it initiated the slide in the pile.

Table 9 give the reported angles for the defined first slide, main slide and final slide. The definition of the angles is as defined in section 2.6 figure 10. The repose angle, the angle of the pile board and the failure angle were measured in-situ when a slide occurred. The critical angles were calculated as the sum of the change in inclination of the pile board since last measure and the last measured failure angle. The computed angles were verified by the video recordings, and adjusted if the calculated value was very different from what could be observed in the video.

Table 9: Overview of measured angles during pile testing at HSVA. All angles are measured in degrees from the horizontal.

Test	*Repose*	*Number*	*First slide*		*Main slide*		*Final slide*
name	*angle*	*of slides*	*critical angle*	*failure angle*	*critical angle*	*failure angle*	*critical angle*
1060	45.7	2	-	-	66.8	57.3	65.0 [v]
2060	42.2	6	51.9	51.1	68.1	51.0	57.2
2061	47.3	2	-	-	80.3	61.2	73.6
3060	45.8	5	76.4	48.6	72.0[v]	64.5	75.0 [v]
3061	41.7	2	73.1	54.8	-	-	66.9
4060	40.9	3	63.8	49.7	62.7	53.6	62.0
5060	42.0	1	71.2	29.2	-	-	-
5061	36.0	3	67.8	42.1	74.5	52.9	66.6

[v] Estimated from video

All slides that occurred in each test, and the measured angles, are given in the laboratory log which is given in appendix E.

4.2.3 Adapted Results

As explained in section 2.6.2, it is possible, with some simplifications, to find a unique relationship between internal angle of friction and cohesion from the tilting of a pile test.

A simple MatLab routine was made to do and plot these calculations. The unique relation between cohesion c and internal angle of friction ϕ (phi) were plotted for the tests as shown in figure 54.

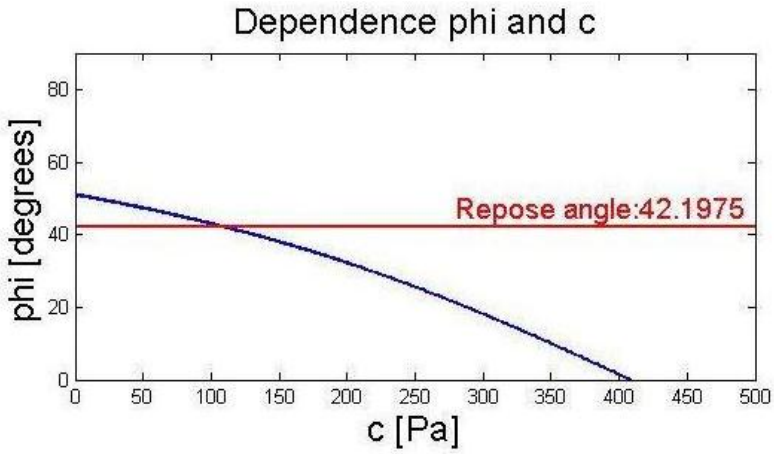

Figure 54: The plotted relation between cohesion c and angle of internal friction ϕ (phi) for pile test 2060. The repose angle is marked as an upper limit for friction angle ϕ.

The calculations was run on all tests with a defined main slide (all except 3061 and 5060), and with a rubble density of $560 kg/m^3$. All results are given in appendix F. The maximum (or extreme) values of the plotted c-ϕ-relation, ϕ(c=0) and c(ϕ=0), are given in table 10.

Table 10: Maximum (or extreme) values from c-ϕ-plots

Test name	*ϕ(c=0) [deg]*	*c(ϕ=0) ([Pa]*
1060	57.3	363
2060	51.0	408
2061	61.2	356
3060	64.5	472
3061	-	-
4060	53.6	352
5060	-	-
5061	52.9	304

5 Discussion

5.1 General

Two experiments using two different methods, examinating two types of artificial rubble, have been conducted. The shear box experiment was conducted together with testing of single freeze-bonds, in order to study freeze-bond mechanisms in rubble and find a correlation between the single freeze-bond strength and rubble behaviour. The pile tests were conducted as a part of the test matrix in the RITAS-project, and the main goal was to access ice rubble parameters. Both methods are relatively simple and with some restrictions to how results can be interpreted. However, some general observations, and some analysis on rubble behaviour can be made.

Deformation in a direct shear box is by Serré et al. (2011) and Hellmann (1984), observed to go through three phases. However, the two studies do not seem consider the same deformation mechanisms when defining the three phases. They both define a first phase, but whereas Hellmann (1984) attribute end of the first phase to the start of shear deformation in rubble, Serré et al. (2011) relate the end of the phase to the breaking of ad freeze-bonds between blocks in rubble.

A first phase was easily identified also in this study, the second and third phase however, were not detected according to the description of Serré et al. (2011) or Hellmann (1984). Therefore all deformation after the first phase was simply referred to as the second phase. The first phase behaviour could be compared to the result of single-freeze-bond testing, and it seems to be a direct relation between single freeze-bond strength and the first peak stress in rubble. This is discussed in section 5.2.

Except for the occurrence of a first phase, the characteristic behaviour of the rubble in the shear box, displayed many similarities with earlier studies: Blocks moved in block-assemblies, there were excessive dilation and some blocks were broken on the shear surface. As explained in section 2.5, the measured response in shear box testing, is a response of both rubble properties and test set-up. As the test proceeds, it seemed that the measured response was governed more and more by the constrains of the set-up. The behaviour of rubble in the second phase is discussed in section 5.3.

The pile tests were aimed at investigating rubble properties in a model scale experiment. The results from the test give rough estimations of properties of ice rubble, and also give useful indications on rubble behaviour. Still the set-up is simple, and test rubble out of water, and interpretation of the results can be difficult. It would

be beneficial to further develop and standardized the method. This is discussed in section 5.4.

There are several aspects with the two test set-ups that may introduce uncertainties, imbalanced relationships between parameters or unphysical simplifications of natural rubble. The uncertainties with testing are commented whenever the results are analysed, but also summarized and further commented in section 5.5. Evaluating the quality of the pile test, was part of the main objectives with pile testing, and is discussed in section 5.4.4. Finally properties and production methods of the artificially created rubble, and how it affects results is discussed in section 5.5.2.

5.2 Shear Box First Phase

5.2.1 General

The results from the shear box testing confirmed earlier assumptions of a "first phase" when rubble deforms. However Hellmann (1984) and Serré et al. (2011) observe a second phase closely following the first phase, where the peak load were included. This as not the case in this study, were the peak load either occurred in the first phase, or later, then related to a block that was breaking.

The first phase was in this study defined as the near linear and sudden increase in force that ended in a peak or a constant force level. According to Hellmann (1984) the first phase is within the first 0.4 % of relative displacement. This correspond to a displacement of $0.4\ \% \cdot 600 = 2.4$ mm or 1.2 seconds, in our study. Ca. 82 % of the tests have the first phase within the same interval as in the study of Hellmann (1984). Serré et al. (2011) reported the first peak within the first 6 seconds of the test, and this interval were used to plot the initial deformation for all test series in figure 37, 38, 39 and 40.

As shown in figure 28, the first signs of deformation in the shear box, were small cracks appearing in between blocks that initially stuck together. The cracks were not visible until the test had run some seconds, still it seem reasonable to relate the occurrence of these cracks to the end of the first phase. No other failure mechanism that could be related to the first peak was observed. There was one exception. For test SB4002 it seemed that a block broke in the very beginning of the test.

Hellmann (1984) relate the first phase to the denser packing of ice rubble, and the end of the phase as the start of shearing in the rubble. This was clearly not the case in our tests, were rubble rather expanded immediately as deformation started. Serré et al. (2011) relate the first phase to the breaking of the rubble skeleton consisting of freeze-bonds between blocks, and this study support this assumption. A convincing argument for the latter, is that dry (unsubmerged) tests without freeze-bonding, displayed almost no tendency of a first phase.

The significance of the first phase shear stress compared to other rubble mechanisms, may very well be overestimated, as the rubble too dense (an average porosity of 0.23) and freeze-bonded area may be too large to simulate natural rubble. This is further described and discussed in section 5.5.2.

The size and shape of the first peaks varied between test configurations. The main differences between test series were the water temperature, and the ice properties of the blocks used to simulate rubble. Since both single freeze-bond tests and shear box tests were conducted for the same water conditions and on the same ice, a comparison of the results could be made, as presented in table 11.

Table 11: A comparison between single freeze-bond strength and first phase values

Shear box series and test configuration	*Single freeze-bond strength [kPa]*	*First peak stress [kPa]*	*Shear modulus [MPa]*
SERIES SB1000			
Ice 1, "warm"	15.6	25.6	8.4
Ice 1, "cold"	17.0	42.7	9.2
SERIES SB2000			
Ice 2, vertical	11.7	12.3	4.5
Ice 2, horizontal	18.5	25.1	7.8
SERIES SB4000			
Ice 3	20.2	-	-
Ice 3, 3.1 kPa	-	11.4	5.4
Ice 3, 18.4 kPa	-	15.9	5.9
Ice 3, 26.6 kPa	-	24.1	5.5
Ice 3, 3.1 kPa (dry)	-	1.0	2.3*
Ice 3, 26.6 kPa (dry)	-	9.1	3.9*

* Not very distinguished first phase

Four main observations on the first phase peak stress and behaviour where made:

1. Series SB1000 displayed some variation with water temperature
2. Series SB1000 displayed higher first peak strength than following series
3. Series SB2000 and SB3000 displayed variation with block orientation
4. Series SB4000 displayed variation with confinement pressure

All these observations are discussed with regards to results from the single freeze-bond testing in the following sections.

5.2.2 Variation with Water Temperature

For test series SB1000 two types of water conditions were tested. Two shear boxes were submerged in a water tank in a room of -1°C ("warm") and 3 boxes in a water tank in a room of -7°C ("cold"). The same variation was done for the single freeze-bond testing. The initial hypothesis was that super cooled water, or more precisely, water in a colder environment, would remove more heat from the submerged ice, and thereby create stronger freeze-bonds.

The measured temperature variation between "warm" and "cold" water was very small. Only 0.1°C separated the warm and the cold basin. The small variation in temperature does not truly describe the situation in the basin, as the "cold" basin contained more slush then the "warm" basin, and clearly was in the process of freezing.

As can be seen in table 6, the effect on the shear strength of single freeze-bonds, was small. The "cold" water gave freeze-bond strengths of 17.0 ± 9.2 kPa, and the "warm" water gave 15.6 ± 7.0 kPa. It seems that water temperature is insignificant for single freeze-bond strength.

The results from the shear box testing on the other hand, show a tendency of a higher first peak, and a more abrupt ending of the peaks, in "cold" tests. This can be seen in the plot of the first 6 seconds of series SB1000 in figure 37. It is common for ice to act more brittle for colder temperatures, and maybe is this also the case for rubble behaviour in the first phase. In general the force seems to fluctuate more for the "cold" tests, while "warm" tests on the other hand seem to deform more softly. It is possible that the individual ice blocks in the "cold" tests kept a lower temperature, and thereby had a higher individual strength and firmness, causing the rubble to deform in a more jagged or uneven manner.

Also, the "cold" submerged boxes looked like they contained more slush then the "warm" submerged boxes. This may give a denser rubble volume, which could be the reason for the differences in behaviour.

Still, only five shear boxes were tested for difference in water submersion temperature, and few conclusions can be drawn based on so few tests. Also if the "cold" tests were more brittle than "warm" tests, the shear modulus should reflect this. That was not the case, as shear modulus was almost the same for "cold" and "warm" tests.

In series following series SB1000, all tests were submerged in a room with "warm" temperature (-1 °C). The decision was made as the water temperature (or room temperature of the submersion basin), seemed to give almost no effect on single freeze-bond strength. Comparing the following tests with the SB1000 series is difficult since the type of ice that was used was different. Still, the following test series all had quite rounded first peaks compared to the "cold" tests of series SB1000.

5.2.3 Variation in First Peak Strength

In general the first peak strength was higher in the SB1000 series, both "cold" and "warm", than in the following series. Most likely this is a result of the difference in ice properties for the ice that was used. Earlier tests (Helgøy, 2011; Astrup, 2011) indicate that the surface structure, or the porosity of blocks, affects the strength of the ad freeze-bonds. The more porous or saline ice blocks, the stronger the freeze-bond between the blocks. Since ice of type 1 was more saline and thereby more porous than ice type 2 and 3, this may explain the higher first peaks in series SB1000.

The results from single freeze-bond testing contradict somewhat with this explanation. Freeze-bond strength was in fact reported higher for the ice blocks used in series SB4000 than those used for series SB1000 (see table 6). However, only five single freeze-bond tests were conducted for this configuration (see table 6), and results are uncertain.

As suggested by Henning Helgøy, the crystal size of ice type 3 were large compared to ice type 1, something that would give a large variation in crystal structure between blocks. This could result in some very weak freeze-bonds. If the first phase peak stress is governed by the weakest freeze-bonds in a rubble volume, this could explain the low first peak strength in series SB4000 compared to series SB1000.

For an equivalent test set-up and test configuration as used in this study, Serré et al. (2011) reported first peak strengths of ca. 10 kPa . For the ice they reported relatively low freeze-bond strengths (3.5 kPa) (Helgøy, 2012). First peak shear stresses reported in this study are higher, and so are single freeze-bond strengths. Still results of Serré et al. (2011) corresponds well to the results from vertical tests in series SB2000/3000 (12.3 kPa) and from series SB4000 (11.4 kPa). Ice parameters in their testing should be the same as intended ice parameters in this study, and similar to ice of type 1. However first peak shear stress in series SB1000 (with ice type 1), are more than double the values of Serré et al. (2011). It is hard to discuss why such different results are reported. One reason is that it is not clear whether the ice parameters reported by Serré et al. (2011) were measured, or were the expected outcome of their method for making ice.

5.2.4 Variation with Block Orientation

The difference in ice surface properties depend on how the ice blocks are cut from an ice sheet. This was the background for testing single freeze-bond strength and shear boxes with blocks of different orientation. In series SB2000 and SB3000 eight shear boxes with blocks cut either horizontally, or vertically (see figure 17), were tested. Every second box was filled with horizontal blocks, and every second box with vertical blocks, everything else was kept the same. The results should therefore be independent of other control parameters.

The result from the single freeze-bond testing indicated that horizontally oriented blocks give stronger freeze-bonds (18.5 ± 11.3 kPa) than vertically oriented blocks (11.7 ± 7.0 kPa). This trend was also observed in the shear box testing. Boxes with horizontally oriented blocks gave stronger peaks (in average 25.1 kPa) than boxes with vertical oriented blocks (in average 12.3 kPa). Also the first phase plot (figure 38), indicate that boxes with horizontal blocks, had a stiffer behaviour (G=7.8 MPa), than boxes with vertical oriented blocks (G=4.5 MPa).

This common behaviour in single freeze-bond tests and shear box tests confirms a direct link between strength of single freeze-bonds and first peak strength of rubble. It also seems that the effect of single freeze-bond strength is quite significant for the rubble strength. When single freeze-bond shear strength increase with a ratio of 18.5 kPa/11.7 kPa=1.6, first peak shear stress increase with a similar ratio 25.1 kPa/12.3 kPa= 2.0.

Something that have not been investigated, is if single freeze-bonds between horizontal blocks, show stiffer behaviour than a freeze-bond between vertical blocks. Then the measured difference in shear modulus for the rubble could be explained with freeze-bond properties. This would be interesting to check, to further link single freeze-bond behaviour and rubble first phase behaviour.

The reason for the relative large difference in freeze-bond strength for the different block types, could be the structure of the ice. A block cut horizontally; have a surface containing more crystals or ice grains, and more brine channels, than a block cut vertically along the direction of the ice crystals. See illustration in figure 55.

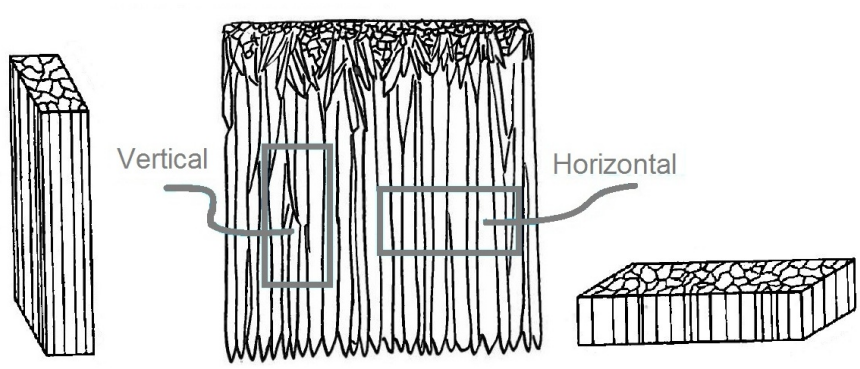

Figure 55: How ice blocks are cut from an ice sheet, and how ice crystals could be distributed in the two block orientations, vertical and horizontal

The freeze-bond formed between horizontal blocks would then be initiated from several small ice grains, which would give small ice crystals and strong ice. Also salt would drain easier from the freeze-bond into the block through the many brine channels, if the block was cut horizontally. This would create a less saline, less

porous and stronger freeze-bond.

The block surface of a vertical block would on the other hand have fewer crystals, and brine channels. It would be denser than a horizontal block, and would not allow the new formed freeze-bond to drain very well. Therefore a freeze-bond between vertical oriented blocks would be weaker.

The results from series SB2000 and SB3000 thereby support the hypothesis that surface structures, or porosity of blocks, have a significant effect on freeze-bond strength.

5.2.5 Variation with Confinement Pressure

In the SB4000 series no first peak occurred, and the first phase simply consisted of a linear increase of force to a constant level. This behaviour could be described as perfect plastic material behaviour.

It was evident than an increase in confinement pressure gave stronger freeze-bonds. The first peak stresses were adapted to Mohr-Coulomb failure criteria, and the cohesion and internal angle of friction were found for both dry and submerged tests. The dry tests displayed almost no cohesion (c = 41.3 Pa), while the submerged tests displayed very strong cohesion (c = 8830.6 Pa). Cohesion measured later in the tests (for average or maximal stress) did not exceed the first phase cohesion. This support the assumption that the cohesion is most significant in the first phase of rubble deformation and that cohesion is related to freeze-bonding.

The shear moduli for all confinements (3.1 kPa, 18.4 kPa and 26.6 kPa) were almost the same (5.4 MPa, 5.9 MPa and 5.5 MPa). This is reasonable since the stiffness of the material should not be affected of a change in the boundary conditions.

The constant shear modulus for increased confinement and the systematic variation of first phase with ice properties and freeze-bond properties all imply that the observed behaviour in the first phase is related to rubble properties and not the set-up. This means that observed trend should be valid also for other testing methods and other types of rubble. It does not mean that reported values for first phase are universal or even in the right ratio of dimensions compared to full scale rubble.

5.2.6 First Phase Summary

All in all the different test configurations all display different behaviour in the first phase. Peak strength varied greatly, but systematically with different ice properties. Results from single freeze-bond testing could be linked to results for first peak strength. An increase of freeze-bond shear strength by a ratio of 1.6 gave an increase in first peak shear strength of rubble by a ratio od 2.0. A change in boundary conditions (applied confinement), gave varying first peak strength, but

the same elastic properties. It seems that the first phase observations mainly are related to rubble properties and not mainly to the set-up.

5.3 Shear Box Second Phase

5.3.1 General

As soon as the first phase had ended, the second phase started. Since the shear box is a direct shear box, it forces the rubble to fail along a specific shear plane, and behaviour is strongly influenced by the boundary conditions.

As soon as the deformation of the shear box started, dilatation of the rubble started. Probably the dilation did not start before the freeze-bonds broke, and the first phase ended, but this was hard to confirm by observation. What was observed was that cracks appeared between blocks as the volume expanded, and after some displacement of the box, blocks started to rearrange. Blocks stuck together in lumps, or block assemblies. For some tests the rubble formed a sort of bridge or arch that lifted the rubble volume upwards (see figure 30).

After the first peak in rubble, the force level slowly decreased until 50 seconds of displacement. This slow decrease was more obvious in tests with high freeze-bond and first peak stress, so it could be the breaking of freeze-bonds is a part of the failure mechanism even after the first peak.

From the force-time-plots an average stress range was defined where effects of freeze-bonding and (excessive) block breaking should be excluded. Some effort was put down in fitting the observed results to a Mohr-Coulomb material description. The obtained values for cohesion and internal angle of friction was not very convincing, and this is discussed in section 5.3.2.

For load calculations the maximal resistance or load applied by a rubble ice feature is interesting. The maximum or overall peak loads were identified in all shear box tests, and some discussion of the failure mechanisms, test behaviour and fitting of results to the Mohr-coulomb criterion are made in section 5.3.3.

5.3.2 Average Shear Stress

In the force-time plots it was observed that from a first phase peak, the force level slowly decreased, and stabilized after ca. 50 seconds of displacement. Until around 175 seconds out in the test, the force level seemed to be rather constant. This interval (50-175 seconds) was used to find a middle or average stress by (eq: 37). See figure 45.

Such an average stress is clearly a simplification. In many tests the volume expanded to the extent that the lid with confinement weights tilted, and some blocks

were pushed up and even forced out of the box. An example shown in figure 29. The picture is taken 84 second after the test was started, and illustrate that the true state of deformation is not well described by equation (eq: 37). Still, the analyses of the average stress give some interesting indications on rubble behaviour, and influence of the set-up.

In the first phase, dry (unsubmerged) rubble displayed cohesion of almost zero. One would not expect this value to change much as rubble was exposed to excessive deformation. The opposite was measured in this study. The cohesion for a dry test in the average stress range (50-157 seconds), was estimated to 1510 Pa (see figure 46) compared to 41 Pa in the first phase. Initially the dry rubble have few and weak freeze-bonds. As the material have not changed, and it is unlikely that a contact force should have developed between dry blocks as the volume deform, the measured increasing cohesion is clearly an effect of constrains imposed by the shear box.

If cohesion in dry tests for the average range, is a set-up effect, one would expect the same overestimation (1510 Pa) for cohesion in submerged tests. In fact, even when accounting for this effect, the submerged tests showed even higher cohesion (6647 Pa). That means that, either the continuous deformation of rubble is not an almost cohesionless process (in disagreement with Ettema and Urroz-Aguirre (1987)), or that some other phenomena additionally increase the cohesion measured for submerged tests. The most likely explanation is linked to the observation of block assemblies.

During the second phase rubble moved together in block assemblies. Block assemblies are clusters of blocks sticking together due to freeze-bonds. As suggested by Serré et al. (2011) this increases the effective block size in the volume and makes the RVE (Representative Volume Element) too small. This means that submerging the tests and allow freeze-bonds to form, give a smaller RVE and thereby behaviour more governed by the set-up. Most likely this is the phenomena that cause the overestimation of the cohesion in submerged tests.

Shafrova (2007) proved the dependence of stress level on the size of blocks, see figure 6. She plots the relation of the ratio of shear box length (L) to block thickness (t) versus measured stress. Ratios under 12 resulted in an overestimation of stress, while ratios over 24, stress gave little overestimation. For this study the shear box length on ice block thickness initially was $600mm/22mm = 27.3$, and chosen dimensions seems to be in the safe range (over 24). When submerged, blocks formed block assemblies that in average consisted of ca. 3 blocks. Then the shear box length on ice block thickness is $600mm/(3 \cdot 22mm) = 9.1$. This is below the ratios studied by Shafrova (2007), and would imply that effective block size is too large and shear force will be highly overestimated.

Serré et al. (2011) also reported that the size of the block assemblies grew with stronger freeze-bonds, and that larger assemblies increased the dilation of the rubble. Similar trends are observed in this study, with the largest block assemblies for test series SB1000, which also had the strongest freeze-bonds. Trends for dilation

are not so obvious. The dilatation of low confinement tests were quite significant, but hard to quantify. It could be possible to use (eq: 11) and calculate a dilation angle, using the volume expansion, and the recorded stress level, for a short time interval. Some modifications to the set-up would then be beneficial, like adding a grid on the shear box to monitor the volume change.

5.3.3 Maximum Stress Level

The maximum stress level was identified for each test. It seemed that for shear boxes filled with ice blocks with high freeze-bond strengths (ice type 1 and horizontal blocks of ice 2), the peak load occurred early (after 0-7 seconds). For shear boxes filled with ice blocks with low freeze-bond strengths (ice type 3 and vertical blocks of ice 2), the peak occurred later, either related to dilation, or to the breaking of one or several blocks.

The tests with low freeze-bond strength resembled more the behaviour described by Serré et al. (2011). In their study the first phase (0-6 seconds) does not include the peak load, which occurs later in the second phase (6-120 seconds) and is related to dilation. The similarity in behaviour of SB4000 series low confinement tests is illustrated by the plot in figure 56. Here the behaviour of the low confinement tests in series SB4000 is plotted in green on top of all low confinement tests in yellow (dry test in black).

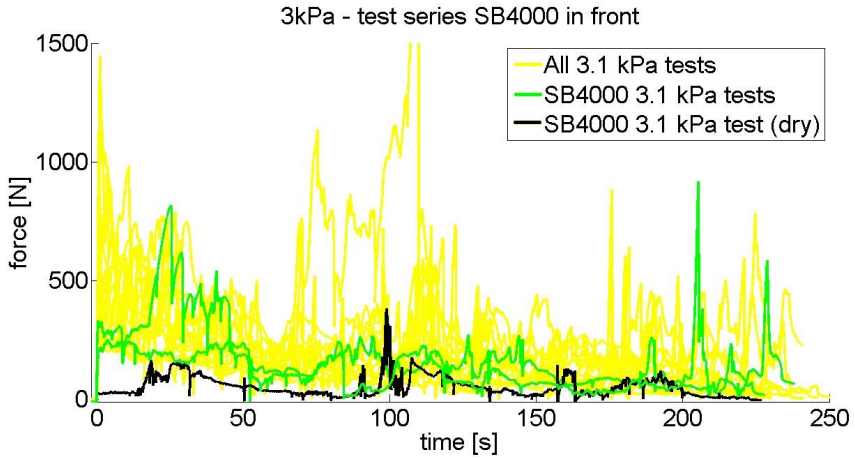

Figure 56: Comparison of behaviour of low confinement tests (3.1 kPa) in series SB4000 to tests of other series

For the maximal stress levels in series SB4000, values for cohesion and internal angle of friction was estimated. They were higher than values suggested in literature (c over 10 kPa and ϕ over 50°). This is most likely a combined effect of the set-up and boundary conditions, and that the maximum stress level were attributed

to different failure mechanisms in each test. For series SB4000 peaks occurred either for the breaking of a single block (one random peak) or when several blocks were packed and crushed at the shear interface (rounded peak/maximum), or for a point of excessive dilation (hard to distinguish from crushing of blocks in the force-displacement plots).

A more correct method of treating the peak stress could be to ignore all single peaks, and focus on the rounded peaks early in the tests. Then the Mohr-Coulomb parameters could be determined for a maximum stress level related to dilation only. However, for high confinements tests, many blocks were crushed on the shear plane, also early in the tests, resulting in rounded peaks in the plot. Therefore locating maximum stress levels, and establishing Mohr-Coulomb parameters, only related to friction and dilation, was difficult.

The observed variations between tests with different ice types, was mostly related to the first phase. Yet it was observed that the trend of arching or bridging in a test was more significant for test series SB1000 and vertical tests of SB2000/3000. Common for these tests is that blocks were oriented vertically.

It is known from ice mechanics that compression strength of ice depend on the crystal direction. Ice in compression is stronger hen force is applied in the direction of crystals than across crystal direction. Therefore it would be reasonable to suggest that vertical oriented blocks did not break as easily as horizontal oriented blocks. That may be the explanation of the tendency of arching in the vertical tests. Yet no less broken blocks were observed in the vertical tests, so it is uncertain whether there are trends varying with ice strength for tests.

The individual compression and flexural strength of blocks influence rubble behaviour, though this is not in-depth investigated in this study. To obtain the right ratio of freeze-bond strength to single block strength, may be difficult, but may be possible be heating the ice or using different submersion times. Future studies should consider this.

As the tests had deformed for 175 seconds, the upper part of the box had moved 350 mm. That means the area of the initial shear surface was already more than halved. Several peaks occurred after this point, and were related to the breaking of blocks at the shear surface. Only blocks directly in contact with the shear plane seemed to be involved in the deformation. It is doubtful whether any analyses beyond this point give any indication of rubble behaviour.

5.3.4 Second Phase Summary

The behaviour in the second phase seems greatly influenced by the set-up constraints. By using the dry shear box tests as a kind reference case, it was found that the effect of the set-up grows with the effective block size. This was expected, as it was known initially that the RVE of the shear box was too small. The maximum shear stress in a test was attributed to either the first phase, the breaking of

one or many blocks or to dilation of the rubble. It seemed that tests with strong freeze-bonds had early peaks and larger block assemblies. Some trends for dilation and variation with ice strength was noted, and should be investigated further.

5.4 Rubble Behaviour in Pile Tests

5.4.1 General

Pile tests were conducted with the aim of reporting rubble properties. Repose angle is easy assessable, and it is the common result reported in previous studies. The extent of analyses was expanded by applying some simple principles of slope stability, and thereby values for cohesion could be suggested. Still it is quite obvious that the set-up tests rubble in a simplified way, in respect to scaling and procedure, so results must be read with that in mind. Also the time-dependence of cohesion was investigated by this test, though it is not well quantified. The test is not a common method, and the set-up needs evaluation.

5.4.2 Rubble Properties

The first objective with the pile testing was to get indications of the model scale rubble properties. For the different pile tests the repose angles ranged from 36.0° to 47.3 °. The initial repose angle in a pile give an estimation, or upper limit for the angle of internal friction. There are no other measurements available to validate this results, but the range of values seem reasonable, compared to values suggested by Liferov and Bonnemaire (2005). Since the level ice thickness, and the ice density varied between tests, one would expect the rubble properties to vary somewhat.

The cohesion was not directly measured in the testing, but from analysis of the main slide that occurred in a pile, a relation between the cohesion c and the internal angle of friction ϕ was found and plotted. This was possible in 6 out of 8 tests. In table 12, values for repose angle is compared to the maximum ϕ and c from the c-ϕ-relation.

Table 12: Some key values from the c-ϕ-relation for pile tests

Test name	*Repose angle [deg]*	*ϕ(c=0) [deg]*	*Cohesion for ϕ = 0° [Pa]*
1060	45.7	57.3	363
2060	42.2	51.0	408
2061	47.3	61.2	356
3060	45.8	64.5	472
3061	41.7	-	–
4060	40.9	53.6	352
5060	42.0	-	–
5061	36.0	52.9	304

Values for cohesion given in table 12 are maximum values, values for cohesion can be read from the c-ϕ-relation corresponding to any friction angle below the maximum values. A more resonable value of cohesion may be taken for a friction angle of 30°. Cohesion for this friction angle, and some ratios to illustrate the relations to other parameters, are given in table 13. H_i is the level ice thickness, H_{pile} is the height of the pile and α_{repose} is the initial repose angle of the pile.

Table 13: Analysis of the c-ϕ-relation for $\phi = 30°$, H_i and H_{pile} are the level ice thickness and the pile height respectively. α_{repose} is the repose angle.

Test name	*Derived cohesion c when $\phi = 30°$ [kPa]*	*c/H_i [kPa/m]*	*c/H_{pile} [kPa/m]*	*c/α_{repose} [kPa/deg]*
1060	0.23	5.33	0.75	$5.01 \cdot 10^{-3}$
2060	0.22	5.05	0.80	$5.14 \cdot 10^{-3}$
2061	0.24	5.63	0.74	$5.12 \cdot 10^{-3}$
3060	0.34	7.28	1.11	$7.47 \cdot 10^{-3}$
3061	-	-	-	-
4060	0.20	3.33	0.78	$4.96 \cdot 10^{-3}$
5060	-	-	-	-
5061	0.17	4.20	0.79	$4.78 \cdot 10^{-3}$

In the literature several values for the ratio of cohesion on block thickness c/t (or c/H_i) are suggested. One of the lowest ratio suggested is $c/t = 12 \pm 6$ kPa/m, based on results from Weiss et al. (1981) and corrected for hydrostatic pressure (Liferov and Bonnemaire, 2005). This is higher than what the adapted results from the pile tests suggest.

For a level ice thickness of ca. 40 mm, the cohesion should by this ratio be in the range of 12 kPa/m $\cdot$ 0.04 m =480 Pa. Even when comparing with the upper limits of the derived cohesion ($\phi = 0°$), the upper limits of cohesion (300 Pa to 470 Pa) are lower than 480 Pa.

It could be that the cohesion of the ice rubble piles truly is low. Especially since the ice used for testing was relatively warm (-0.6 to -0.8 °C). Referring with the test program of Weiss et al. (1981), who lay basis for some of the suggested c/t ratio, they used colder ice (-2.5°C to -7.0°C). Still, one would expect that piles with thicker ice blocks, (like 61 mm for test 4060), would display a larger cohesion. The results give no such indication.

The assumption that cohesion depend on block thickness is not intuitive, as cohesion is attributed to contact forces and logically should depend mostly on surface properties and confinement. Yet, earlier studies post that cohesion is large for large blocks, and small for small blocks. This seems to be the same relation that Shafrova (2007) found when investigating the effect of block size in shear box tests. This means that observations of cohesion depending on block thickness could be a scaling effect when shear boxes was used to obtain results. Also no considerations about thermal scaling seem to have been done in derivation of the cohesion dependence of block thickness.

Scaling ice experiments are difficult, and an issue for pile tests is the problem of scaling of ice strength to freeze-bonding and friction. Since the ice is warmed and thereby weak, a failure in the pile is most likely a combination of failure between blocks (friction and cohesion) and failure of blocks (flexural strength). This makes results difficult to analyse, and more consideration should be payed to thermal scaling of the experiment.

The smallest piles (4060 and 5061) seem to give the lowest cohesion, and the lowest angle of friction. As the c/H_{pile} ratio is the same for big and small piles, the cohesion seem to be proportional to the pile size, and not block thickness. This may very well be due to how cohesion is calculated. From equation (eq: 33) we see that cohesion is sensitive to the ratio $\frac{A_{slide}}{L_{slide}}$ and to the failure angle. Further investigations on how sensitive cohesion is to these parameters should be done when further developing the analysing method.

The property values suggested based on the derived relations are not unreasonable, but it is impotent to stress that these values are obtained by using considerable simplifications. Also the number of tests is few, and one should be very careful to draw any conclusions supported by these results.

5.4.3 Time Dependence of Cohesion

Since the goal for the testing is to get values for the internal angle of friction and cohesion, how fast cohesion develops is crucial for the interpretation of results.

From the tilting of the piles it was evident that the cohesion developed fast. After a consolidation time of 6-20 min, the critical angles of the first slide were 9.7° to 31.8° steeper than the initial repose angles.

In some tests series two pile tests were run on the same type of rubble (series 2000

and 3000). Test 2060 and 3060 had a short consolidation times (less than 18 and 20 min) and test 2061 and 3061 had a long consolidation times (more than 38 and 37 min). A comparison of measured angles between these tests, or derived cohesion, is difficult. The number of tests is too small, and the individual variation in behaviour of the tests is too large.

Still the number of slides in each test indicate that the cohesion have developed significantly. 5-6 slides were observed in the tests with short consolidation times, and only 2 for the long consolidation times. It seems that for long consolidation times, the pile acts less like a loose assembly of blocks and more like one unit. That means less small slides, and that the whole pile fails at the same time as a slide along the plate.

5.4.4 Test Evaluation

The last objective with the pile testing was to evaluate the test method. Even if several studies (Ji, 2011; Ettema and Urroz-Aguirre, 1989) suggest pile testing as a validation for values for internal angle of friction, few have described the set-up or evaluated the method. This study only found one: Serré et al. (2009).

Based on the experience from the testing, some comments and recommendations for pile-tests in general can be made. Firstly, the pile needs to be of a certain size. In this case, a base line larger than 400 mm for ice with thickness of 40 mm. This is a question of getting enough blocks to simulate a rubble material, and that the pile is large enough to allow a slide inside the pile when it is tilted.

Secondly the consolidation time of the pile should be monitored, as cohesion in the pile develops fast. In geology were this test also is used, the materials (mostly sand) are near cohesionless, and the observed repose angles are much closer to the true angle of internal friction. If one could establish how fast cohesion develops in ice rubble, results could be corrected for this.

The way rubble is gathered and how the pile is made is neither trivial. Serré et al. (2009) stacked the piles manually between frame pieces, while this study poured the rubble from a perforated box. It would be beneficial to have a standardized way to agree on, if the method is to be used frequently.

Adaption of slope analysis to the pile test, and the derivation of the c-ϕ-relation made for this thesis could surely be improved and developed. Results could be compared to results from more sophisticated tests, like the results from the buoyancy box in the RITAS-project, which testes rubble stability under water, or simulated with finite element analysis.

To obtain good results from whatever analysing method, accuracy of the input parameters should be improved. The method is sensitive to the input angles for slides and the rubble porosity. Also the crane sometimes tugged the plate, something that caused a failure sooner than in an undisturbed test.

5.4.5 Pile Test Summary

Directly from the testing one gets an indication or upper limit for the internal angle of friction (repose angle). Combined with the c-ϕ-relation obtained from tilting the pile, values for internal angle of friction and cohesion can be suggested. Results are not unreasonable, but needs further validation. The cohesion in rubble increase rapidly with time and this governs the behaviour of rubble in the tests. Pile testing implies some simplifications and uncertainties in relation to scaling, investigating rubble out of water and to coarse measurements of pile geometry. The set-up and the method should be further tested and developed.

5.5 Summary of Uncertainties

Results from both test methods are associated with considerable limitations and uncertainties. All factors will not be discussed here, but section 5.5.1 give the most important limitations of the testing. Section 5.5.2 give a discussion of artificial rubble.

As the shear box constrains governed the observed rubble behaviour, the set-up influence has to a large extend been discussed together with the results. Some comments on pile test set-up is already given in section 5.4, and measuring uncertainties in instruments etc. for both tests are small in comparison to other uncertainties with the testing, and will not be discussed.

5.5.1 Limitations

Scaling of the shear box experiment was simply adopted from Serré et al. (2011), and this was a limitation of the study. Also the interpretation of result is somewhat subjective, and classifications of results and observations of behaviour are to some extent dependent on the person observing.

As the pile tests were a part of the RITAS-project, assumptions for scaling were given by the general test set-up, as where ice parameters and time available for testing.

5.5.2 Artificial Ice Rubble

The conclusions and observed trends are greatly dependent on the ice and ice rubble properties. The artificial rubble is supposed to simulate natural rubble, only in small scale. For the shear box, small rubble blocks were cut manually from large ice blocks, while rubble for the pile testing were made from breaking the level ice into large irregular pieces. Some uncertainties and difficulties with these methods are given below.

SHEAR BOX:

- Ice properties were not all as intended (crystal size, salinity)
- Rubble porosity was low
- Very regular shape of blocks

PILE TEST:

- Large present of slush in some tests
- Uncertain density measurement

The ice for the shear boxes did not all have the intended ice properties. As reported in table 3, the values for ice salinity in the NTNU experiment varied significantly in between batches of ice, and was for ice of type 2 and 3 far off the intended value of 3 ppt. Also the crystal size and the structure were different for the different ice types. The explanation is probably the difference in growth time and the fluctuations in room temperature when the ice was formed.

Porosity for the shear boxes were much smaller than intended, with an average of 0.23. This is among the lowest values observed in nature (0.25-0.45). In addition a 2D case is constraining the volume even more than a (natural) 3D case, so the rubble is clearly too compact in comparison to values for in-situ ridges. This leads to a high dilation of the rubble volume. Another effect was that water did not drain as easily right before and during testing of the shear box in the rig. This may have affected the observed behaviour.

It has also been observed that cohesion seems to plays a more important role than the frictional resistance if rubble is tightly packed (Wong et al., 1990). Cohesion is mainly related to the first phase, and it may be that the first peak stress is overestimated in comparison to the stress levels at continuous shear.

we made some effort to produce rubble with higher porosities, but the very regular shape of blocks made this difficult. The blocks were to be distributed randomly, yet with certain gaps. We discovered that this was difficult when all blocks were equal and rectangular. An example is given in figure 57.

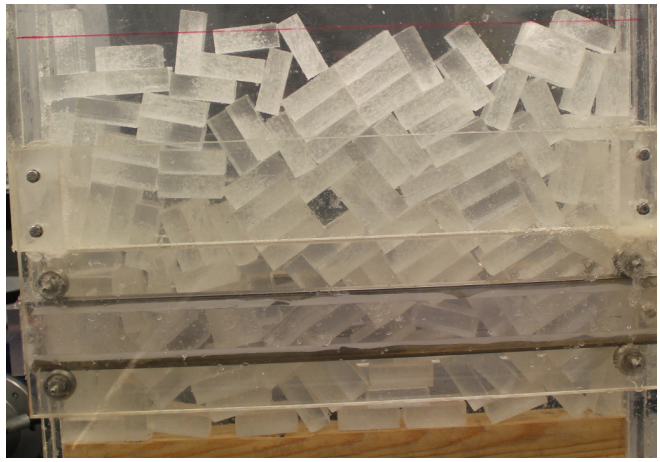

Figure 57: The regular stacking of blocks in test SB2003 (before submersion)

The very regular shape of ice blocks may have given more freeze-bonded area than natural rubble. This may have lead the rubble behaviour was dominated by the first peak strength, to an extent that will not be observed in nature. All in all one should be careful to draw to many parallels from the shear box tests to behaviour of full scale rubble. The testing is based on many simplifications, and a simple scaling of parameters. And rubble in its natural surroundings displays large variability in properties and behaviour.

Level ice produced at HSVA in Hamburg, was well controlled. Ice parameters were as intended and scaling was well defined. Rubble was made by breaking the level ice cover into blocks, much like it happens in nature. The only difficulty was that the ice was warm, as this was necessary to scale down the flexural strength of the ice for interaction tests. It may be that pile test results were failing due to by the low individual strength of blocks, and not in friction and cohesion between blocks. The warm ice made the rubble mushy and gave a lot of crushed ice in the piles. Collecting the rubble in careful manner, improved the consistency of the rubble somewhat.

The measure for the rubble density, was associated with a large estimated uncertainty (560 kg/m^3 $\pm$ 100 kg/m^3). The method for measuring was somewhat improvised, and could surely be improved.

There are many advantages on having a standardized way of creating saline ice, as HSVA have. NTNU would benefit from having some guidelines for making saline ice in FRYSIS II, or some system of reported input parameters (water salinity, temperature, time, seeding/no seeding of ice) and the measured output parameters (ice thickness, salinity, density and crystal diameter).

6 Conclusions

Two tests have been presented in this thesis: the shear box test and the pile test. Both tests are relatively simple, but give information on the characteristics of ice rubble behaviour.

6.1 Shear Box Tests

With the purpose of investigating the relation between single freeze-bond strength and rubble behaviour, an experiment with shear box testing was conducted in the cold lab at NTNU. Simultaneously tests of single freeze-bond shear strength were conducted for the same ice. The shear box was a direct shear box, filled with rectangular ice block simulating rubble in a 2D state. It was submerged for 10 minutes and tested by forcing the rubble to fail in shear.

22 tests were conducted, and the main results were:

1. A first phase with a near linear force-deformation-relation was identified in all submerged tests. Observed behaviour was:
    - Colder submerging water temperature gave more brittle and higher first peak strengths, without single freeze-bond tests showing a significant change in strengths.
    - Rubble with ice blocks oriented horizontally with high freeze-bond strength (18.5 kPa), gave in average stiffer and higher first peaks (G=7.8 MPa and τ=25.1 kPa), than blocks oriented vertically (G=4.5 MPa and τ=12.3 kPa) with low freeze-bond strengths (11.7 kPa).
    - More saline or porous ice blocks gave stronger first peak strength of rubble
    - Varying boundary conditions (applied confinement), gave varying first peak strength, but the same elastic properties (G-modulus).
    - Mohr-coulomb parameters for submerged test for the fist phase peak shear stress were: ϕ_p=28.0° and c=8830.6 Pa.
2. After the first phase, a second phase of rubble deformation started, and lasted until the end of the test. Observed behaviour was:
    - All tests displayed dilation, but tests with low confinement more than high confinement

- Rubble moved together in block assemblies, it seemed stronger freeze-bonds gave bigger block assemblies
- In average 3.3 blocks broke in each test
- Mohr-coulomb parameters for submerged tests for the average stress level over an interval (50-175 seconds) were: ϕ_c=43.3° and c=6647 Pa.
- the overall peak strength in tests was related to either the first phase peak, the breaking if one or many blocks or dilation.

From results it was concluded that the first phase is related to the breaking of freeze-bonds between blocks. The peak strength varies greatly, but systematically with different ice properties and confinement. It seems that the observed behaviour could be related to rubble properties, and is general trends for rubble material.

In the second phase it became evident that the behaviour was strongly governed by constrains of the shear box as blocks broke at the shear plane, and unphysical cohesions was measured. Since blocks clustered together in block assemblies, the effective block size grew and clearly the volume of rubble that was tested was too small to allow continuous deformation of the material.

6.2 Pile Tests

Pile tests were conducted as a part of the RITAS-project at HSVA, with the purpose of reporting model scale rubble parameters and developing and evaluating the use of the method. Pile tests were done by letting rubble form an elongated pyramid-shaped pile, and tilting it to one side to initiate a failure in the pile. Principles for slope stability were applied to evaluate results.

Eight test were conducted, and main results were:

- Piles displayed repose angles ranging from 36.0° to 47.3°.
- Cohesion for an assumed angle of friction of 30° was in the range of 172 Pa to 342 Pa.
- Cohesion developed after only 6 minutes

The repose angles are indications for internal angle of friction and were not unreasonable. Derived values for cohesion was lower than values reported in literature, this could be due to warm ice. There are several challenges with the method, and it involve simplifications that greatly affects result. Both the method and the analysing tool for the results should be developed further.

6.3 Recommendations for Further Work

The shear box testing it is well suited to investigate properties of the first deformation phase of rubble. It is doubtful whether the first phase peak stress dominates the rubble behaviour in nature, and this needs to be further investigated. The behaviour of rubble in the second phase is not well simulated by the shear box, but the process still can give some indications on rubble behaviour.

Some further work related to the shear box work could be:

- To check the deformation stiffness of single freeze-bonds. Compare for example the horizontal and the vertical oriented tests to see if the change in shear module in the shear box testing is attributed to a change in freeze-bond stiffness.
- To do testing with even larger variations in ice properties than tested in this study.
- To do field test to investigate the amount of freeze-bonded areas in rubble. Then shear box testing could be conducted with artificial rubble better simulating natural occurring rubble.
- To do shear box testing aimed at investigating dilation of rubble, and perhaps combine this with investigating the effect of ice strength
- To do shear box tests and vary other control parameters, like submersion time and deformation velocity.

The pile test has potential to give good indications on rubble properties and the set-up is simple, but some more work should be done on standardizing the method and minimizing uncertainties.

Some further work could be:

- To do pile tests under and over water, and compare results.
- To compare results from the present study with results from the buoyancy box test in the RITAS-study.
- To do finite element analysis of pile tests.
- To find the c-ϕ-relation for more slides, and evaluate the method further.
- Find a time-dependence of cohesion, and correct results for pile tests for consolidation time.

Bibliography

Astrup, O. S. (2011). Rubble properties and ad freeze-bonds in first-year ridges. Specialization Project, course TBA4550 Marine Civil Engineering.

Emdal, A., Grande, L., and Nordal, S. (2006). Geoteknikk beregningsmetoder. Kompendium for bruk i emne TBA4105 Vår 2006.

Ettema, R. and Schaefer, J. A. (1986). Experiments on freeze-bonding between ice blocks in floating ice rubble. *Journal of Glaciology*, (Vol. 32, No.112). 397-403.

Ettema, R. and Urroz-Aguirre, G. E. (1987). Simple shear box experiments with floating ice rubble. *Cold Regions Science and Technology*, (14). pp. 185-199.

Ettema, R. and Urroz-Aguirre, G. E. (1989). On internal friction and cohesion in unconsolidated ice rubble. *Cold Regions Engineering*, (16). 237-247.

Ettema, R. and Urroz-Aguirre, G. E. (1991). Friction and cohesion in ice rubble reviewed. *Cold Regions Engineering*, (12). 317-326.

Fransson, L. and Sandkvist, J. (1985). Brash ice shear properties - laboratory tests. In *Proc. of the 8th Int. Conf. on Port and Ocean Eng. under Arctic Conditions (POAC), Hamburg, Germany*, volume 1, 1: pp. 75-87.

Gale, A. D., Wong, T. T., Sego, D. C., and Morgenstern, N. R. (1987). Stress-strain behaviour of cohesionless broken ice. In *Proc. of the 9th Int. Conf. on Port and Ocean Eng. under Arctic Conditions (POAC), Fairbanks, Alaska*, volume 3, pp. 109-119.

Helgøy, H. (2011). Study of freeze-bond strength in relation to the contact surfaces for small-scale experiments. Specialization Project, course TBA4550 Marine Civil Engineering.

Helgøy, H. (2012). Experimental investigations of freeze-bonds between saline ice-blocks ice-properties and reproducibility. Master's thesis, NTNU.

Hellmann, J.-H. (1984). Basic investigations of mush ice. In *Proc. of the 7th Int. Symp. on Ice (IAHR), Hamburg, Germany*, 3 : pp. 37-55.

Houlsby, G. (1991). How the dilantancy of soils effect their behaviour. In *Soil Mechanics report*, number 121/91.

Irgens, F. (2008). *Continuum mechanics*. Springer-Verlag Berlin Heidelberg.

ISO/FDIS/19906 (2010). Petroleum and natural gas industries - arctic offshore structures. Technical report, International Standard, International Standardization organization, Geneva, Switzerland.

Ji, W. (2011). Finite element modelling of a shear box experiment in ice rubble. Master's thesis, NTNU.

Liferov, P. and Bonnemaire, B. (2005). Ice rubble behaviour and strength, Part I: Review of testing methods and interpretation of results. *Cold Regions Science and Technology*, (41, 2). 135-151.

Liferov, P. A. (2005). *First-year ice ridge scour and some aspects of ice rubble behaviour*. PhD thesis, Norwegian University of Science and Technology. 155 p.

Løset, S., Shkhinek, K. N., Gudmestad, O. T., and Høyland, K. V. (2006). *Actions from Ice on Arctic Offshore and Coastal Structures*. LAN St. Petersburg, ISBN S-8114-0703-3. 266 p.

Mellor, M. (1983). *Mechanical behavior of sea ice*. Hanover, N.H. : United States Army, Corps of Engineers, Cold Regions Research and Engineering Laboratory. 105 p.

Prodanovic, A. (1979). Model tests of rubble strength. In *Proc. of the 5th Int. Conf. on Port and Ocean Eng. under Arctic Conditions (POAC), Trondheim, Norway*, volume POAC'79, pp.89-105.

Repetto-Llamazares, A., Høyland, K. V., and Evers, K.-U. (2011). Experimental studies on shear failure of freeze-bonds in saline ice Part I: Set-up, Failure Mode and Freeze-bond Strength. *Cold Regions Science and Technology*, 65. 286-297.

RITAS-participants, Borge, J., and Lundamo, T. (2012). Daily reports from the RITAS-project.

Sayed, M. (1987). Mechanical properties of model ice rubble. In *"Materials and Member behaviour" Proceeding Structures Congress'87 Orlando, Florida, U.S.A.*, 647-659.

Sayed, M., Timco, G. W., and Sun, L. (1992). Testing model ice rubble under proportional strains. In *Offshore Mecanics and Artic Engineering (OMAE 92)*, pp. 335-341.

Serré, N., Liferov, P., and Jochmann, P. (2009). Model testing of ridge keel loads on strucutres Part III: Investigation of model ice rubble mechanical properties. In *Proc. of the 20th Int. Conf. on Port and Ocean Eng. under Arctic Conditions (POAC), Luleå, Sweden*, volume Paper #150.

Serré, N., Repetto-Llamazares, A. H. V., and Høyland, K. V. (2011). Experiments on the relation between freeze-bonds and ice rubble strength part I: Shear box experiments. In *Proc. of the 21th Int. Conf. on Port and Ocean Eng. under Arctic Conditions (POAC), Montreal, Canada*, volume Abstract submitted.

Shafrova, S. (2007). Initial failure of the ice rubble in plain strain direct shear tests. In *Proc. of the 19th Int. Conf. on Port and Ocean Eng. under Arctic Conditions (POAC), Dalian, China*, 1: pp. 256-266, ISBN 978-7-5611-3631-7.

Timco, G. W. and Cornet, A. (1999). Is ϕ a constant for broken ice rubble? In *Proc. of the 10th Workshop on River Ice, Winnipeg, Candada*, pp. 318-331.

Timco, G. W., E. R. Funke, M. S., and Laurich, P. H. (1992). A laboratory apparatus to measure the behaviour of ice rubble. In *Proc. Offshore Mechanics and Artic Engineering (OMAE'92), Calgary, Canada*, volume IV, pp. 369-375.

Weiss, R., Prodanovic, A., and Wood, K. (1981). Determination of ice rubble shear porperties. In *Proc. of the 6th Int. Symp. on Ice (IAHR), Quebec, Canada*, pp. 860-870.

Wong, T. T., Morgenstern, N. R., and Sego, D. C. (1990). A constitutive model for broken ice. *Cold Regions Science and Technology*, (17). pp. 241-252.

A Task Description

NTNU
Fakultet for ingeniørvitenskap og teknologi
Institutt for bygg, anlegg og transport

MASTER DEGREE THESIS

Spring 2012
for

Student: Oda Skog Astrup

Experimental Investigations of Ice Rubble: Shear Box and Pile Testing

BACKGROUND
First year ice ridges are characteristics for sea areas with seasonal ice cover, and an encounter with such a feature may give the dimensioning load for ships and structures located in these waters. An ice ridge consists of broken ice blocks that are fully or partly frozen together. To investigate the unconsolidated rubble material in the laboratory, one often use shear boxes. Pile tests are used to easily access material properties.

TASK DESCRIPTION
The goal of the thesis is to investigate rubble behaviour by experimental and analytical methods, using two tests: the shear box test and the pile test. This includes a literature study on the mechanical properties of ice rubble, earlier shear box studies, scaling and other aspects of forming experiments. Set-ups for two experiments must be formed: Shear box testing at NTNU and pile testing at HSVA.

Laboratory work in the cold lab at NTNU is aimed at finding relations between single freeze-bond testing and shear box testing. In combination with single freeze-bond testing, variations in rubble behaviour in relation to submersion water temperature and block orientation should be investigated. In addition general rubble behaviour and the influence of the set-up should be studied.

Laboratory work at HSVA (Hamburg Ship Model Basin) is a part of the collaboration project about rubble transport on arctic structures (RITAS), and must be planned in respect to this. Pile tests should be used to access rubble parameters by simple observations and by using principles of slope stability. The time dependence of cohesion in a pile, and the potential for the method should be considered.

NTNU
Fakultet for ingeniørvitenskap og teknologi
Institutt for bygg, anlegg og transport

General about content, work and presentation

The text for the master thesis is meant as a framework for the work of the candidate. Adjustments might be done as the work progresses. Tentative changes must be done in cooperation and agreement with the professor in charge at the Department.

In the evaluation thoroughness in the work will be emphasized, as will be documentation of independence in assessments and conclusions. Furthermore the presentation (report) should be well organized and edited; providing clear, precise and orderly descriptions without being unnecessary voluminous.

The report shall include:

- Standard report front page (from DAIM, http://daim.idi.ntnu.no/)
- Title page with abstract and keywords.(template on: http://www.ntnu.no/bat/skjemabank)
- Preface
- Summary and acknowledgement. The summary shall include the objectives of the work, explain how the work has been conducted, present the main results achieved and give the main conclusions of the work.
- Table of content including list of figures, tables, enclosures and appendices.
- If useful and applicable a list explaining important terms and abbreviations should be included.
- The main text.
- Clear and complete references to material used, both in text and figures/tables. This also applies for personal and/or oral communication and information.
- Text of the Thesis (these pages) signed by professor in charge as Attachment 1..
- The report musts have a complete page numbering.

Advice and guidelines for writing of the report is given in: "Writing Reports" by Øivind Arntsen. Additional information on report writing is found in "Råd og retningslinjer for rapportskriving ved prosjekt og masteroppgave ved Institutt for bygg, anlegg og transport" (In Norwegian). Both are posted posted on http://www.ntnu.no/bat/skjemabank

Submission procedure

Procedures relating to the submission of the thesis are described in DAIM (http://daim.idi.ntnu.no/). Printing of the thesis is ordered through DAIM directly to Skipnes Printing delivering the printed paper to the department office 2-4 days later. The department will pay for 3 copies, of which the institute retains two copies. Additional copies must be paid for by the candidate / external partner.

On submission of the thesis the candidate shall submit a CD with the paper in digital form in

NTNU
Fakultet for ingeniørvitenskap og teknologi
Institutt for bygg, anlegg og transport

pdf and Word version, the underlying material (such as data collection) in digital form (eg. Excel). Students must submit the submission form (from DAIM) where both the Ark-Bibl in SBI and Public Services (Building Safety) of SB II has signed the form. The submission form including the appropriate signatures must be signed by the department office before the form is delivered Faculty Office.

Documentation collected during the work, with support from the Department, shall be handed in to the Department together with the report.

According to the current laws and regulations at NTNU, the report is the property of NTNU. The report and associated results can only be used following approval from NTNU (and external cooperation partner if applicable). The Department has the right to make use of the results from the work as if conducted by a Department employee, as long as other arrangements are not agreed upon beforehand.

Tentative agreement on external supervision, work outside NTNU, economic support etc.
Separate description to be developed, if and when applicable. See http://www.ntnu.no/bat/skjemabank for agreement forms.

Health, environment and safety (HSE) http://www.ntnu.edu/hse
NTNU emphasizes the safety for the individual employee and student. The individual safety shall be in the forefront and no one shall take unnecessary chances in carrying out the work. In particular, if the student is to participate in field work, visits, field courses, excursions etc. during the Master Thesis work, he/she shall make himself/herself familiar with " Fieldwork HSE Guidelines". The document is found on the NTNU HMS-pages at http://www.ntnu.no/hms/retningslinjer/HMSR07E.pdf

The students do not have a full insurance coverage as a student at NTNU. If you as a student want the same insurance coverage as the employees at the university, you must take out individual travel and personal injury insurance.

Start and submission deadlines
The work on the Master Thesis starts on January 16, 2012

The thesis report as described above shall be submitted digitally in DAIM at the latest at 3pm June 11, 2012

Professor in charge: Knut Høyland

Other supervisors:

NTNU
Fakultet for ingeniørvitenskap og teknologi
Institutt for bygg, anlegg og transport

Trondheim, January 16, 2012. (revised: 07.06.2012)

Professor in charge (sign)

B Force-time Plots Shear Box

B.1 Series SB1000

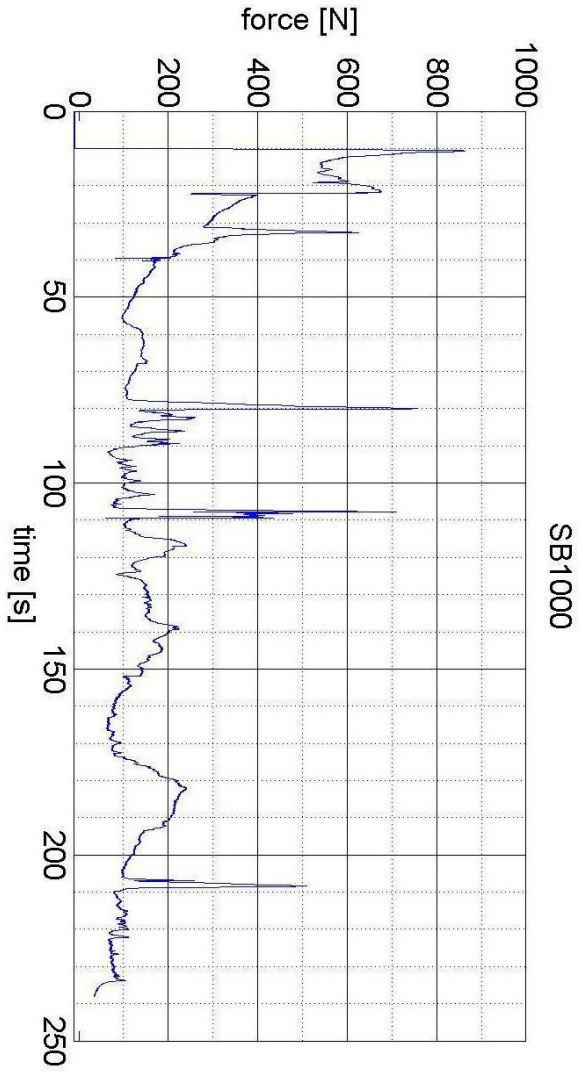

Figure 58

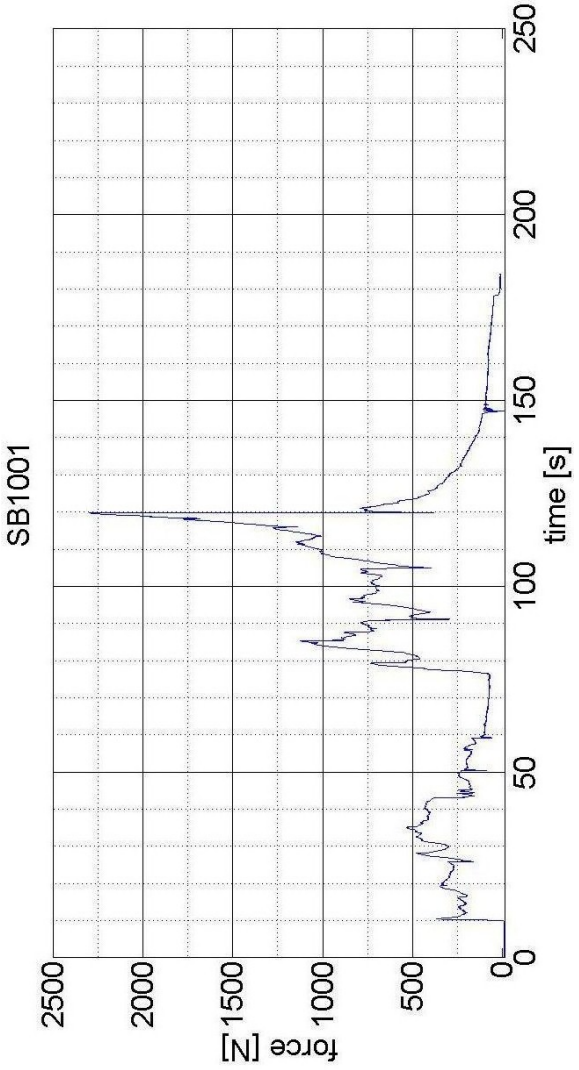
SB1001
force [N]
time [s]
0
500
1000
1500
2000
2500
0
50
100
150
200
250

Figure 59

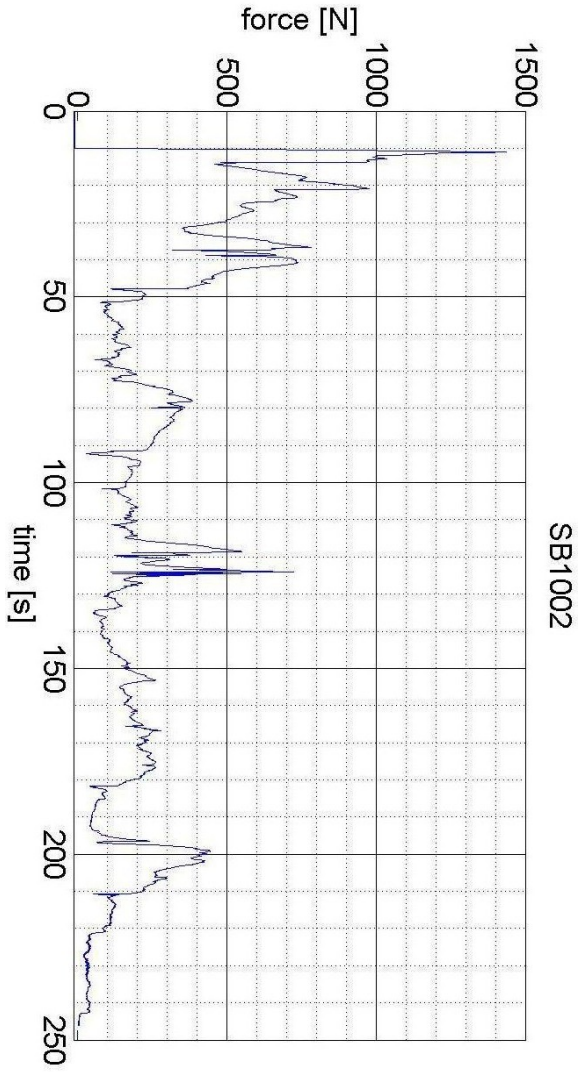

Figure 60

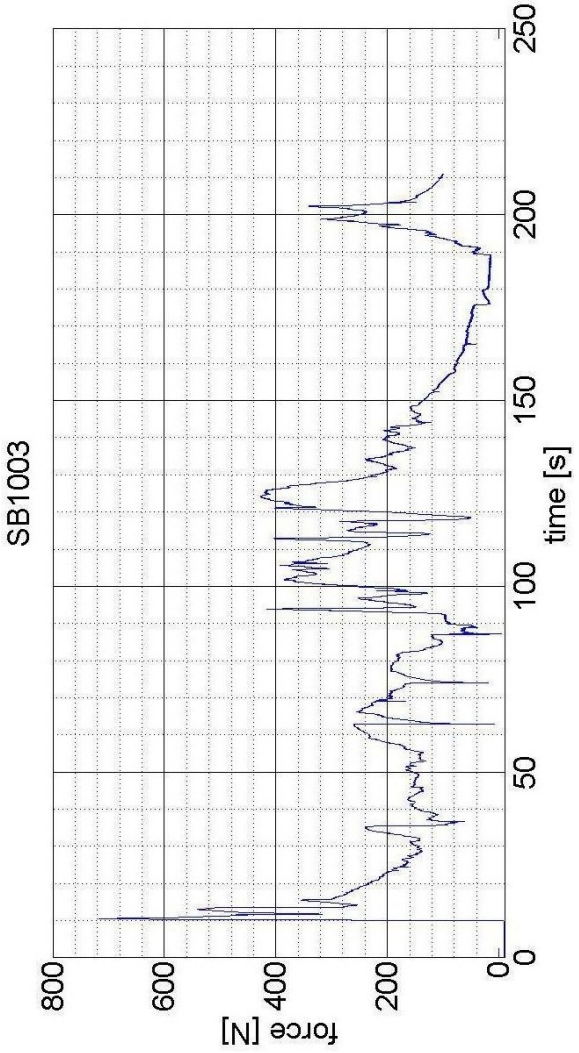

Figure 61

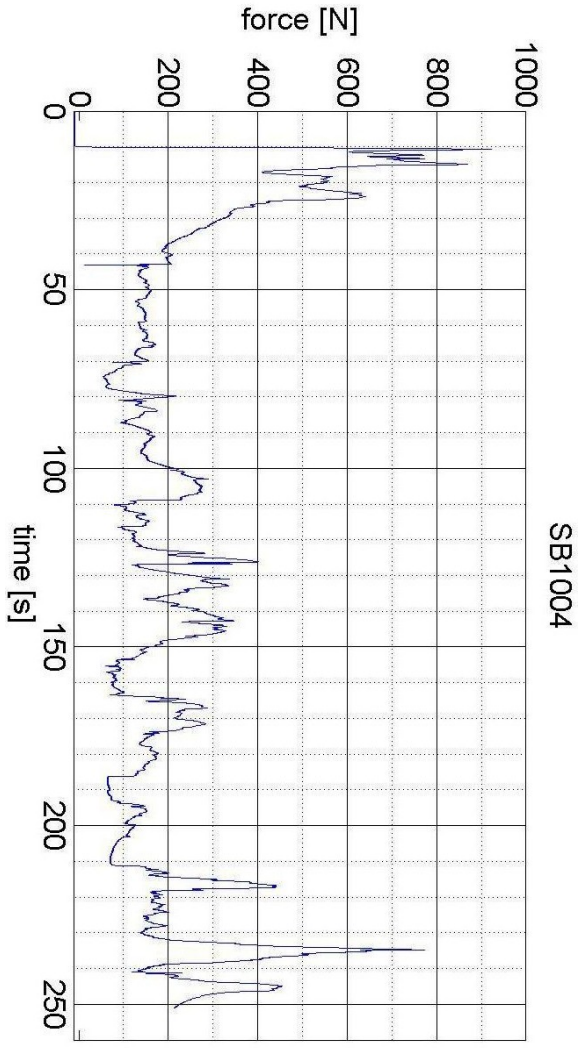

Figure 62

B.2 Series SB2000

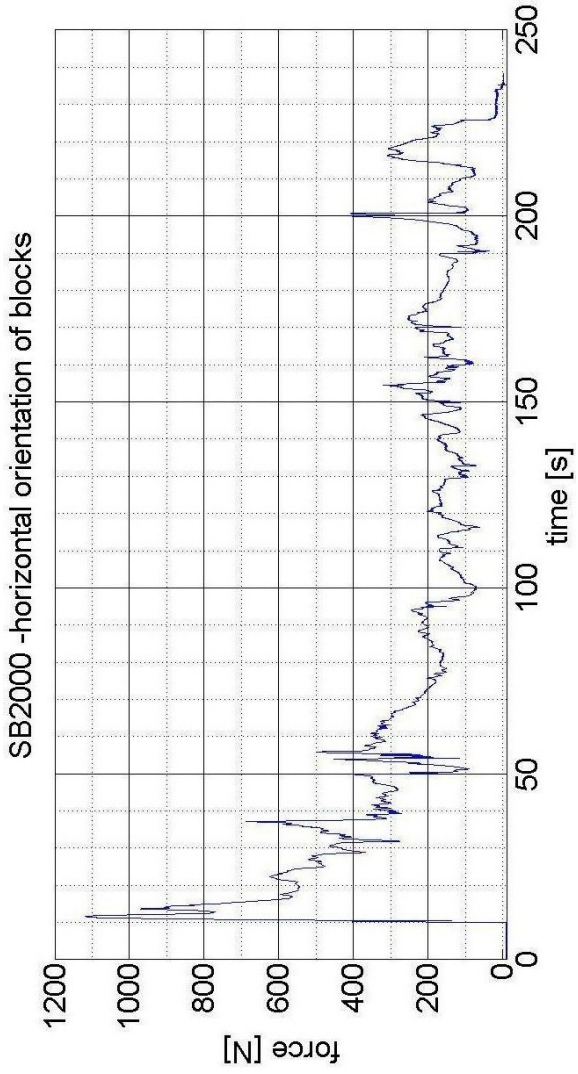

Figure 63

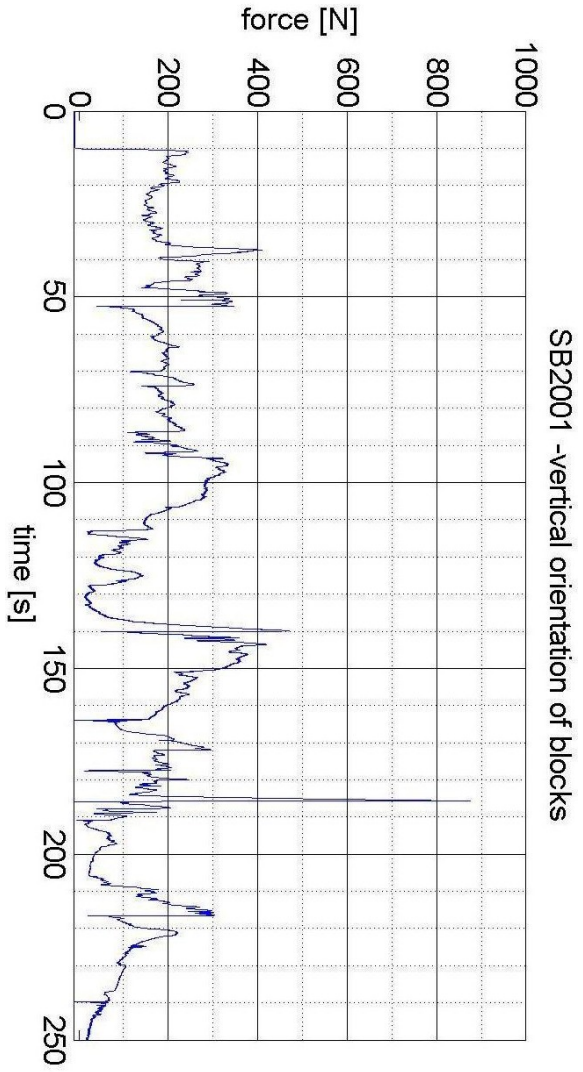
force [N]
0
200
400
600
800
1000
time [s]
0
50
100
150
200
250
SB2001 -vertical orientation of blocks

Figure 64

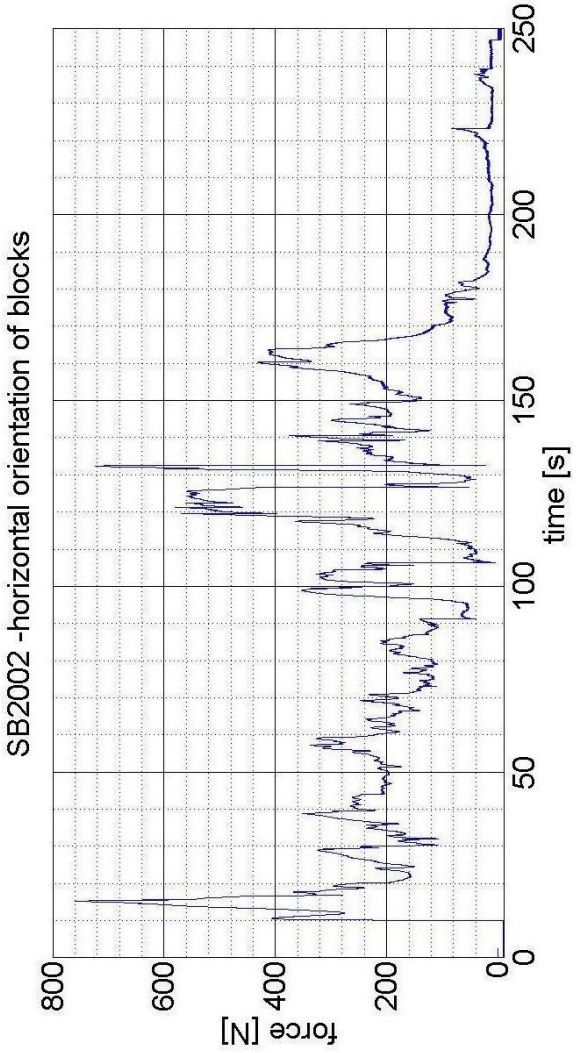
SB2002 -horizontal orientation of blocks
force [N]
time [s]
0
200
400
600
800
0
50
100
150
200
250

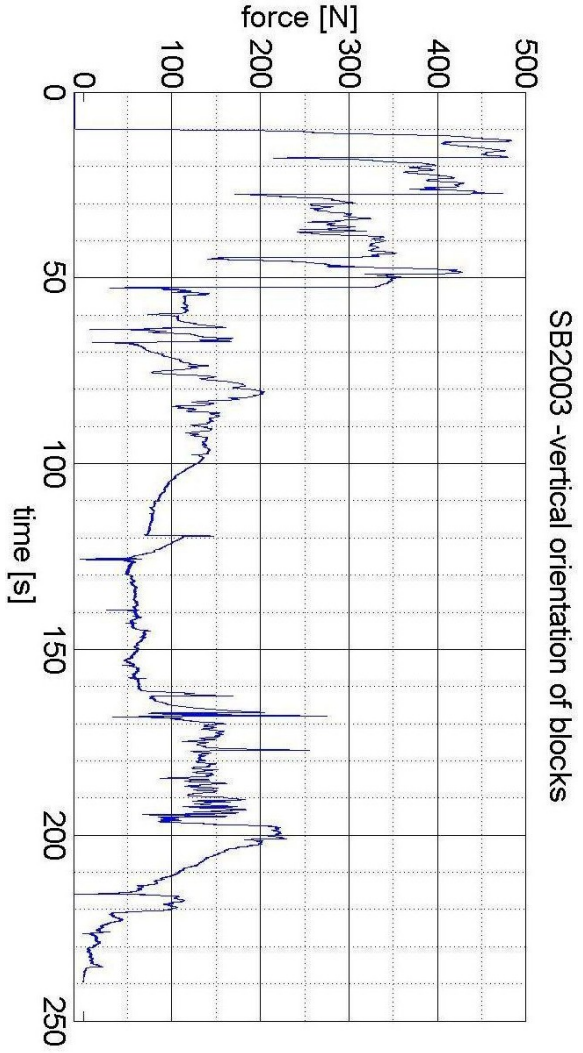
force [N]
0
100
200
300
400
500
time [s]
0
50
100
150
200
250
SB2003 -vertical orientation of blocks

Figure 65

B.3 Series SB3000

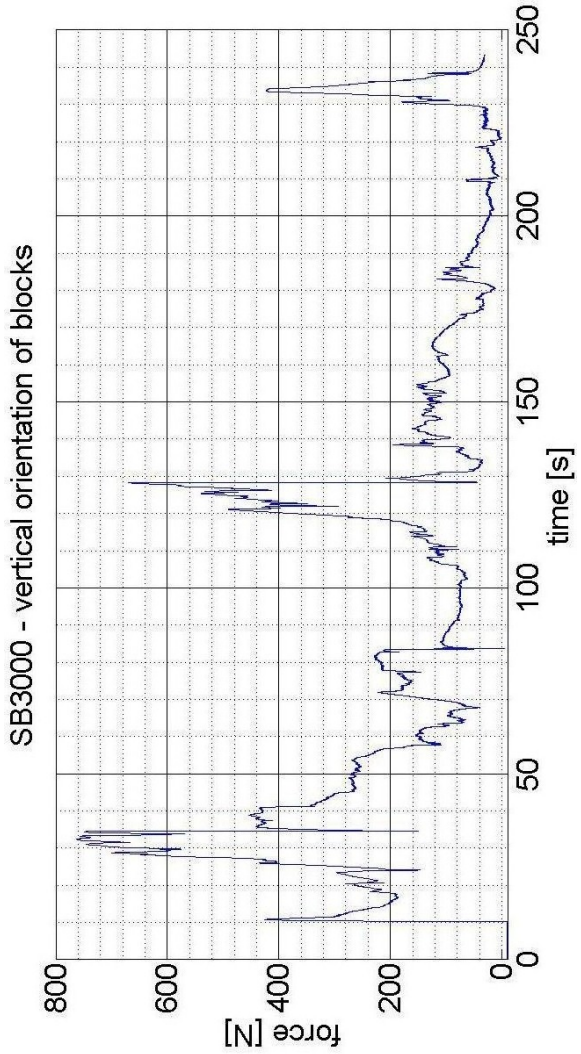

Figure 66

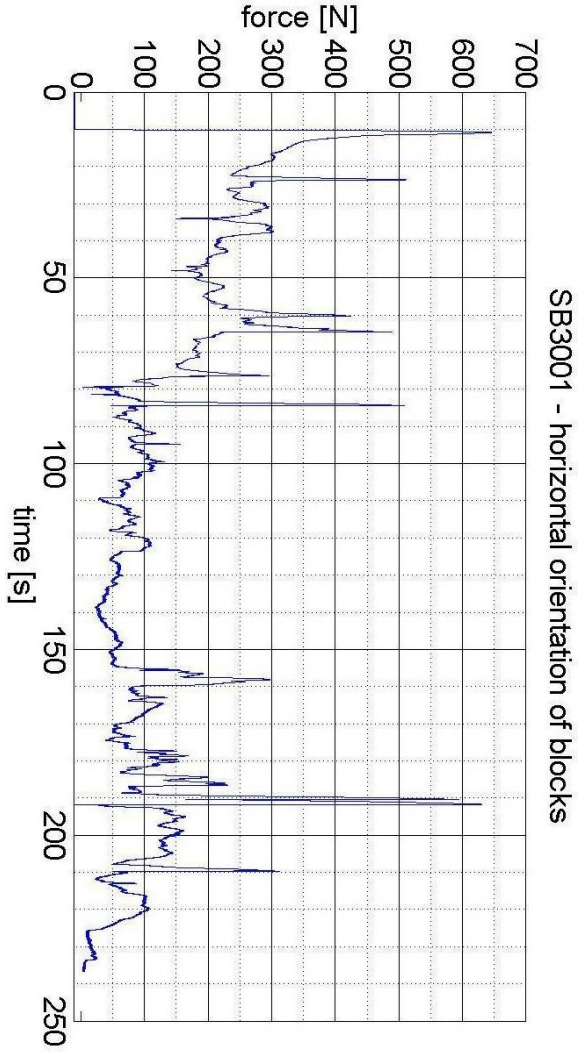
force [N]
0
100
200
300
400
500
600
700
time [s]
0
50
100
150
200
250
SB3001 - horizontal orientation of blocks

Figure 67

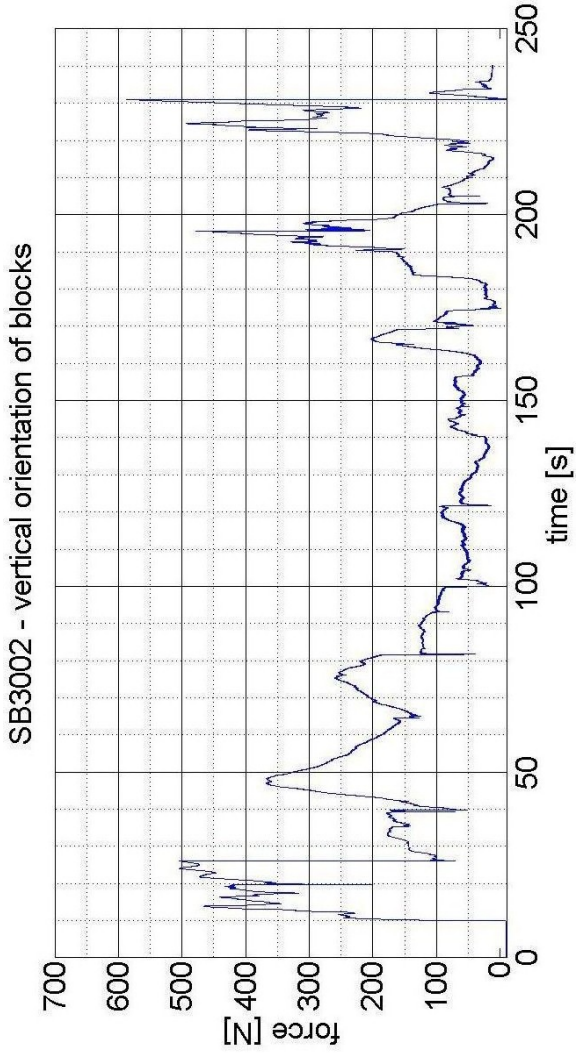
SB3002 - vertical orientation of blocks
force [N]
0
100
200
300
400
500
600
700
0
50
100
150
200
250
time [s]

Figure 68

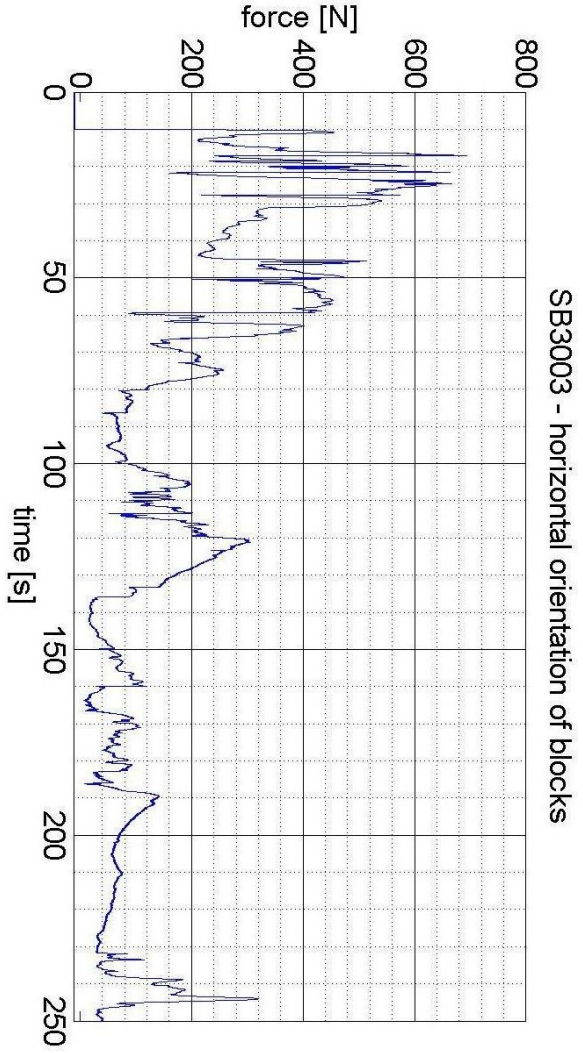
force [N]
0
200
400
600
800
time [s]
0
50
100
150
200
250
SB3003 - horizontal orientation of blocks

Figure 69

B.4 Series SB4000

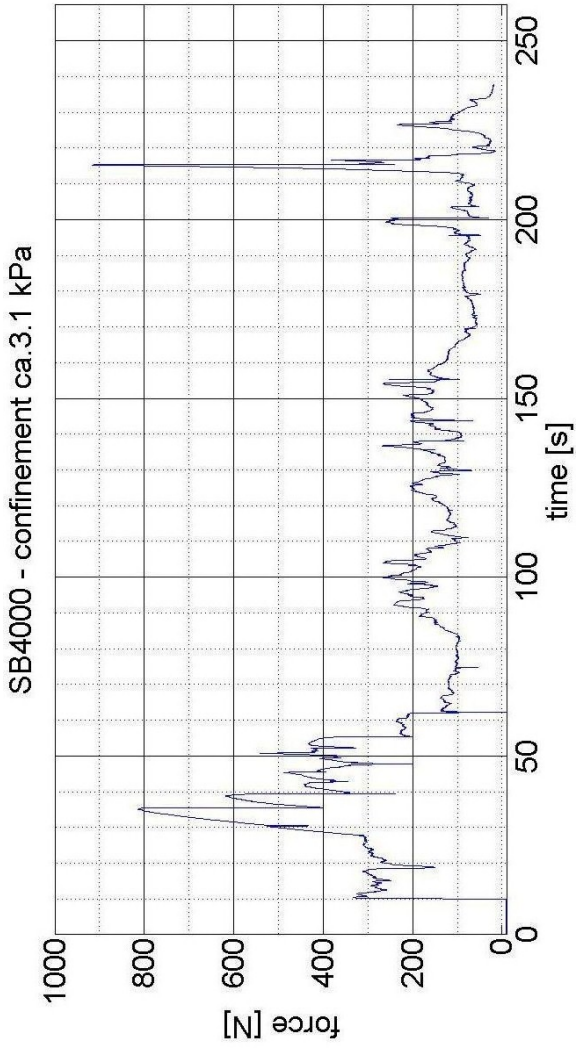

Figure 70

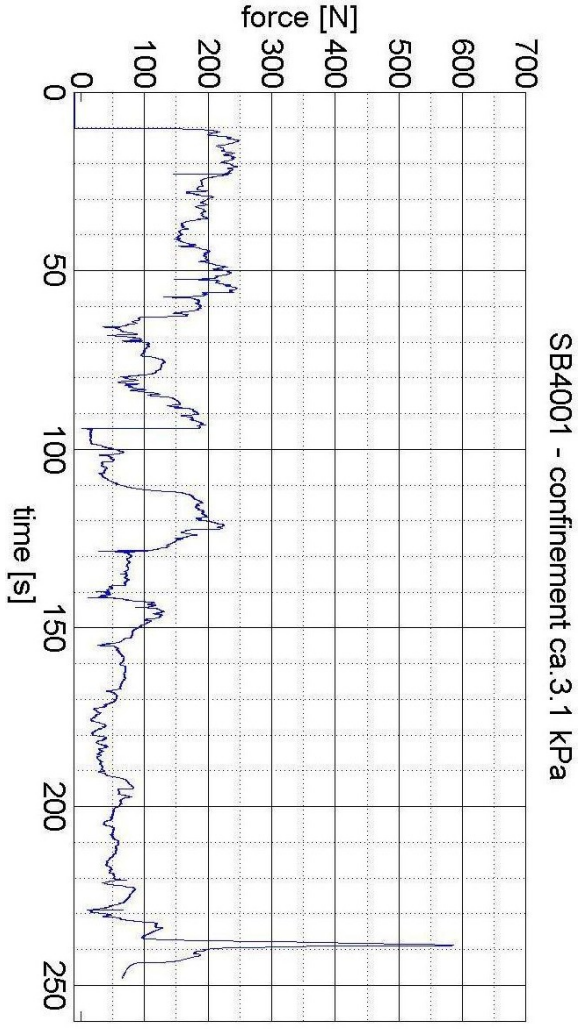
force [N]
0
100
200
300
400
500
600
700
time [s]
0
50
100
150
200
250
SB4001 - confinement ca.3.1 kPa

Figure 71

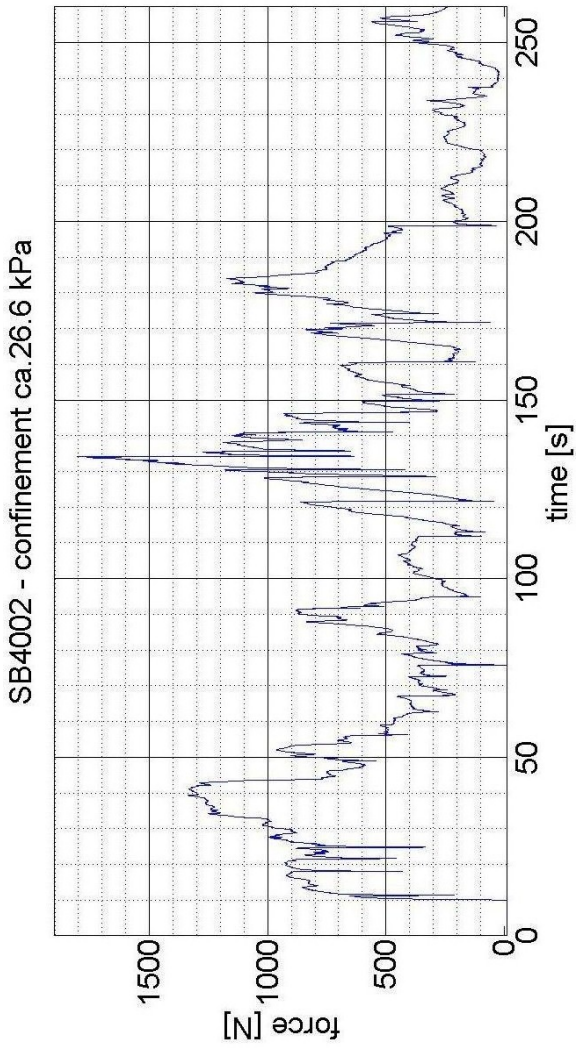
SB4002 - confinement ca.26.6 kPa
force [N]
0
500
1000
1500
0
50
100
150
200
250
time [s]

Figure 72

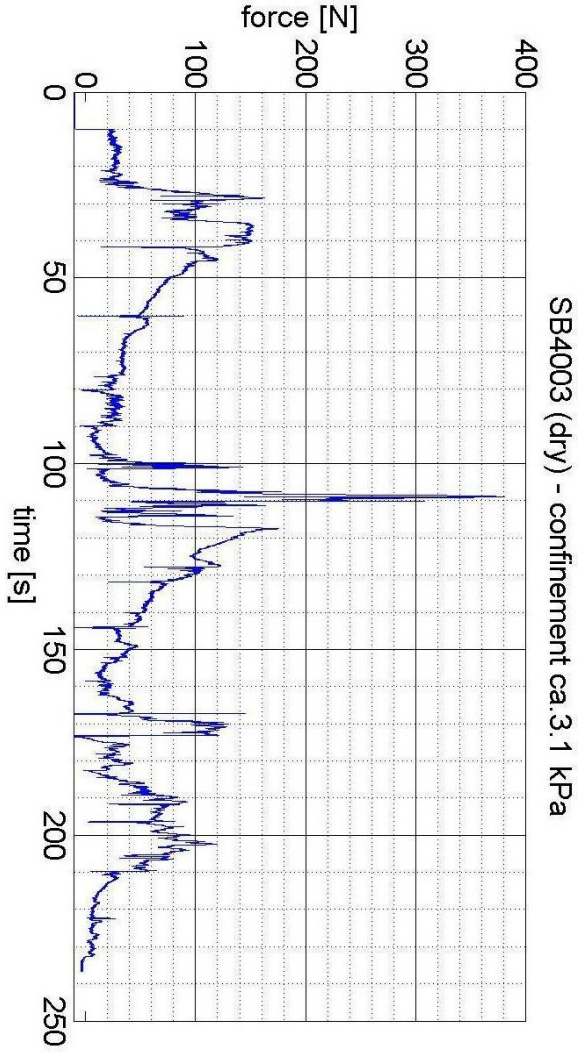
force [N]
0
100
200
300
400
time [s]
0
50
100
150
200
250
SB4003 (dry) - confinement ca.3.1 kPa

Figure 73

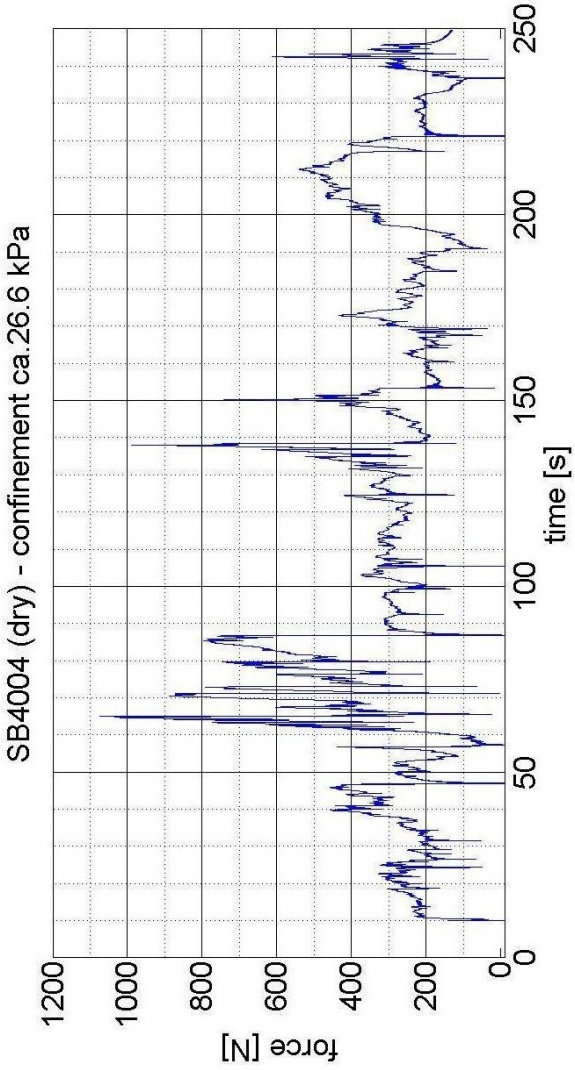
SB4004 (dry) - confinement ca.26.6 kPa
force [N]
time [s]
0
200
400
600
800
1000
1200
0
50
100
150
200
250

Figure 74

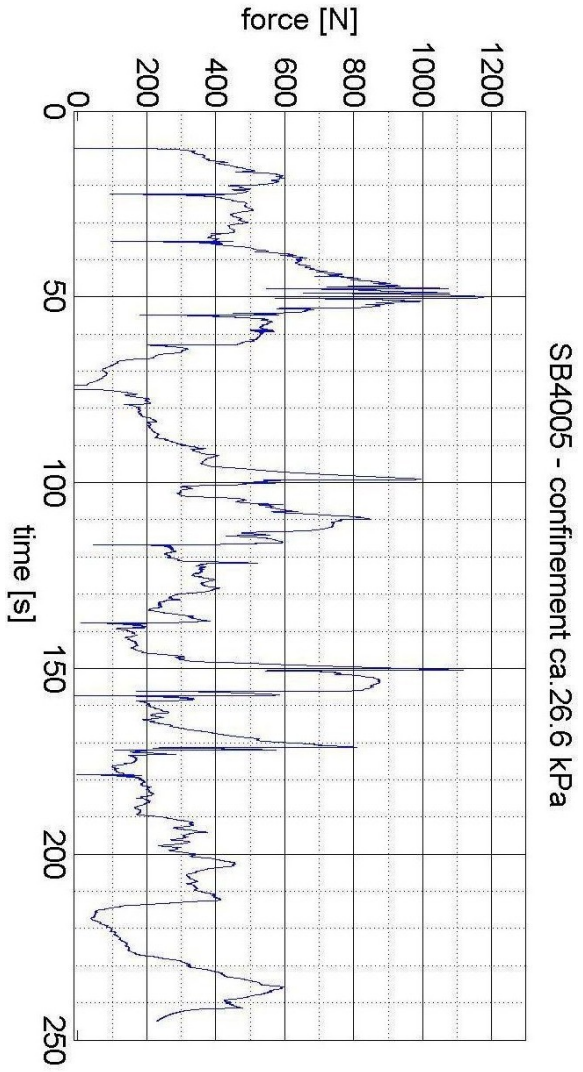
force [N]
0
200
400
600
800
1000
1200
time [s]
0
50
100
150
200
250
SB4005 - confinement ca.26.6 kPa

Figure 75

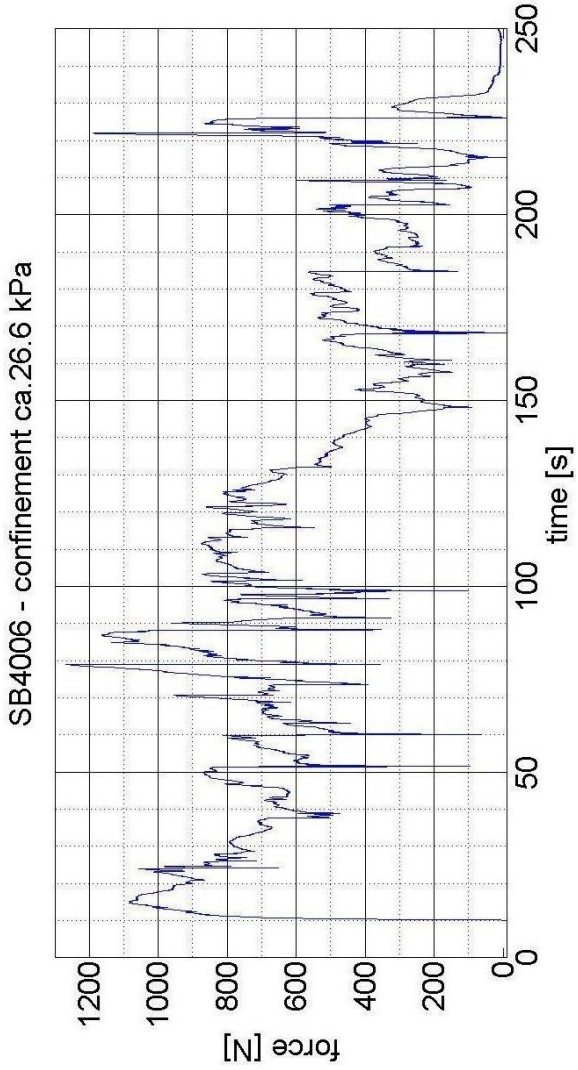
SB4006 - confinement ca.26.6 kPa
force [N]
time [s]
0
200
400
600
800
1000
1200
0
50
100
150
200
250

Figure 76

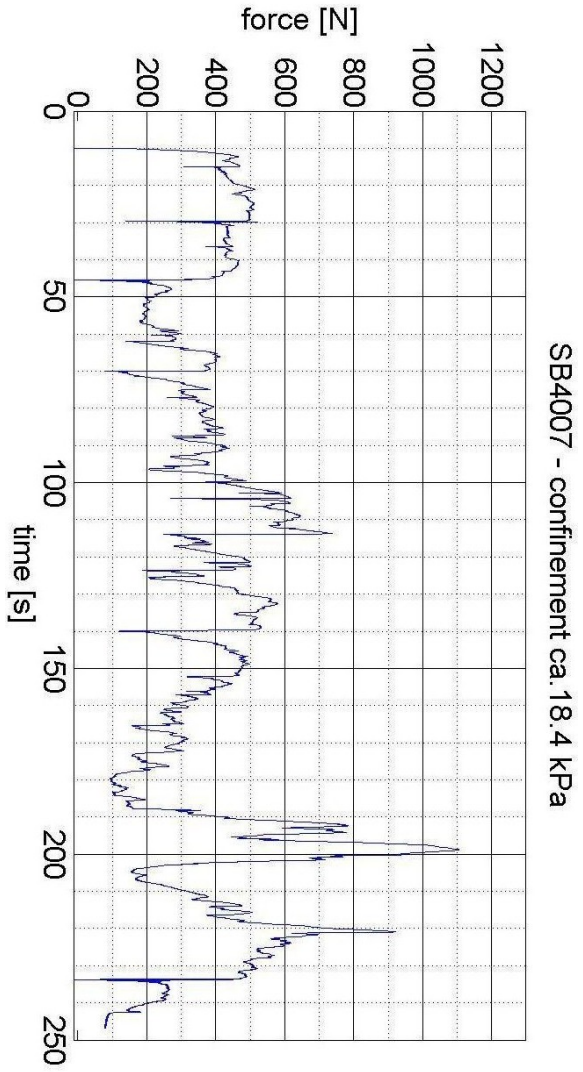
force [N]
0
200
400
600
800
1000
1200
time [s]
0
50
100
150
200
250
SB4007 - confinement ca.18.4 kPa

Figure 77

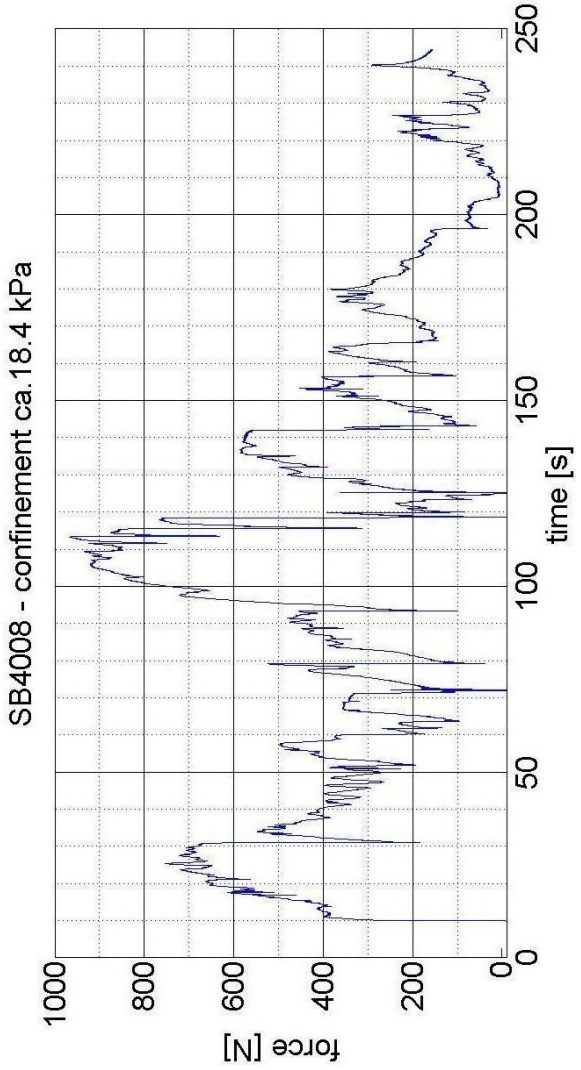
SB4008 - confinement ca.18.4 kPa
force [N]
time [s]
0
200
400
600
800
1000
0
50
100
150
200
250

Figure 78

C Thin Sections

C.1 Ice type 1

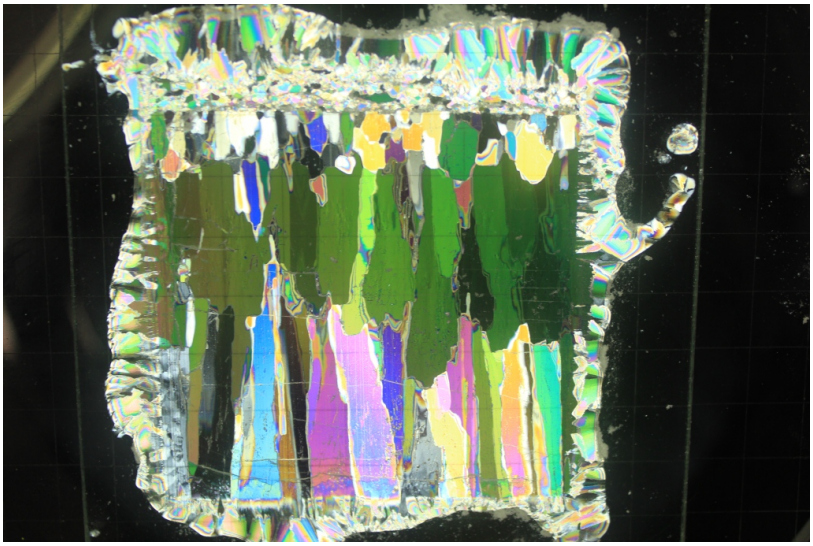

Figure 79: Upper 6 cm

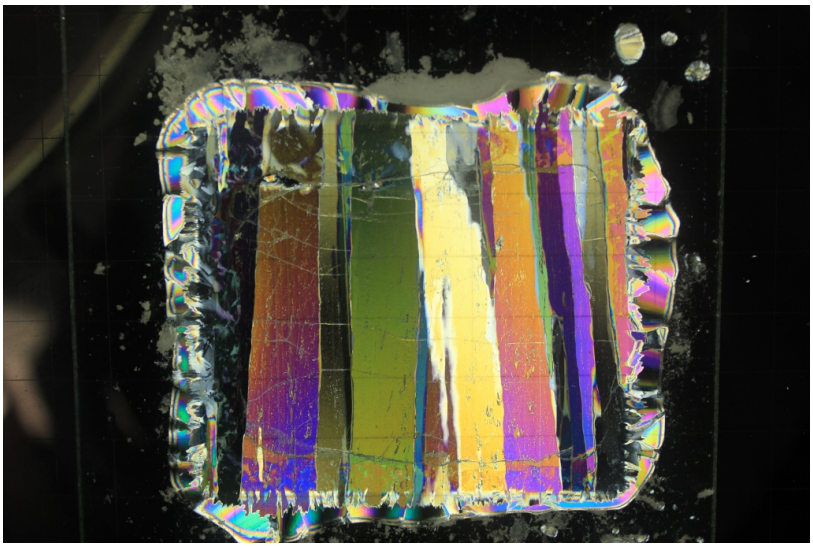

Figure 80: Middle 6 cm

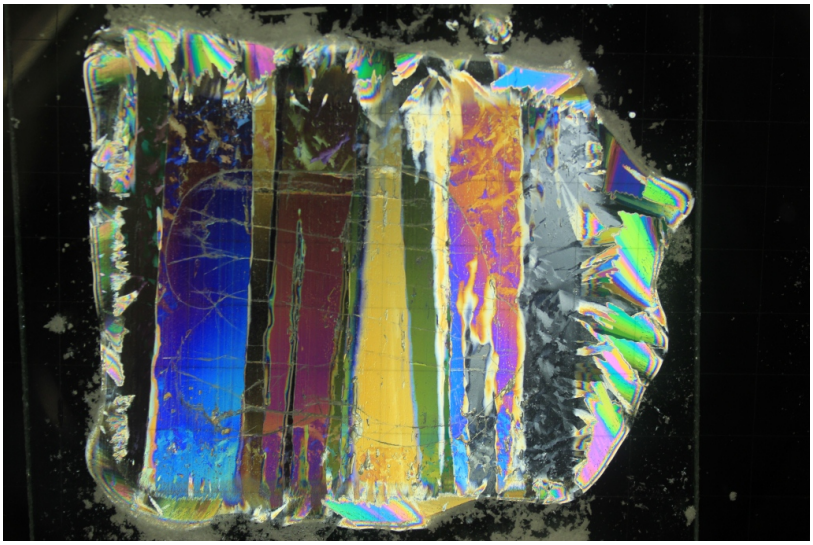

Figure 81: Lower 6 cm

C.2 Ice type 2

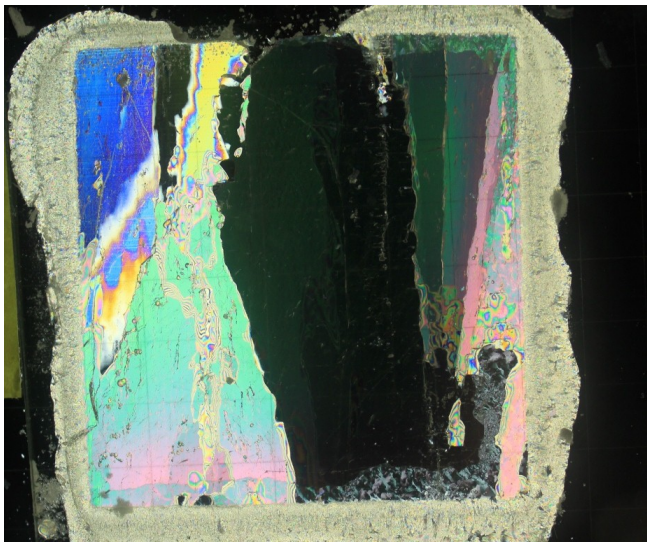

Figure 82: Upper 7 cm

Figure 83: Lower 7 cm

C.3 Ice type 3

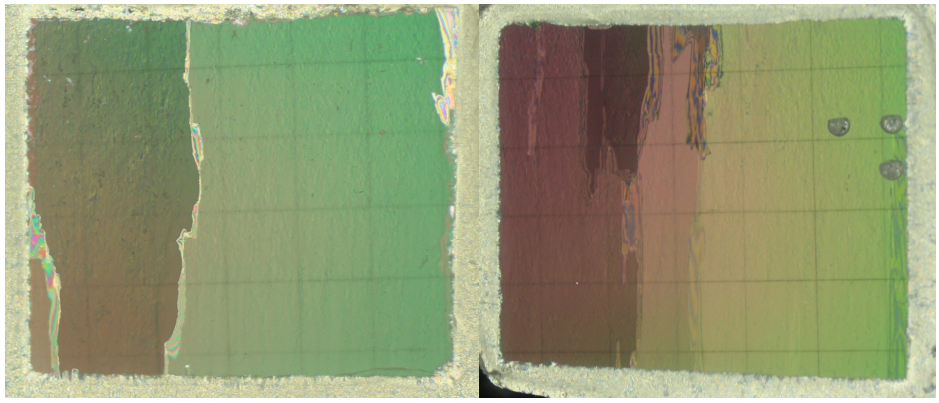

(a) (b)

Figure 84: Upper 5 cm

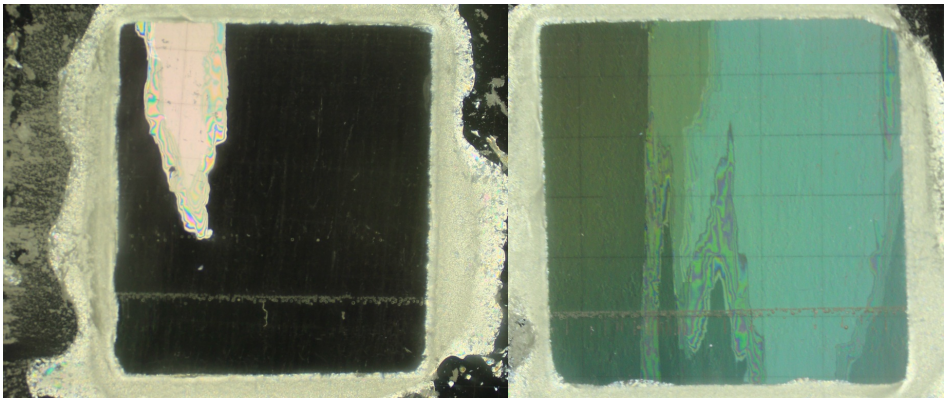

(a) (b)

Figure 85: Lower 5 cm

C.4 Block assemblies from shear box

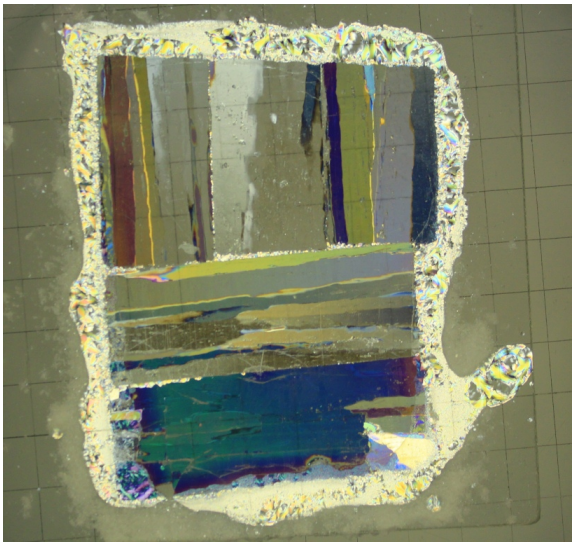

Figure 86: Block assembly from SB1000, vertically oriented blocks

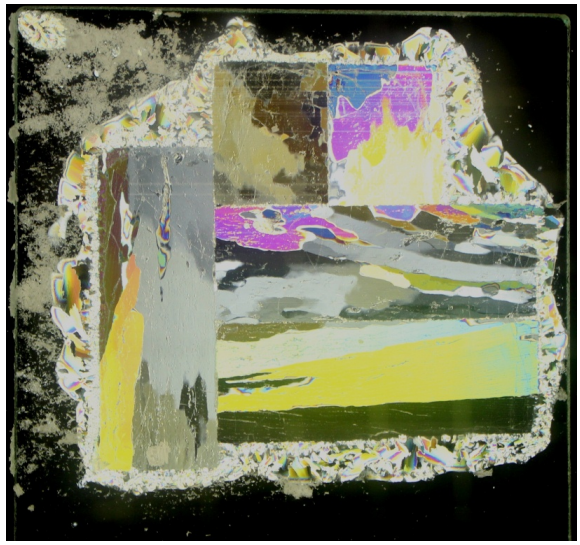

(a) Vertically oriented blocks

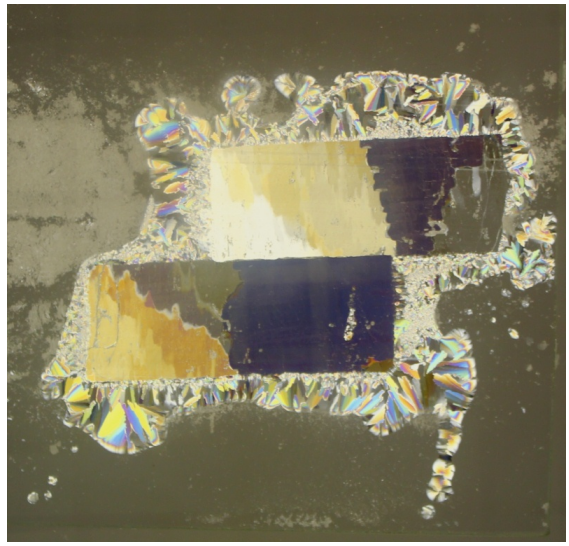

(b) Horizontally oriented blocks

Figure 87: Block assembly from (a) SB3000 and (b) SB3001

D Data from Shear Box Testing

NAME	Control parameters					
	Date	Temp. Basin [C]	Ice type	Confinement [kPa]	Orientation of blocks	Porosity SB
SERIES 1000						
SB1000	7. feb.	warm (-0,43)	1	3,07	vertical	0,239
SB1001	7. feb.	warm (-0,43)	1	3,07	vertical	0,202
SB1002	8. feb.	cold(-0,53)	1	3,07	vertical	0,230
SB1003	8. feb.	cold(-0,54)	1	3,07	vertical	0,212
SB1004	8. feb.	cold (-0,53)	1	3,07	vertical	0,239
SERIES 2000						
SB2000	15. feb.	-0,51	2	3,07	horizontal	0,194
SB2001	15. feb.	-0,5	2	3,07	vertical	0,195
SB2002	15. feb.	-0,53	2	3,07	horizontal	0,186
SB2003	15. feb.	-0,54	2	3,07	vertical	0,233
SERIES 3000						
SB3000	16. feb.	-0,44	2	3,07	vertical	0,225
SB3001	16. feb.	-0,44	2	3,07	horizontal	0,225
SB3002	16. feb.	-0,44	2	3,07	vertical	0,252
SB3003	16. feb.	-0,44	2	3,07	horizontal	0,260
SERIES 4000						
SB4000	23. feb.	-0,52	3	3,07	horizontal	0,218
SB4001	23. feb.	-0,52	3	3,07	horizontal	0,243
SB4002	23. feb.	-0,52	3	26,57	horizontal	0,208
SB4003	23. feb.	(tørr)	3	3,07	horizontal	0,216
SB4004	23. feb.	(tørr)	3	26,57	horizontal	0,203
SB4005	23. feb.	-0,52	3	26,57	horizontal	0,249
SB4006	23. feb.	-0,52	3	26,57	horizontal	0,245
SB4007	23. feb.	-0,52	3	18,39	horizontal	0,226
SB4008	23. feb.	-0,52	3	18,39	horizontal	0,269
AVERAGE						

NAME	Block properties							
	Number of blocks	H_rubble [mm]	L_block [mm]	B_block [mm]	t_block [mm]	Weigth block (dry) [g]	Density block [g/cm3]	Temp. block [C]
SERIES 1000								
SB1000	141	400	58,9	39	22	49,5	0,9795	
SB1001	146	395	58,9	39	22	49,5	0,9795	
SB1002	139	390	58,9	39	22	49,5	0,9795	
SB1003	146	400	58,9	39	22	49,5	0,9795	
SB1004	141	400	58,9	39	22	49,5	0,9795	
SERIES 2000								
SB2000	134	380	59,9	38,9	22,9	44,4	0,8321	-6,60
SB2001	135	390	60,9	35,9	22,9	43,9	0,8768	-5,60
SB2002	134	370	58,9	38,9	22,9	43	0,8195	-6,20
SB2003	132	400	60,9	35,9	22,9	43,8	0,8748	-6,20
SERIES 3000								
SB3000	130	390	60,9	40,9	22,9	46,2	0,8100	-5,70
SB3001	140	395	59,9	38,9	21,9	45	0,8818	-6,20
SB3002	125	380	60,9	40,4	22,4	46	0,8347	
SB3003	132	390	59,9	38,9	21,9	44,3	0,8681	
SERIES 4000								
SB4000	143	380	58,95	38,65	21,15			
SB4001	142	390	58,95	38,65	21,15			
SB4002	141	370	58,95	38,65	21,15			
SB4003	149	395	58,95	38,65	21,15			
SB4004	140	365	58,95	38,65	21,15			
SB4005	141	390	58,95	38,65	21,15			
SB4006	138	380	58,95	38,65	21,15			
SB4007	149	400	58,95	38,65	21,15			
SB4008	139	395	58,95	38,65	21,15			
AVERAGE								-6,08

NAME	Submerging time		Salinity			
	Time down	Time up	Salinity (dry) block [ppt]	Sal. wet block (top SB) [ppt]	Sal. wet block (Bottom SB) [ppt]	sal. Basin [ppt]
SERIES 1000						
SB1000	14:28:00	14:38:00		2,38		
SB1001	16:25:00	16:35:00		2,02	2,16	8,14 ppt
SB1002	12:33:00	12:43:00		2,83		8,30 ppt
SB1003	13:09:30	13:19:30		2,37		
SB1004	13:50:50	14:00:50		2,82		
SERIES 2000						
SB2000	14:21:10	14:31:10	2,13	1,51	1,38	
SB2001	15:04:50	15:14:50	2,11	2,08	1,78	
SB2002	16:11:00	16:21:00		2,58	2,22	
SB2003	16:54:10	17:04:10		1,7	2,05	
SERIES 3000						
SB3000	13:13:20	13:23:20	1,65	2,3	2,65	
SB3001	13:52:35	14:02:35	1,45	2,2	1,84	
SB3002	14:29:45	14:39:25		1,18	1,62	
SB3003	15:42:25	15:52:25		2,33	1,19	
SERIES 4000						
SB4000	09:29:10	09:39:10	0,63	1,6	1,36	8,5 (kl11.50)
SB4001	10:05:00	10:15:00	0,63	0,85	0,76	
SB4002	10:57:10	11:07:10	0,63	0,92	0,73	
SB4003			0,63			
SB4004			0,63			
SB4005	13:21:00	13:31:00	0,63	0,81	0,94	
SB4006	13:56:10	14:06:10	0,63	0,68	0,83	
SB4007	15:09:30	15:19:30	0,63	1,33	1,32	
SB4008	15:45:10	15:55:10	0,63	1,12	0,78	
AVERAGE						8,31

	Velocity				First Phase			
NAME	Aveerage velocity [mm/s]	std velocity [mm/s]	Velocity check	system friction [N]	Peak load [N]	Sec. after start [s]	peak stress phase 1 [Pa]	G [MPa]
SERIES 1000								
SB1000	2,06	0,13	OK	9,7	34	0,06	35995,83	10,39
SB1001	1,81	0,56	OK	9,7	400	0,36	15283,33	6,35
SB1002	1,95	0,34	OK	9,7	342	0,43	59775,00	9,42
SB1003	1,84	0,59	OK	9,7	727	0,49	29887,50	8,22
SB1004	1,96	0,19	OK	9,7	376,5	0,51	38454,17	10,08
SERIES 2000								
SB2000	1,90	0,21	OK	9,7	415	0,57	37500,00	7,74
SB2001	2,02	0,26	LOWER	9,7	435	0,62	10012,50	4,62
SB2002	1,83	0,40	OK	9,7	932,6	0,65	16887,50	7,34
SB2003	2,08	0,29	OK	9,7	873,6	0,67	11179,17	3,50
SERIES 3000								
SB3000	1,97	0,36	OK	9,7	357,5	0,80	17720,83	5,72
SB3001	2,02	0,35	OK	9,7	655	0,83	26887,50	8,58
SB3002	1,93	0,54	OK	9,7	250	0,84	10220,83	4,19
SB3003	1,90	0,21	OK	9,7	255	0,84	18970,83	7,69
SERIES 4000								
SB4000	2,01	0,29	OK	9,7	465	0,85	13845,83	6,23
SB4001	1,99	0,20	OK	9,7	224	1,00	8929,17	4,55
SB4002	1,80	0,42	OK	17,8	236	1,00	27175,00	5,91
SB4003	2,04	0,26	OK	9,7	411	1,00	1012,50	2,29
SB4004	1,98	0,21	OK	17,8	1444,3	1,08	9091,67	3,89
SB4005	1,89	0,50	OK	17,8	670	1,33	14154,17	5,27
SB4006	1,98	0,10	OK	17,8	480	2,27	30966,67	6,54
SB4007	1,99	0,24	OK	14,8	492	3,15	15341,67	4,16
SB4008	2,01	0,25	OK	14,8	1100	4,81	16508,33	6,77
AVERAGE	1,95	0,31						

NAME		Maximum stress			
	Average stress (50-175 s) [Pa]	Max load [N] [N]	sec. after start [s]	Max stress [Pa]	Broken blocks
SERIES 1000					
SB1000		863,9	0,6	36067,97	4
SB1001		2297	109,7	150880,19	3
SB1002		1435	1,08	60007,69	5
SB1003		717,3	0,5	29937,40	4
SB1004		922,9	1,6	38660,36	4
SERIES 2000					
SB2000		1118	1,6	46833,11	4
SB2001		875,6	175,8	34531,16	3
SB2002		759,7	5,3	32223,45	4
SB2003		483	3,2	20341,98	3
SERIES 3000					
SB3000		762	22,5	34324,32	2
SB3001		645,5	0,91	26977,67	4
SB3002		587,7	221	22226,14	2
SB3003		693,4	7,1	29592,01	4
SERIES 4000					
SB4000	923055,56	915,6	205,3	37054,72	3
SB4001	595277,78	585,4	228,6	10476,44	1
SB4002	1811666,67	1807	124,3	128557,20	over 10
SB4003	67500,00	308,7	99	19197,76	0
SB4004	606111,11	1074	55	54795,92	over 20
SB4005	943611,11	1181	30	54675,93	9
SB4006	2064444,44	1267	68,9	68530,94	over 10
SB4007	1022777,78	1105	188,8	47062,95	ca 12
SB4008	1100555,56	966,3	103	61313,45	ca12
AVERAGE					3,333333333

NAME	Comment
SERIES 1000	Gennerally: cold tests looked more slushy, ran two friction tests of the systen (one wet and one dry)
SB1000	
SB1001	Obvious that the rubble moves in lumps (block assemblies)
SB1002	
SB1003	
SB1004	The top lid collided with the testing rigg at the end of testing
SERIES 2000	Temperature of submerging basin was somewhat difficult to interpretate
SB2000	Low salinity? Very clear ice.
SB2001	Weak, at least 3 broken blocks and one peak clearly corresponds to the breaking of a block
SB2002	Rubble heigth a little low (-2 cm)
SB2003	
SERIES 3000	Note on ice type 2: measured salinity of one clear block (0,33 ppt) and one non-transperant (1,91)
SB3000	single block breaking correspond to peak on plot. Wet upper part of SB, large block assemblies move together
SB3001	Uper part of shear box (SB) is not fully covered in water, very wet SB
SB3002	
SB3003	Rubble was compressed when we put on confinement, well drained test
SERIES 4000	For SB4000: ran three friction tests, two for 65 kg and one for 45 kg confinement weigth
SB4000	Lot of dialation, heard two blocks breaking, last one is obvious on the force-disp-graf
SB4001	Moovement looks smooth, few peaks
SB4002	Weigths are only added 8 min during submerging
SB4003	Smooth movement, rotates freely, no breaking of blocks
SB4004	A lot of blocks are breaking, rubble volume is redused when the confinement weigth is added
SB4005	Rubble volume is not redused when adding weigth
SB4006	Rubble volume is not redused when adding weigth
SB4007	More movement, less breaking than 26.6 kPa-confinement tests
SB4008	Added a 25 l volume tank in the water so the water level in submerging basin increased
AVERAGE	

E Log from Pile Testing

Log from pile testing in the RITAS-project at HSVA, 23.04.12-03.05.12

1.0 Initial geometry and rubble properties

Table 1 Initial geometry of tests

Test name	Width [mm]	Bottom length [mm]	Top length [mm]	Average height [mm]	Repose angle [deg]	Description of ice rubble	Consolidation time [min]
1060	760	1800	-	308 (258 over framework)	45.7	Very warm ice, and very mushy rubble pile, thickness 43 mm	0 (time to make the pile: 20)
2060	600	1400	-	272	42.2	More distinguished pieces, and less slush then 1060, thickness 43 mm	0 (time to make the pile: 20)
2061	600	1500	-	325	47.3	Uses some new, and some of the same rubble as test 2060, thickness 43 mm	33 (time to make the pile: 5)
3060	600	1600	800	308	45.8	quite distinguished blocks and pieces of ice thickness 47 mm	0 (time to make the pile: 18)
3061	600	1470	690	267	41.7	Uses some new, and some of the same rubble as test 3060, thickness 47 mm	32 (time to make the pile: 5*)
4060	600	1800	1000	260	40.9	Large block pieces (61 mm thick)	0 (time to make the pile: 15)
5060	400	1300	1200	180	42.0	Pile too small, for satisfying results LI-Thickness 41 mm	0 (time to make the pile :6)
5061	600	1800	800	218	36.0	Thickness 41 mm	0 (time to make the pile :6)

The dry density of rubble was estimated two times, for series 3000 and series 5000. The density was estimated to 560 kg/m^3 (3000-series, low density) and 558 kg/m^3 (5000-series, base case).

The scale that was used had an accuracy of 0.5 kg, and the volume measure had an accuracy of ca. ±5000 cm^3 this gave the density an accuracy of roughly around ±100 kg/m^3.

2.0 Slides and tilting of the piles

Table 2 all slides that occurred

	Angle of board	Critical angle	Failure angle	Type of slide
1060				
initial	0	34.2		
1.slide	32.6	34.2 + 32.6 = 66.8	57.3	*Main slide*
2.slide	38.7	Ca.65 estimated from video	50.7	*Final slide* Slide initiated along the board, then friction developed, and we measured angle of the slide
2060				
initial	0	42.2		
1.slide	9.7	42.2 + 9.7 = 51.9	51.1	*First slide* A few blocks
2.slide	27.1	51.1-9.7 + 27.1 = 68.5	40.3	Quite some blocks
3.slide	29.4	40.3 -27.1 +29.4 = 42.6	61.1	A tug from the crane shakes the pile, and some blocks fall off
4.slide	36.4	61.1 -29.4 +36.4 =68.1	51.0	*Main slide* A tug from the crane makes the top of the pile slide off, the rest of the pile consists of one layer of blocks between the frame pieces
5.slide	42.6	51.0-36.4+42.6 =57.2	42.6	*Final slide* Slide is in the angle of the plate
6.slide	61.2			All blocks slides off
2061				
initial	0	47.3		
1.slide	33.0	47.3+33.0=80.3	61.2	*Main slide* Initiated by a tug from the crane
2.slide	45.4	61.2-33.0+ 45.4 =73.6	45.4 (36.6)	All rubble slides off the board,(failure angle measured outside the board)
3060				
initial	0	45.8		
1.slide	30.6	45.8 +30.6=76.4	48.6	*First slide* Small slide, at two locations
2.slide	36.4	48.6-30.6 +36.4	49.7 (60 I	Two big slides at two locations at *the sides*

		= 54.4	video)	
3.slide	44.5	48.6-30.6+44.5 = 62.5 (72 from video)	64.2	*Main slide* Top of pile slides off (in the centre of the pile)
4.slide	55.7	62.2-44.5 +55.7 =73.4	55.7	Some few blocks
5.slide	65.5	Ca.75 (estimated from video)		*Last slide* All blocks slides off
3061				
initial	0	41.7		
1.slide	31.4	41.7 +31.4=73.1	54.8	*First slide* Small local slide from the top
2.slide	43.5	54.8-31.4+43.5 =66.9		Some top block slides, the tilting is stopped, but right after the entire pile slides off the plate.
4060				
Initial	0	40.9		
1.slide	22.9	40.9 +22.9=63.8	49.7	*First slide* Small slide in one location
2.slide	35.9	49.7-22.9+35.9 = 62.7	53.6 , 38.0	*Main slide* The hole pile slides at the same time, measure slide angle at two locations
3.slide	44.3	53.6-35.9+44.3= 62.0		*Last slide* The top of the pile slides off, and only a layer between the frame pieces remain.
5060				
Initial	0	42.0		
1.slide	29.2	42+29.2=71.2	29.2	Pile top collapses when the plate had an angle of 29.2 deg. Seems like the width is too small to make a real pile shaped pile. The testing was stopped.
5061				
initial	0	36.0		
1.slide	31.8	36.0 +31.8=67.8	42.1	*First slide* Two small slides
2.slide	38.5	36+38.5 = 74.5	52.9	*Main slide* Some small slides due to stop-and-go of test, then one slide in the area around the centre
3.slide	52.2	52.9-38.5+52.2= 66.6		*Last slide* All rubble slides off the board,

The critical angle is computed as follows:

Critical angle Initial = repose angle

Critical angle 1.slide = repose angle + angle of board at 1.slide

Critical angle 2.slide = Failure angle 1.slide - angle of board at 1.slide + angle of board at 2.slide

Note: failure angle is measured at one location of the pile, and is therefore not always valid for the entire pile.

Definitions of slides are as follows:

When the piles were tilted, several small local slides were registered and the local failure angles were measured in-situ. The first of these local slides is referred to as *the first slide*. It also occurred that all or most of, the pile deformed at the same time. This is referred to as *the main slide*. In some of the tests the failure of the pile was simply a friction failure against the pile board, and rubble slid off the board. After such a failure the test was stopped and this is referred to as *the final slide*.

Oda Skog Astrup, 15.05.12

F Adapted Results from Pile Tests

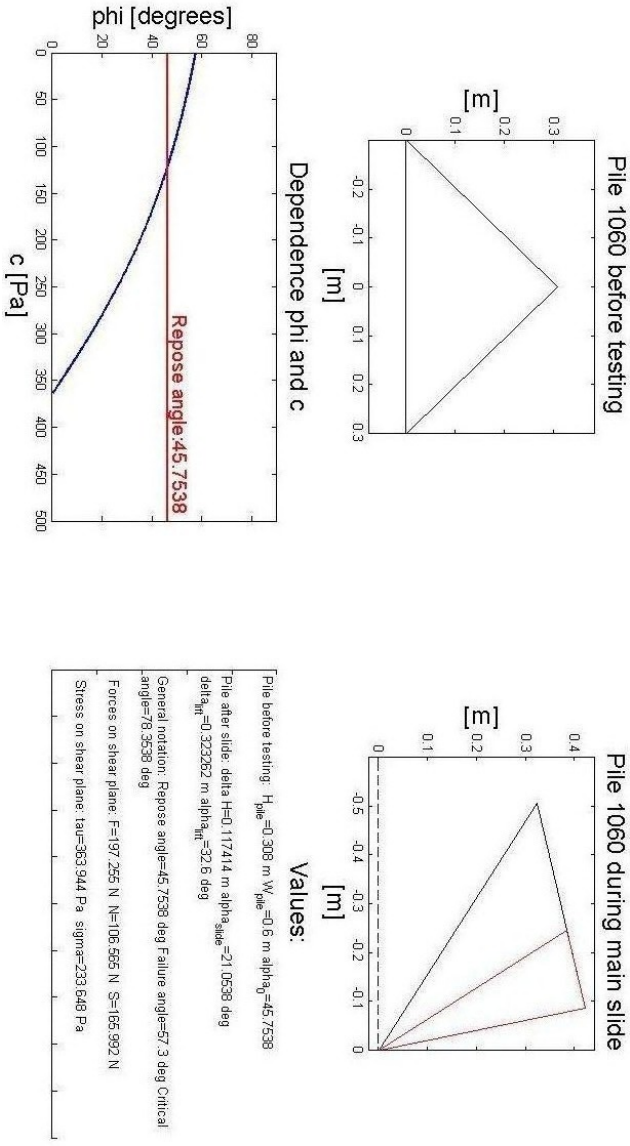

Figure 88: Pile 1060

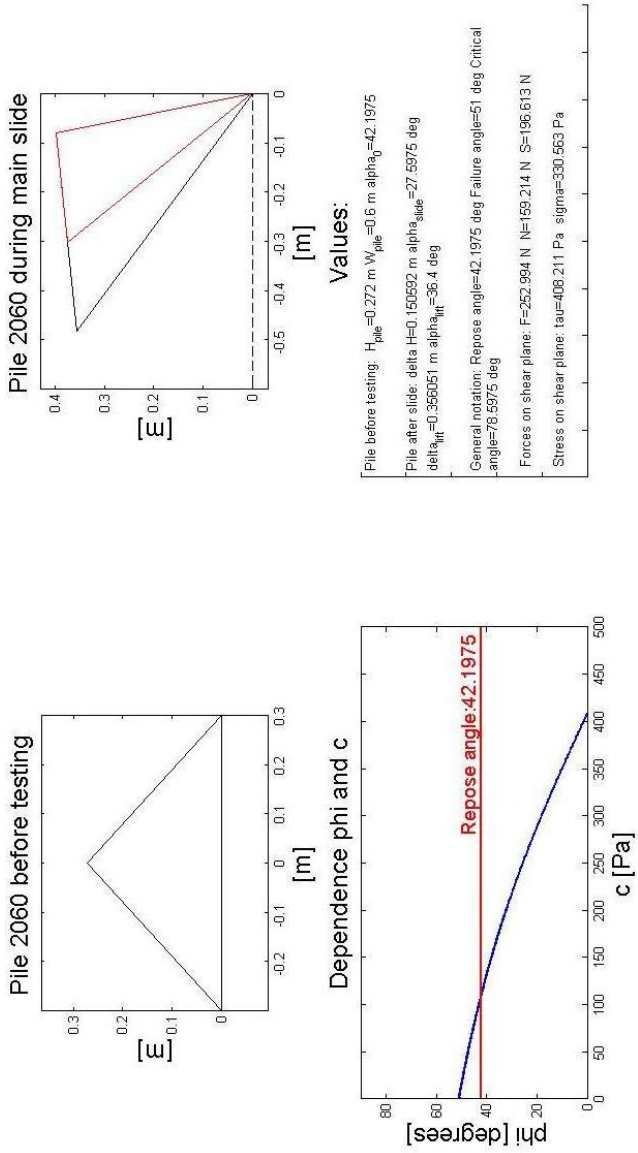

Figure 89: Pile 2060

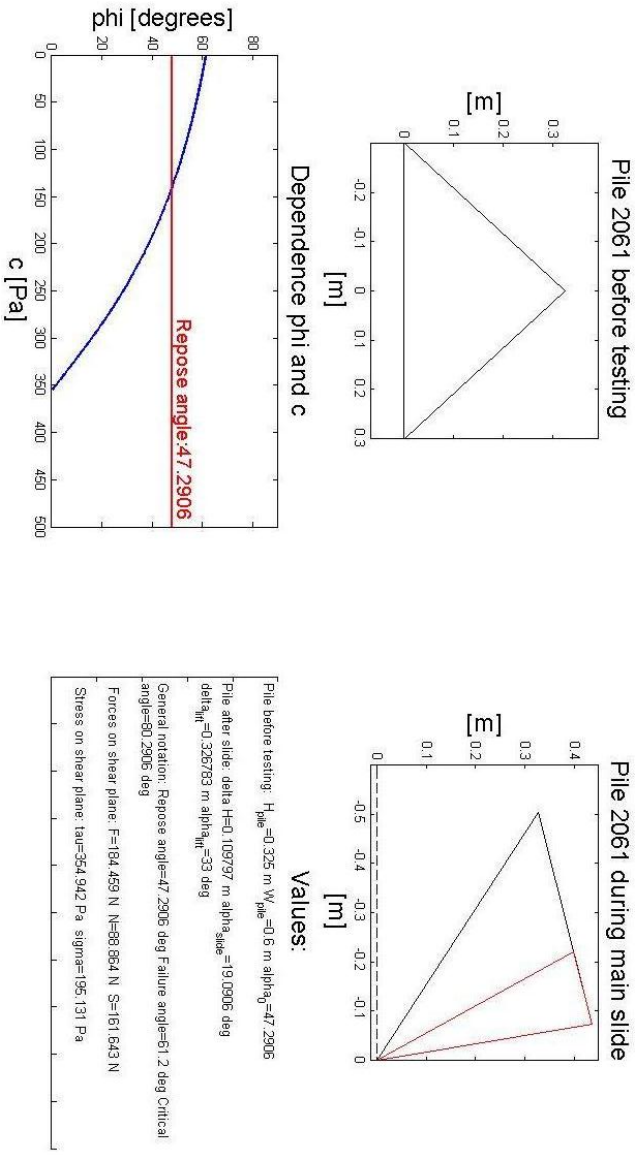

Figure 90: Pile 2061

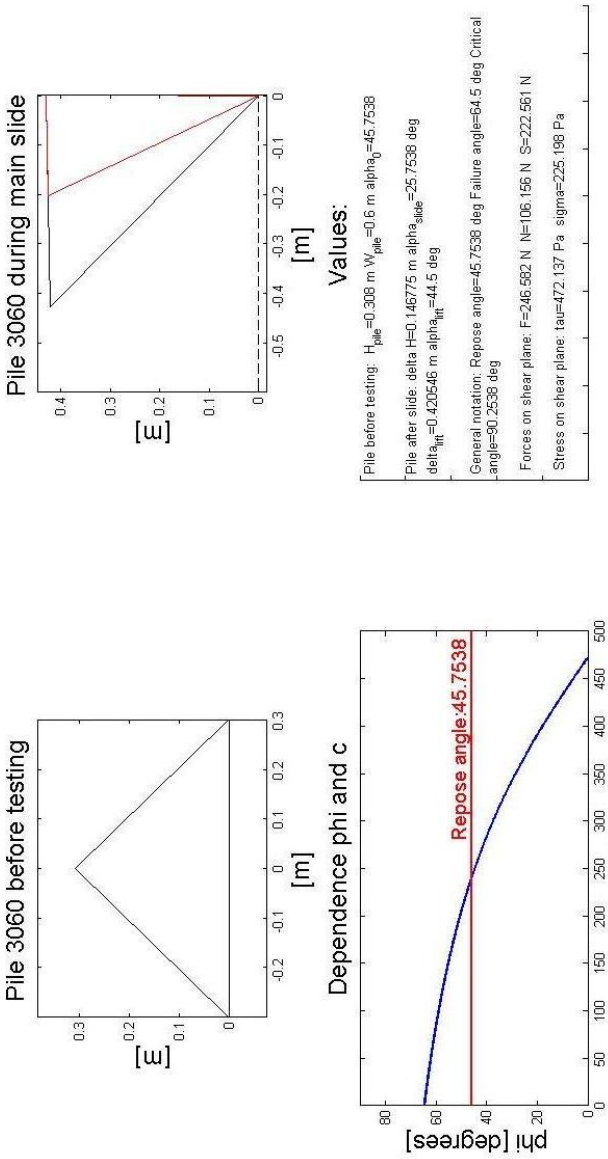

Figure 91: Pile 3060

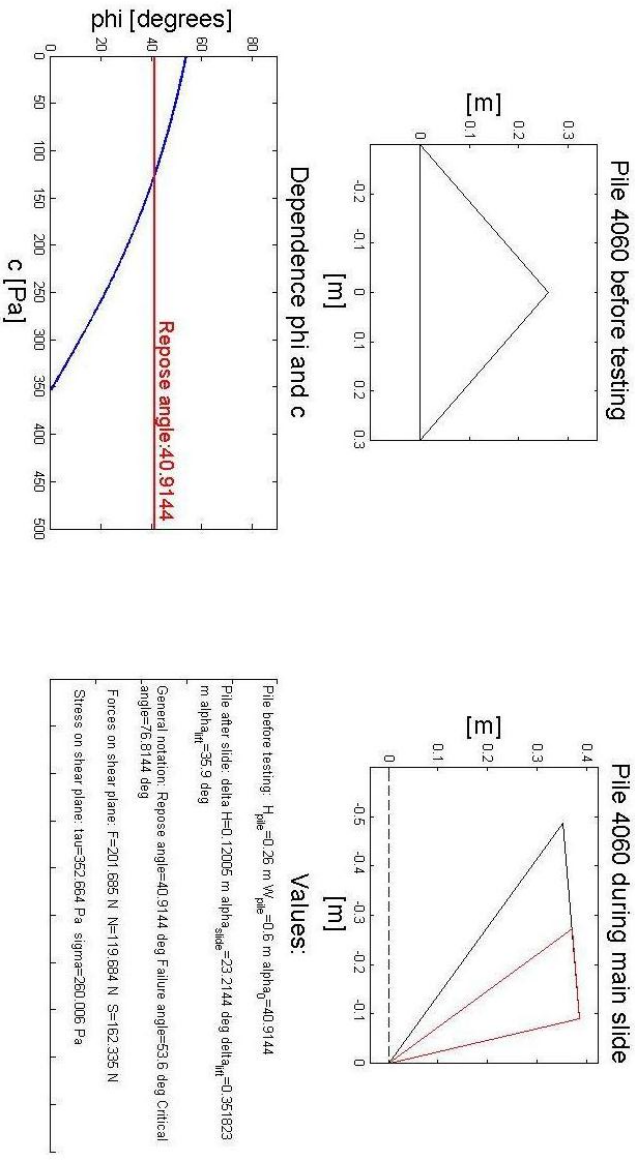

Figure 92: Pile 4060

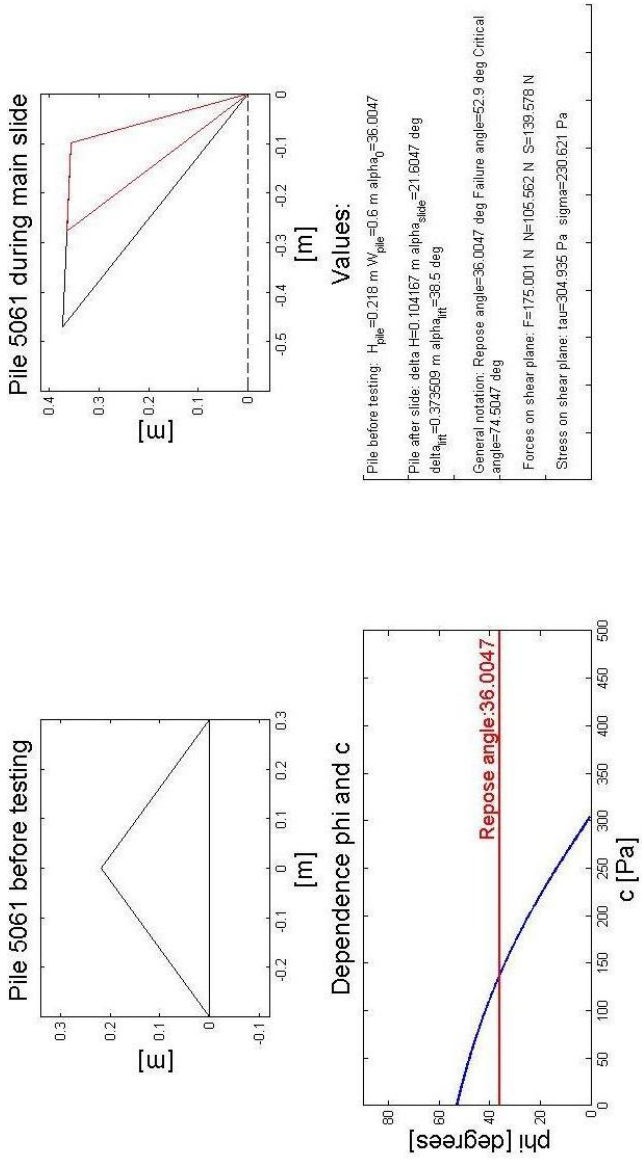

Figure 93: Pile 5061